

DOCTORAL THESIS

Role of Metal Ions in Amyloidogenic Properties of Insulin and Superoxide Dismutase

Julia Gavrilova

TALLINN UNIVERSITY OF TECHNOLOGY
DOCTORAL THESIS
44/2022

**Role of Metal Ions in Amyloidogenic
Properties of Insulin and Superoxide
Dismutase**

JULIA GAVRILOVA



Tallinn University of Technology

School of Science

Department of Chemistry and Biotechnology

This dissertation was accepted for the defense of the degree of Doctor of Philosophy in Gene Technology 12.07.2022

Supervisors:

Professor Peep Palumaa

Department of Chemistry and Biotechnology

Tallinn University of Technology

Tallinn, Estonia

Vello Tõugu, PhD

Department of Chemistry and Biotechnology

Tallinn University of Technology

Tallinn, Estonia

Opponents:

Professor Wojciech Bal

Institute of Biochemistry and Biophysics

Polish Academy of Sciences

Warsaw, Poland

Professor Ago Rinke

Institute of Chemistry

University of Tartu

Tartu, Estonia

Defense of the thesis: 23.08.2022, Tallinn

Declaration:

Hereby I declare that this doctoral thesis, my original investigation and achievement, submitted for the doctoral degree at Tallinn University of Technology has not been submitted for doctoral or equivalent academic degree.

Julia Gavrilova

signature



European Union
European Regional
Development Fund



Investing
in your future

Copyright: Julia Gavrilova, 2022

ISSN 2585-6898 (publication)

ISBN 978-9949-83-883-7 (publication)

ISSN 2585-6901 (PDF)

ISBN 978-9949-83-884-4 (PDF)

Printed by Koopia Niini & Rauam

TALLINNA TEHNIKAÜLIKOO
DOKTORITÖÖ
44/2022

Metallioonide roll insuliini ja superoksiidi dismutaasi amüloidgeensetes omadustes

JULIA GAVRILOVA



Contents

List of publications	6
Author's contribution to the publications	7
Introduction	8
1 Review of the literature	10
1.1 Roles of zinc and copper ions in proteins	10
1.2 Insulin	11
1.2.1 Insulin synthesis and secretion	12
1.2.2 Role of zinc in the functioning of insulin.....	13
1.2.3 Structure of insulin	14
1.2.4 Fibrillization of insulin.....	15
1.2.5 Diabetes mellitus and the role of zinc in it	17
1.3 Superoxide dismutases	19
1.3.1 Structure of Human Superoxide Dismutase 1 (SOD1)	21
1.3.2 Human Superoxide Dismutase 1 (SOD1) stability and properties	22
1.3.3 Post-translational maturation of SOD1	23
1.3.4 Amyotrophic lateral sclerosis and ALS-related SOD1 mutations.....	24
2 Aims of the study	26
3 Materials and methods	27
4 Results	28
Publication I	28
Publication II	28
Publication III	28
5 Discussion.....	30
6 Conclusions	35
References	36
Abstract.....	46
Lühikokkuvõte.....	47
Appendix	49
Publication I	49
Publication II	59
Publication III	67
Curriculum vitae.....	81
Elulookirjeldus.....	83

List of publications

The current thesis is based on the following publications, which will be referred to in the text by their Roman numerals.

- I. Noormägi, A., Gavrilova, J., Smirnova, J., Tõugu V., Palumaa, P. "Zn(II) ions co-secreted with insulin suppress inherent amyloidogenic properties of monomeric insulin" (2010) *Biochem J.*; 430(3):511-518.
- II. Gavrilova, J., Tõugu V., Palumaa, P. "Affinity of zinc and copper ions for insulin Monomers" (2014) *Metallomics*; (6) 1296-1300.
- III. Smirnova, J., Gavrilova, J., Noormägi, A., Valmsen, K., Pupart H., Luo, J., Tõugu, V., Palumaa, P. "Evaluation of Zn²⁺- and Cu²⁺-binding affinities of native Cu,Zn-SOD1 and its G93A mutant by LC ICP MS" (2022) *Molecules*; (27) 3160.

Author's contribution to the publications

- I. The author participated in experimental design, performed fluorimetric experiments, and analyzed the data.
- II. The author participated in experimental design, performed the experimental work, analyzed the data, and wrote the draft of the manuscript.
- III. The author participated in the methodology development, experimental work, and writing of the manuscript draft.

Introduction

One of the most challenging problems of proteins and peptides is the physical instability and tendency to form amyloid fibrils. Amyloid formation starts typically from soluble monomeric precursors, which undergo remarkable conformation changes associated with the polymerization into 8- to 10-nm wide fibrils with dominantly cross-beta structure. Protein tendency to form fibrils is associated with more than 40 human diseases, including the neurodegenerative disease amyotrophic lateral sclerosis (ALS) and metabolic disorder type 2 diabetes mellitus. Proteins can form fibrils at intra- or extracellular sites causing different pathologies. In vitro fibrillization causes many challenging problems in the production and storage of artificially produced peptide hormones and therapeutic proteins.

Proteins often require cofactors to perform their biological functions. Such cofactors are often metal ions. That is why it is very important to investigate the physical and chemical properties of protein-metal complexes. In addition, it has been demonstrated that metal ions such as Zn(II) and Cu(II) have a pronounced effect on the fibrillization of various amyloidogenic peptides and proteins. However, the roles of metal ions in the fibrillization of metalloproteins as well as affinity parameters of metal-protein complexes are still largely unknown, although they are of fundamental importance for the understanding of protein functioning and dysfunction.

One goal of this study was to gain more understanding of the molecular mechanism of protein fibrillization in the example of insulin. We also examined the effect of Zn(II) ions on insulin fibrillization and revealed insulin fibrillization kinetics at physiological pH. We have determined the dissociation constant value for the monomeric 1 : 1 Zn(II) – insulin and Cu(II) – insulin complexes. We showed that Zn(II) inhibits the fibrillization of monomeric insulin at physiological pH values by forming a soluble Zn(II)-insulin complex. The obtained results demonstrate that Zn(II) ions might suppress the fibrillization of insulin at its release sites. In circulation, it is, however, not possible due to the low concentration of free Zn(II) in the environment. Based on the obtained results we proposed a model for the assembly and fibrillization of insulin in the presence of Zn(II) ions and indicated that dimerization is an off-pathway in this process.

The second goal of this study was the investigation of the demetallation of Cu,Zn-SOD1, and its ALS-related G93A mutant in the presence of different standard metal ion chelators at varying temperatures by using an LC-ICP MS-based approach. Our results showed that both metal ions Zn(II) and Cu(II) are released simultaneously according to the slow first-order kinetics from the protein at elevated temperatures. The rate of the release depends on the concentration of chelating ligands but is almost independent of their metal-binding affinities. Metal-binding affinities of native and G93A mutant of Cu,Zn-SOD1 have been estimated from the extrapolation of the Arrhenius plot to physiological temperatures.

The obtained results give us a better understanding of the mechanisms of amyloid formation on the molecular level in the absence and presence of metal ions and reveal the affinities of many protein-metal ion complexes.

Abbreviations

β -amyloid	Amyloid- β peptide
AAS	Atomic absorption spectroscopy
ALS	Amyotrophic lateral sclerosis
CCS	Copper Chaperone for Superoxide Dismutase
CPE	Carboxypeptidase E
DTPA	Diethylenetriaminepentaacetic acid
EDTA	Ethylenediaminetetraacetic acid
ER	Endoplasmic reticulum
LC-ICP MS	Liquid Chromatography-Inductively Coupled Plasma Mass Spectrometry
MND	Motor neuron disease
MT	Metallothionein
$O_2^{\cdot-}$	Superoxide anion
PC1/3, PC2	Prohormone convertases 1/3, 2
SEC	Size-exclusion chromatography
SOD1	Superoxide Dismutase 1
T1D	Type 1 diabetes mellitus
T2D	Type 2 diabetes mellitus
TEM	Transmission electron microscopy
ThT	Thioflavin T
ZnT8	Zinc transporter 8

1 Review of the literature

1.1 Roles of zinc and copper ions in proteins

It is known that nearly thirty percent of all proteins contain metal ions. There is a term “metalloproteins” which denotes proteins whose function is regulated by metal ions (Mounicou, Szpunar et al. 2009). Metal ions serve a variety of functions in proteins. The most important function is to take part in the catalytic processes of enzymes (Glusker 1991). Metal ions are well suited for these functions because of the following properties: (i) metal ions are usually positively charged and, hence, electrophilic. They can act as Lewis acids in binding and activating substrates; (ii) many metals can exist steadily in several different oxidation states differing by one or by several units. This allows these metals to participate in various types of oxidation-reduction processes; (iii) metal ions generally bind four or more ligands. By binding several protein side chains, metals can act as cross-linking agents (Berg 1987). Another role of metal ions is to enhance the structural stability of the protein in the conformation required for biological function. The most common metal ions included in the composition of metalloproteins are zinc and copper.

Copper is an essential trace metal found in all living organisms. It is required for survival and serves as an important catalytic cofactor in redox chemistry for proteins that carry out fundamental biological functions required for growth and development (Linder and Hazegh-Azam 1996). Copper serves as an essential cofactor for the activity of cytochrome C oxidase in mitochondria, the enzyme that is central for respiration, and for Cu,Zn-dependent superoxide dismutase (SOD), which plays an important role in the detoxification of superoxide radicals. In addition, many cells require copper in the secretory pathway, where enzymes like ceruloplasmin, dopamine- β -hydroxylase, peptidyl- α -mono-oxygenase, tyrosinase, and others incorporate copper as a cofactor in their catalytic sites. These enzymes contribute critically to several key physiological processes, such as iron influx into the cells, the production of neuroendocrine peptides and neurotransmitters, pigmentation, blood clotting, and others. Copper deficiency decreases the activity of these enzymes and thus affects adversely the corresponding physiological processes (Johnson and Anderson 2008; Nelson and Prohaska 2009).

Genetic and biochemical studies identified several proteins that play key roles in the uptake, and export of copper from the cells. These include a high-affinity transporter CTR1, a low-affinity transporter CTR2, and the copper efflux transporters ATP7A and ATP7B. It has also become apparent that, in addition to membrane transporters, cells contain a complex network of soluble regulator molecules – copper chaperones (CCS, Atox1, Cox17, SCO1, and SCO2), that allow for the fine-tuning of copper homeostasis and precise temporal and spatial distribution of copper in a cell (Lim, Cater et al. 2006; Gupta and Lutsenko 2009). In organism Cu ions can only be found in the composition of proteins because the concentration of free copper ions in the cytoplasm of eukaryotic cells is very low, estimated to be under 10^{-18} M (Rae, Schmidt et al. 1999).

Copper can exist in biological conditions in two redox states – Cu(II) and Cu(I) with the redox potential of Cu(II)/Cu(I) couple of 153 mV (Strehlow 1978). Copper in its reduced (Cu(I)) form can interact mainly with thiol and thioether groups of Cys and Met. Oxidized (Cu(II)) form interacts with imidazole nitrogen of His or carboxyl groups of Asp or Glu. Copper-containing proteins are important electron carriers and redox catalysts thanks to switching between two redox states (Wittung-Stafshede 2015).

Zinc is a vital biometal involved in numerous aspects of cellular metabolism. The content of zinc in β -cells of pancreas is one of the highest in the body and it appears to be an important metal for insulin-secreting cells. Zinc ions are essential cofactors for the activity and folding of up to ten percent of mammalian proteins (Vallee and Falchuk 1993) and can modulate the function of many others. It is, therefore, not surprising that zinc deficiency has catastrophic consequences, reflected in the retarded growth and impaired immune functions (Udechukwu, Collins et al. 2016) also in other syndromes, like erosion of the gastrointestinal tract, skin lesions, cardiac failure, and malformations of the brain and the male reproductive system (MacDonald 2000; Maret and Sandstead 2006). Zinc, particularly the “free” or loosely-bound form of the ion, is nevertheless profoundly toxic to mammalian cells (Frederickson, Koh et al. 2005). Thus, both zinc deficiency and free zinc excess are toxic to mammalian cells (Lemaire, Ravier et al. 2009). Dysregulation of free zinc has also been implicated in the formation of β -amyloid plaques associated with Alzheimer’s disease (Cherny, Atwood et al. 2001). These paradoxical aspects of cellular zinc dictate that it is distributed in highly regulated gradients with respect to the plasma membrane and intracellular compartments. The cellular distribution of zinc into organelles is precisely managed to provide the zinc concentration required by each cell compartment (Sekler, Sensi et al. 2007). It secures that an adequate supply of this ion is available to the numerous zinc-binding proteins while preventing its accumulation and the potentially devastating effects it can readily initiate (Sekler, Sensi et al. 2007).

The uniqueness of zinc, in contrast to other abundant transition metals in the body, e.g., iron and copper, is that it lacks redox activity (Sekler, Sensi et al. 2007). Zn(II) is redox-stable and it functions as a Lewis-acid type catalyst to accept a pair of electrons. In proteins, Zn(II) ions are bound to His, Cys, Glu and Asp residues (Berg and Shi 1996; McCall, Huang et al. 2000; Swart 2013). In proteins, zinc ions are essential for enzymatic activity, folding or conformational changes. Zn(II) is a very important metal ion for the functioning of more than 300 different enzymes that regulate cell growth, cell division and apoptosis, gene expression, and immune response. Moreover, Zn(II) functions as structural a component in many transcription factors, such as zinc-fingers, which represent one of the largest protein families coded by the mammalian genome.

1.2 Insulin

Insulin is a small peptide hormone that is crucial for the control of glucose metabolism (Ahmad, Uversky et al. 2005) and the regulation of the biosynthesis of triglycerides by adipose cells (Haas, Vohringer-Martinez et al. 2009). Defects in insulin secretion and action result in diabetes mellitus, a severe metabolic disorder, the hallmark of which is hyperglycemia (high blood sugar) (Chimienti 2013). If untreated then diabetes mellitus will lead to serious health problems and ultimately to death (Alberti and Zimmet 1998). Insulin is secreted in the islets of Langerhans by the β -cells both tonically (at a constant low-level release rate) and as a high-level spike in response to an immediate glucose load such as a meal (Chausmer 1998). The Zn content in pancreatic β -cells is among the highest in the body and it is an important metal ion for insulin-secreting cells (Chimienti, Favier et al. 2005). Zn deficiency has not been very well documented in diabetes; however, it is suggested that there may be additional requirements for Zn. Different studies have found decreased physiological levels of Zn status in diabetics (Tepaamorndech, Kirschke et al. 2016), (2017).

1.2.1 Insulin synthesis and secretion

Insulin is secreted primarily in response to elevated blood glucose concentrations. This is reasonable as insulin is responsible for promoting glucose entry into cells. Some neural stimuli (such as vision and taste of food) and increased blood concentrations of other fuel molecules, including amino acids and fatty acids, also contribute to insulin secretion. Insulin is synthesized in significant quantities only in beta cells of the pancreas. The insulin mRNA is translated as a single chain precursor called preproinsulin. Later when its signal peptide is eliminated upon incorporation into the endoplasmic reticulum, proinsulin is formed (Weiss, Steiner et al. 2000).

Proinsulin consists of three regions: a carboxy-terminal A chain, an amino-terminal B chain, and a connecting peptide in the middle known as the C peptide. Within the endoplasmic reticulum, proinsulin is exposed to several specific endopeptidases which excise the C peptide, thereby generating the mature form of insulin (Fig. 1). Insulin and free C peptide are packaged in the Golgi complex into secretory granules together with amylin (Landreh, Alvelius et al. 2014).

When the beta cells are appropriately stimulated, insulin is released from the cell by exocytosis and diffuses into the capillary blood of the islets. C peptide is also secreted into the blood but has no known biological activity (Davidson 2004).

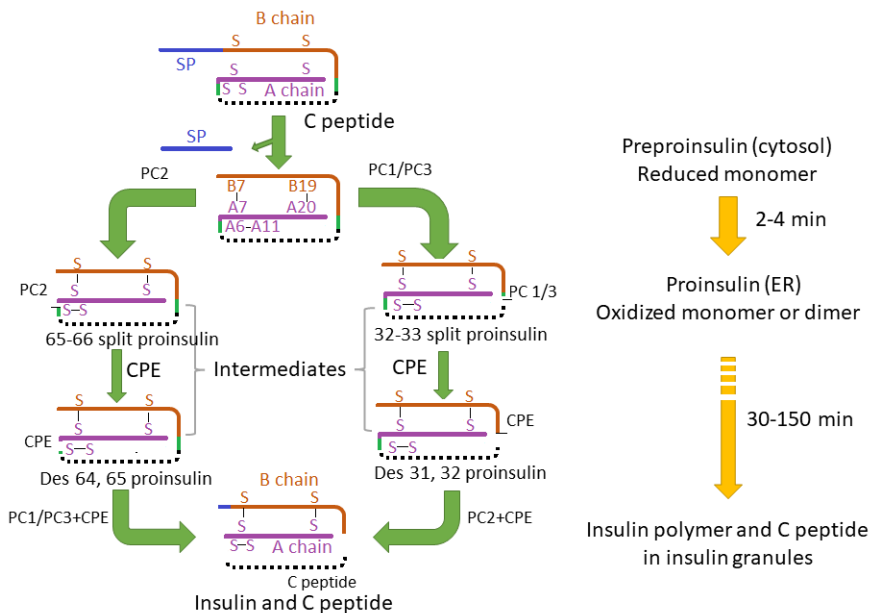


Figure 1. Insulin biosynthesis in pancreatic beta cells. Insulin biosynthesis begins with the synthesis of a precursor, preproinsulin, within the cytosol. Preproinsulin is composed of signal peptide (blue), insulin B-chain (brown), C peptide (black), and insulin A-chain (purple). Newly synthesized preproinsulin undergoes co- and posttranslational translocation into the endoplasmic reticulum (ER), where it is cleaved by a signal peptidase, forming proinsulin. The proinsulin folds in the ER, forming three evolutionarily conserved disulfide bonds, including two interchain disulfide bonds B7–A7 and B19–A20, and one intrachain disulfide bond A6–A11. Properly folded proinsulin forms dimers and exits from the ER, trafficking through The Golgi complex into secretory granules where prohormone convertases (PC1/3 and PC2) in concert with carboxypeptidase E (CPE) are cleaving proinsulin into C peptide and two-chain mature insulin stored in the insulin granules (adapted from Liu, Wright et al. 2014).

Insulin molecules are stored in secretory granules of pancreatic β -cells in the hexameric state. Each hexamer is stabilized by at least two Zn(II) ions coordinated by the imidazole side chains of HisB10 (Hua 2010). *In vitro* studies showed that the hexameric state of insulin can exist in three distinct forms: T6, T3R3, and R6 (where R stands for relaxed and T represents tight conformations). These forms differ from each other by the conformations of the N-terminal regions of their B-chains (residues B1–B9).

In the T6 hexameric conformation, both Zn(II) sites are octahedral and coordinated by three symmetry-related His imidazole rings (HisB10) as well as three symmetry-related water molecules (Frankaer, Knudsen et al. 2012; Frankaer, Sonderby et al. 2017). The R6 hexameric conformation has tighter tetrahedral coordination around the Zn(II) ions comprising the three HisB10 residues and a lyotropic anion such as chloride (Frankaer, Knudsen et al. 2012). Finally, in the T3R3 hexameric conformation, both the octahedral and the tetrahedral coordination geometries are present (Frankaer, Sonderby et al. 2017). Currently, it is assumed that the T3R3 conformation is the pancreatic storage form of insulin (Kosinova, Veverka et al. 2014).

From the structural point of view, it is clear that the hexameric state is more stable against various stressogenic conditions than the monomeric form (Akbarian, Yousefi et al. 2020). From the biological activity standpoint, however, insulin must be monomeric to be functional. Only the monomeric form of this hormone can bind to its receptor (Shepherd and Kahn 1999). However, this functionality, which requires dissociation also decreases the conformational stability of insulin, weakens its structure, and increases the vulnerability and predisposition of this hormone to pathological self-assembly. It has been shown that during insulin fibrillization, the hexameric form dissociates into monomers or dimers, then the partial unfolding makes insulin susceptible to fibrillization (Hong and Fink 2005; Akbarian, Ghasemi et al. 2018).

1.2.2 Role of zinc in the functioning of insulin

The importance of zinc in insulin crystallization was recognized about a decade after the discovery of insulin. It was discovered that the addition of Zn(II) to a phosphate-buffered solution containing insulin induced the formation of characteristic rhombohedral insulin crystals (Scott 1934). Thereafter a direct effect of Zn(II) ions on the action of insulin was demonstrated. Further, it was decided to measure the zinc content in the pancreas of groups of normal and diabetic individuals because of the close association between insulin and Zn(II) (Scott and Fisher 1938). It was found that the content of Zn in the pancreas of diabetics is half that of healthy people, while there was no difference in Zn concentration in the liver, raising the possibility that at least part of the Zn in the pancreas could be connected with the storage of insulin (Chimienti 2013). In this way, the understanding of the link between insulin and zinc was born.

The concentration of Zn(II) in the insulin-containing granules of β -cells is high with an estimated range between a few mM to 20 mM (Hutton 1983; Grodsky and Schmid-Formby 1985; Foster, Leapman et al. 1993). Normally Zn(II) is tightly bound to proteins, which limits the extent of cytosolic free Zn(II) concentration (Vallee and Falchuk 1993; Outten and O'Halloran 2001). If secreted Zn(II) at the interstitial space reaches the level of 1–10 μ M, the concentration difference between the cytosol of the β -cells and the interstitial space could be as great as 1000-fold (μ M to nM) (Li 2013). Zn(II) uptake following its secretion could, therefore, be similar to that described for other ions: a passive process in which Zn(II) moves from an area of high concentration in the extracellular to an area of low concentration within the cytosol of β -cells (Li 2013).

Quantitative electron probe microanalysis of the granular Zn(II) to insulin ratio has shown that β -cell granules contain Zn(II) in 1.5-fold excess of that necessary to form Zn-insulin hexamers (Foster, Leapman et al. 1993), which leads to release of more free Zn(II) (Li 2013). The level of free Zn(II) appears to mediate multiple signaling pathways including apoptotic signaling cascades, indicating that Zn(II) can act as an intracellular signaling molecule and regulate cellular metabolism and functional activities (Bellomo, Meur et al. 2011; Slepchenko and Li 2012).

It is known that monomeric insulin coexists in equilibrium with other higher-order multimers (Bocian, Sitkowski et al. 2008). Effects of Zn(II) on native-state insulin aggregation were not initially linked to its influence on multimer equilibria. It was found that excess Zn(II) results in the aggregation of insulin at $\text{pH} > 4$ (Klostermeyer and Humbel 1966). Also, it was reported that the solubility of insulin decreased rapidly as the amount of Zn(II) added at neutral pH became sufficient to form hexamers complexed with 3–6 Zn(II) ions (Grant, Coombs et al. 1972). This solubility decrease after adding Zn(II) was explained by the neutralization of net 12 negative charges on insulin hexamer at neutral pH by 6 Zn(II) ions (Xu, Yan et al. 2012). The effect of zinc on insulin aggregation was further supported by the fact that chelating Zn(II) by ethylenediaminetetraacetic acid (EDTA) improved solubility and slowed the aggregation of Zn-insulin (Quinn and Andrade 1983). Thus, the speciation of insulin is controlled by the protein concentration and strongly influenced by Zn(II), which controls aggregation (Xu, Yan et al. 2012).

1.2.3 Structure of insulin

After many years of research the X-ray structure of rhombohedral insulin crystals was resolved (Adams, Blundell et al. 1969). Insulin was one of the first proteins to have its X-ray structure uncovered. It was shown that the crystals are formed by six insulin molecules and two Zn(II) atoms and the intramolecular zinc coordination spheres were determined. However, physiological interactions between Zn(II) and insulin were known decades before the crystal structure of the Zn(II)–insulin complex was resolved. Moreover, as early as the 1930s, it was known that the addition of Zn(II) to insulin delayed its action when administered to diabetic patients (Scott 1934).

The insulin molecule is built up of a 21-residue A chain containing an intrachain disulfide bond and a 30-residue B chain which are connected by two interchain disulfide bonds (Baker, Blundell et al. 1988) (Fig. 2). The A-chain consists of two short α -helices formed by residues A1–A8 and A13–A19. The B-chain is folded around a central helix (B9–B19) flanked by stretches of extended structure at both termini. Two disulfide bridges, A7–B7 and A20–B19, link the two chains covalently. Additionally, there is an intrachain disulfide from A6 to A11 (Steensgaard, Schluckebier et al. 2013).

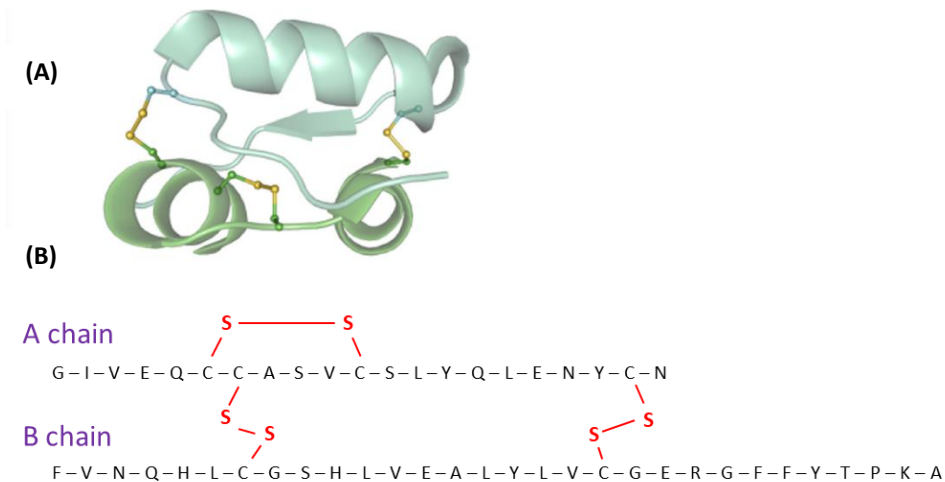


Figure 2. (A) Crystal structure of insulin displaying the A chain (21 residues) colored green which contains an intrachain disulfide bond, and the B chain (30 residues) colored cyan with two additional inter-chain disulfide bonds shown as balls and sticks (PDB ID: 4E7T).

(B) The primary structure of bovine insulin.

Like other globular proteins, insulin tends to adopt and maintain a three-dimensional structure in which its hydrophobic residues are buried by the folding of individual residues. However, changes in the native conformation can be provoked by a variety of factors. Usually, insulin solutions are composed of mixed populations of monomers, dimers, and hexamers that are in dynamic equilibrium. The amount of each species in the solution is dependent on the concentration and pH of the solution (Pohl, Hauser et al. 2012). At neutral pH and high concentration (>0.1 mM), this equilibrium favors the zinc-stabilized hexamer (molecular weight ~36 kDa), which consists of three dimers of insulin arranged around two Zn(II) ions on the 3-fold symmetry axis, while at low concentrations (10^{-5} to 10^{-8} M) or low pH, the monomer is prevalent (Brange, Owens et al. 1990). The hexameric form of insulin is relatively stable and it is the commonly used pharmacologic form (Chausmer 1998). Each zinc ion coordinates to three B10 His imidazole groups and by extrinsic ligands complete either tetrahedral or octahedral ligand geometry. The eight N-terminal residues of the B-chain can exist in extended β - or α -helical conformation.

Under the influence of heat, low pH, and exposure to hydrophobic surfaces, insulin has the propensity to undergo conformational changes resulting in successive aggregation and formation of a viscous gel or insoluble precipitates (Brange, Langkjaer et al. 1992).

1.2.4 Fibrillization of insulin

Insulin fibril formation is a physical process in which partially unfolded insulin molecules cooperate with each other to form linear assemblies (Brange, Andersen et al. 1997). Many hypotheses about the molecular mechanisms of the *in vivo* and *in vitro* fibrillization of amyloidogenic proteins have been proposed. However, despite decades of studies, we still do not completely understand how soluble globular insulin molecules assemble into long, micrometer-long fibrils with a diameter of 8–10 nm (Ivanova, Sievers et al. 2009; Akbarian, Yousefi et al. 2020).

It has been proposed that insulin fibrillization process takes place through the dissociation of oligomers into monomers, which undergoes a structural change to a conformation having a strong propensity to fibrillate (Ahmad, Millett et al. 2004). Thus, a minimum pathway for insulin fibrillization is hexamer → monomer → partially unfolded monomer → fibrils (Ahmad, Millett et al. 2004).

Fibril formation is not dependent on the presence of carboxyl groups, whereas a marked decrease in the tendency to fibrillization is observed when the amino groups are acetylated (Brange, Andersen et al. 1997).

The typical fibril formation process is characterized by a lag phase during which nucleation occurs, but no detectable fibrils are formed. The lag phase is followed by an elongation phase in which fibrils are formed over a period often shorter than the lag phase. Eventually, the process reaches equilibrium when most soluble proteins are converted into fibrils. The lag phase is known to be the rate-determining step and hence controlling this step is of utmost importance. The length of the lag phase and the fibril growth rate depend upon factors such as the initial peptide concentration and pH, both of which affect the degree of supersaturation in solution. Other factors include the addition of fibril seeds, the ionic strength of the solution, and the intensity of agitation (Nayak, Dutta et al. 2008).

The formation of insulin fibrils precedes precipitation. It was shown that heat precipitation involves three reactions: formation of active centers (nucleation), elongation of these centers to fibrils (growth), and floccule formation (precipitation) (Brange, Andersen et al. 1997). Flocculation – a process where colloids come out of suspension in the form of floc or flakes.

The nucleation reaction, which is the slowest process, requires the nearly simultaneous interaction of 3 to 4 insulin molecules (Brange, Andersen et al. 1997). Essentially undistorted insulin is involved in these interactions, which are mainly between nonpolar side chains (hydrophobic interactions) of dimeric or monomeric insulin. Whereas nucleation occurs at temperatures above normal, the growth into fibrils can proceed at ambient or even lower temperatures. Depending on the conditions, the growth leads to long fibers resulting in a thixotropic gel or to shorter fibers with a tendency to arrange radially to spherulites with precipitation as the consequence (Krebs, Macphee et al. 2004). The growth of fibrils is a function of the surface area of the fibril population and the concentration of insulin in solution, and thus it is a highly cooperative process able to quantitatively remove the insulin from the solution into the fibrous form. An increase in ionic strength increases the rate of growth and, in particular, nucleation whereas a high concentration of organic acids, urea, and phenol suppresses the nucleation reaction while allowing the growth reaction to proceed. Heterogeneous surfaces accelerate the insulin nucleation process which is the rate-determining step during amyloid fibril formation. The observed shorter lag (nucleation) phase correlates both with the surface wetting ability and surface roughness. Surfaces promote faster nucleation possibly by increasing the local concentration of peptide molecules (Brange, Andersen et al. 1997). A composite parameter combining both surface wetting ability and roughness suggests that the ideal surface for slower nucleation should be hydrophilic and smooth (Nayak, Dutta et al. 2008).

The classic method to induce insulin fibrillization process is to heat insulin in an acidic solution. The formation of the fibrils can be observed as an increase in viscosity or precipitate formation. A more recent method is an agitation of neutral solutions of

insulin in the presence of a hydrophobic surface (air or polymeric material) at ambient or slightly increased temperature (Brange, Andersen et al. 1997).

Amyloid fibrils are characterized by a specific local arrangement of cross β -sheet structures (Fig.3). The same structural features have been observed in amyloid fibrils obtained *in vitro* from many proteins, even those that are not related to any known disease. This indicates that the capability to form amyloid fibrils is a generic property of many polypeptide chains (Fodera, Librizzi et al. 2008).

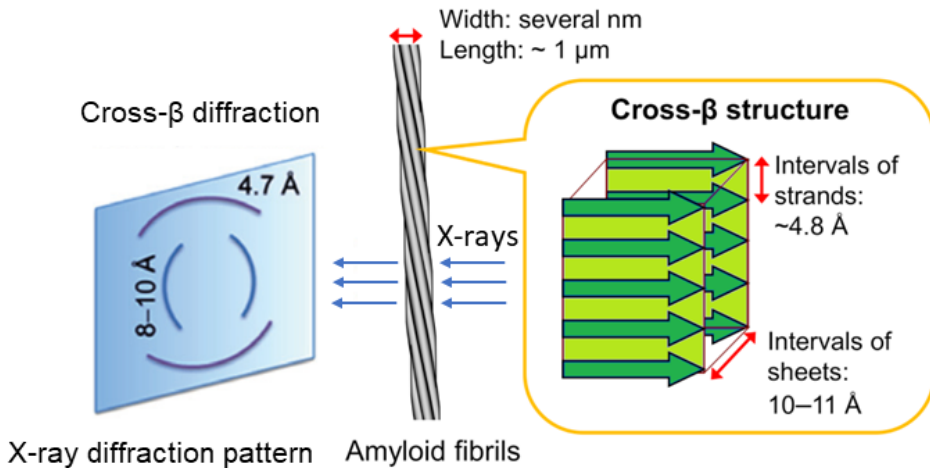


Figure 3. Schematic representation of the cross- β X-ray diffraction pattern typically produced by the amyloid fibrils. The cross- β pattern is consistent with a core of the fibrils being formed by extensive β sheets arranged along the longitudinal axis of the fibril, while the β strands forming them are arranged perpendicular to this. The reflections at 4.7 and 10 Å, which are typical of the cross- β diffraction pattern, reflect, respectively, the inter-strand and the inter-sheet spacing characterizing the cross-beta structure (adapted from del Pozo-Yauner, Wall et al. 2014).

Insulin fibrillization is very sensitive to environmental conditions (Ahmad, Millett et al. 2004), especially at low pH and high temperature (Ahmad, Uversky et al. 2005), (Fodera, Librizzi et al. 2008).

In acidic solutions, insulin maintains its tertiary structure but is mainly monomeric below pH 2 whereas an increasing population of dimers and hexamers dominates the mixture of monomers and dimers at pH above 2. Insulin fibrillization in aqueous solutions at pH 7 is a much slower and more complicated process than in acidic solutions. In neutral, aqueous solution the insulin molecule is typically associated with mainly hexameric units and insulin fibrillization does not occur to any significant extent in aqueous solution at moderate temperatures in the absence of hydrophobic surfaces or agitation (Brange, Andersen et al. 1997). The fibrillization of insulin at physiological pH in the absence of denaturing agents is practically not studied.

1.2.5 Diabetes mellitus and the role of zinc in it

Diabetes mellitus is a group of metabolic disorders characterized by hyperglycemia resulting from defects in insulin secretion, insulin action, or both. In Type 1 diabetes (T1D) there is a lack of insulin production, in T2D there exists a resistance to the effects of insulin. Both T1D and T2D have the same long-term complications (Chausmer 1998).

During T1D there is the destruction of the β -cells of the Islets of Langerhans in the pancreas, most often on an autoimmune basis, resulting in termination of insulin production. Without insulin, muscle, adipose, and liver cells cannot transport glucose from the blood to the intracellular space. In intracellular starvation conditions, fats become the primary intracellular energy source. This form of energy generation results in the production of ketone bodies and organic acids, primarily acetoacetic and beta-hydroxybutyric acids, with the consequence of the development of severe metabolic acidosis (increased acidity in the blood and other body tissue) (Chausmer 1998). These patients are dependent on insulin for survival.

In T2D the pancreatic islet cells are capable of making large quantities of insulin, at least at the beginning of the disease. In a healthy individual, insulin binds to a cell membrane insulin receptor, which initiates events leading to the transport of glucose through the membrane. The intracellular events associated with the activation of glucose transport after receiving the signal from the insulin-receptor complex are called the "post-receptor" events (Chausmer 1998). To a great extent, it is the failure of the post-receptor events that results in hyperglycemia (high blood sugar) in T2D. In response to hyperglycemia, the pancreatic islets produce increasing quantities of insulin, which results in down-regulation of the number of insulin receptors on the cell membrane. This results in both hyperglycemia and hyperinsulinemia (excess levels of insulin circulating in the blood). Additionally, the β -cells cannot make enough insulin to normalize the glucose, suggesting an error in the ability of the β -cell to synthesize insulin (Chausmer 1998). It follows that, in T1D, hyperglycemia is the major hallmark of the disease, whereas T2D is characterized also by hyperinsulinemia.

A link between zinc and diabetes has been proposed in 1998 (Chausmer 1998), as many studies have shown that zinc is secreted from pancreatic β -cells in response to elevated glucose concentration (Zalewski, Millard et al. 1994; Chimienti, Devergnas et al. 2006). The interest of the scientific community in the role of Zn(II) in the development of diabetes has been constantly growing. There are studies investigating the effect of Zn(II) supplementation in the prevention, treatment, and complications of diabetes. Moreover, genome-wide association studies have discovered polymorphisms in zinc-related genes, for example, ZnT8 and metallothionein (MT), linked to diabetes (Chimienti 2013).

MT is an intracellular low-molecular-weight, a cysteine-rich protein with high metal-binding capacity (Maret 2011). MT was used in numerous research studies describing the effects of Zn(II) on reducing diabetic complications associated with oxidative stress (Islam and Loots du 2007). MT can buffer and distribute Zn(II) to apoproteins, including transcription factors since they can move from the cytosol to cellular compartments such as the nucleus (Levadoux, Mahon et al. 1999). MT is crucial to protect the β -cells from cell death during diabetes (Li 2013). It functions physiologically by accepting Zn(II) from other Zn-binding ligands, including Zn(II) binding proteins, on the one hand, and can also function as Zn(II) donor to other Zn-binding proteins. MT plays a role in both Zn(II) homeostasis and the regulation of the cellular redox state (Li 2013). In the latter context, these proteins release Zn(II) in response to oxidative damage, a condition often found in the tissues of T2D patients (Lee, Geiser et al. 2003). Several of the complications of diabetes may be related to increased intracellular oxidants and free radicals associated with decreases in intracellular Zn(II) and Zn(II) dependent antioxidant enzymes (Chausmer 1998).

The relationship between diabetes and zinc deficiency is also complex. It is suggested that zinc deficiency can exacerbate the cytokine-induced damage in the autoimmune

attack, which destroys the islet cell in T1D. Since zinc plays an important role in the synthesis, storage, and secretion of insulin as well as conformational integrity of insulin in the hexameric form, the decreased Zn(II), which affects the ability of the islet cell to produce and secrete insulin, might then become the problem, particularly in case of T2D. The addition of Zn(II) to solutions of insulin in case of insulin therapy changes the time course for the effect of a given dose of insulin, which prolongs the duration of action of the insulin by delaying its absorption from the subcutaneous injection site, thus requiring fewer insulin injections. The behavior of insulin in the presence of Zn(II) suggested that it plays an important role in insulin's secretion from the β -cells (Li 2013).

Many genetic and functional studies have provided a better understanding of the importance of Zn(II) for pancreatic islet cells at the molecular level. It is now clear that Zn(II) has a beneficial effect on many steps in the pathophysiology of diabetes, including insulin synthesis and secretion, β -cell function and mass, islet cell communication, protection against complications, and modulation of the immune system in T1D. The overall useful effect of Zn(II) supplementation on glucose control in blood in both types of diabetes suggests that Zn(II) is a candidate ion for the prevention and therapy of diabetes (Chimienti 2013).

Despite the importance of insulin interaction with Zn(II) ions, the affinity of the formation of zinc-insulin complexes and the effects of Zn(II) ions on insulin fibrillization at physiological pH values have not been thoroughly studied.

1.3 Superoxide dismutases

Superoxide anion ($O_2^{\cdot-}$), a free radical of oxygen, is the initial product of the hydrogen peroxide formation. It is produced by the one-electron reduction of molecular oxygen.

Excessive reactive oxygen species, especially superoxide anion ($O_2^{\cdot-}$), play important roles in the pathogenesis of many cardiovascular diseases, including hypertension and atherosclerosis. Superoxide dismutases (SODs) are the major antioxidant defense systems against $O_2^{\cdot-}$, which consist of three isoforms of SOD in mammals: the cytoplasmic Cu,Zn SOD (SOD1), the mitochondrial Mn SOD (SOD2), and the extracellular Cu,Zn SOD (SOD3) (Table 1). All the isoforms require catalytic metal (Cu or Mn) for their activation (Fukai and Ushio-Fukai 2011). Two types of SODs, SOD1, and SOD3 contain Cu(II) and Zn(II) in their active site (Zelko, Mariani et al. 2002). A third isozyme – SOD2 uses manganese as a cofactor (Weisiger and Fridovich 1973).

Table 1. Comparison of three human SOD isoforms.

	SOD1	SOD2	SOD3
Location	cytoplasm	mitochondria matrix	extracellular matrix, cell surface, extracellular fluids
Metal ions in the catalytic center	Cu, Zn	Mn	Cu, Zn
Molecular mass	32 kDa	96 kDa	135 kDa
Quaternary structure	homodimer	homotetramer	homotetramer

All three SODs have a distinctive color because of bound metal ions. Cu,Zn-SOD1 exhibits a distinctive blue-green color, however, if the Zn(II) ion is released, the protein exhibits a blue color, but when the Cu(II) is reduced, then protein is colorless (Beckman, Estevez et al. 2001), Mn-SOD2 is wine-red (McCord and Fridovich 1969).

All types of SOD catalyze the same reaction – the conversion of the superoxide anion (Figure 4). It occurs in two steps: firstly, superoxide is oxidized to dioxygen and copper atom cycles in SOD1 from Cu(II) to Cu(I). Secondly, superoxide is reduced to hydrogen peroxide requiring two protons and copper cycles back to Cu(II) (Valentine, Doucette et al. 2005; Nedeljkovic, Gokce et al. 2003).

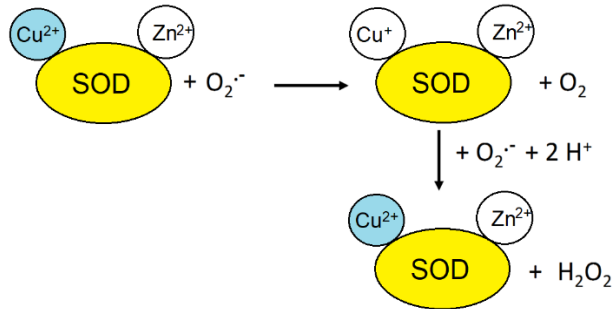


Figure 4. The conversion of the superoxide anion and cycling of the copper in SOD1 from Cu(II) to Cu(I) and back to Cu(II).

Zn(II) does not participate in this reaction but is essential for the structuring of the active site.

The harmful by-product H₂O₂ is in cellular conditions converted by glutathione peroxidase and catalase (hydroperoxidase) into less-reactive molecular oxygen and water molecules (Figure 5) to prevent cellular damage (Mondola, Damiano et al. 2016).

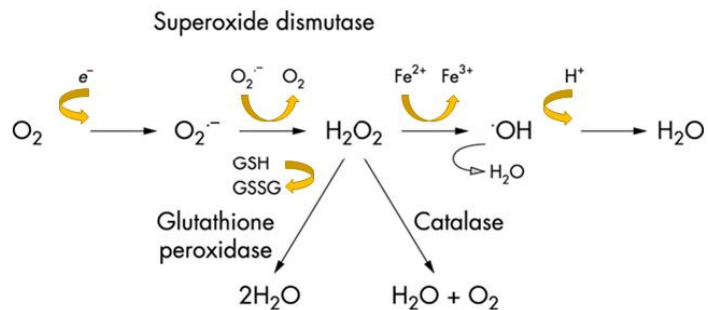


Figure 5. Generation of reactive oxygen species. Molecular oxygen (O₂) reacts with an unpaired electron (e⁻) to form the superoxide anion (O₂•⁻). Superoxide is converted to hydrogen peroxide (H₂O₂) by the enzyme superoxide dismutase. Hydrogen peroxide undergoes metal-catalyzed conversion to the highly reactive hydroxyl radical (•OH). Alternatively, it can be detoxified via either glutathione peroxidase or catalase to water (H₂O) and oxygen (GSH, reduced glutathione; GSSG, oxidized glutathione) (adapted from Nedeljkovic, Gokce et al. 2003).

In addition, SODs play a critical role in inhibiting oxidative inactivation of nitric oxide, thereby preventing peroxynitrite formation and endothelial and mitochondrial dysfunction (Fukai and Ushio-Fukai 2011).

1.3.1 Structure of Human Superoxide Dismutase 1 (SOD1)

The structure of human SOD1 was determined in 1992 (Parge, Hallewell et al. 1992). The amino acid sequence, as well as the structure of SOD1, is highly conserved among eukaryotic species. As was previously mentioned, the human SOD1 is a 32-kDa homodimeric metalloenzyme and each subunit binds one copper ion and one zinc ion (Figure 6). Zn(II) is important for SOD1 structure and stabilization of the entire SOD1 protein (Nedd, Redler et al. 2014). Redox-active Cu is responsible for catalysis (Fetherolf, Boyd et al. 2017; Sirangelo and Iannuzzi 2017).

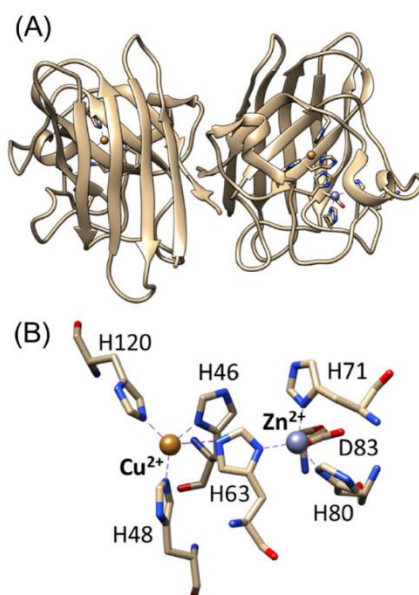


Figure 6. Spatial structure of SOD1 (A) and the structure of its metal-binding site (B). PDBID: 1PU0 (Takahashi, Nagao et al. 2020).

In the monomer, a polypeptide of 153 residues folds into an eight-stranded Greek key β -barrel motif connected by seven loops (Figure 6 A). The active site consists of two structural loops, the zinc loop (loop IV, residues 49–84) and the electrostatic loop (loop VII, residues 122–143), and contains one copper ion and one zinc ion per subunit. The charged residues of the electrostatic loop do not have a catalytic role (Rakhit and Chakrabarty 2006). In contrast, the zinc loop has many residues crucial for the binding of metal ions. Active sites of subunits are located on the opposite sides of the dimer (Furukawa and O'Halloran 2006; Perry, Shin et al. 2010). Metallated SOD1 contains an intra-subunit disulfide bond between two Cys residues. The subunits are held together primarily by hydrophobic interactions with a dissociation constant of $\sim 1.0 \times 10^{-10} \text{ M}^{-1}$ (Furukawa and O'Halloran 2006).

Zn(II) ion is tetrahedrally coordinated to three His residues (His63, His70, His80) and to one Asp residue (Asp83) (Figure 6 B). The copper ion is coordinated according to its oxidation state. Cu(II) is coordinated irregularly by four His residues (His46, His48, His63, His120) (Figure 6 B) while Cu(I) state is coordinated trigonally by three His residues

(His46, His48, and His120). The bridge between Cu(II) and Zn(II) ions is formed by the imidazolate group of His63 and is released upon reduction (Fetherolf, Boyd et al. 2017) (Rakhit and Chakrabartty 2006).

1.3.2 Human Superoxide Dismutase 1 (SOD1) stability and properties

Cu,Zn -SOD1 is an unusual enzyme with many specific properties. For example, SOD1 is quite unique in terms of its stability. As an enzyme it is catalytically active even at 80 °C and the melting point of a protein can exceed 90 °C. In addition, SOD1 is also very resistant to proteolytic digestion (Arnesano, Banci et al. 2004; Furukawa and O'Halloran 2006; Fetherolf, Boyd et al. 2017).

The stability of SOD1 is supported by several structural properties. The backbone β -barrel is a distinctive structural motif of SOD1, which is independent of the presence of metal ions or an intramolecular disulfide bond. Regardless, only a fully metalated and disulfide-oxidized homodimer exhibits such unconventional stability, while the monomeric state exists only before post-translational modifications. A reduction of the intramolecular disulfide bond can also lead to the dissociation of the dimer. However, this bond is very stable and is maintained even in the reducing environment of the cytoplasm. The dimeric state can be restored by adding Zn(II) to the reduced unstable apo-SOD1, which indicates that Zn(II) binding contributes significantly to the stability of SOD1. The thermal stability of SOD1 is also associated with free Cys residues located in the β -barrel strand (Cys6) and another one (Cys111) in a loop region that is accessible to solvents (Valentine, Doucette et al. 2005; Bafana, Dutt et al. 2011; Sirangelo and Iannuzzi 2017).

In the absence of both metal ions, SOD1 produces high and stable amyloid-like protein aggregates under physiological pH and temperature conditions, suggesting that metal binding can play a key protective role against the *in vivo* SOD1 aggregation process (Sirangelo and Iannuzzi 2017). It has been shown that both copper and zinc greatly increase the thermodynamic stability of SOD1 (Lepock, Arnold et al. 1985; Biliaderis, Weselake et al. 1987). Dimer formation reduces the solvent-accessible surface area, greatly increasing the stability of SOD1. Dimerization is also essential to protein functionality (Zhuang, Liu et al. 2014; Arnesano, Banci et al. 2004; Yamazaki and Takao 2008).

Cu,Zn-SOD1 denaturation process could proceed through several various mechanisms. One unfolding pathway involves simultaneous dimer dissociation and zinc release that is followed by a slow conformational change in the protein's core, which, in turn, is followed by rapid copper release (Figure 7) (Mulligan, Kerman et al. 2008). It is suggested that zinc release occurs at the beginning of the denaturation process, whereas copper release is the final event of the denaturation process.

Another Cu,Zn-SOD1 unfolding model suggests that native dimeric SOD1 dissociates to produce a largely folded, metal-bound monomeric intermediate, which then unfolds, releasing copper and zinc simultaneously (Rumfeldt, Stathopoulos et al. 2006).

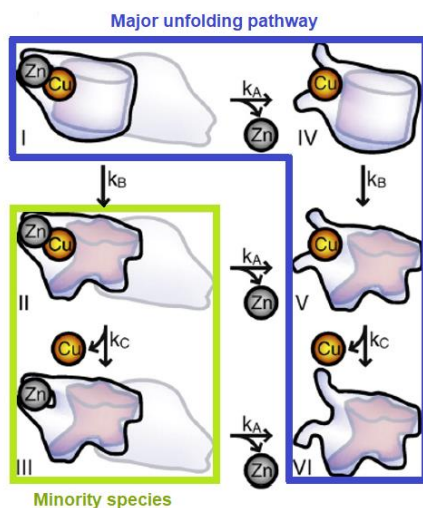


Figure 7. SOD1 denaturation process is characterized by three events: almost simultaneous zinc release and dimer dissociation (k_A), conformational change that affects Trp residue at position 32 (W32), and SOD1 β -barrel (k_B) and copper release (k_C) (adapted from Mulligan, Kerman et al. 2008).

The final level of dissociation depends on the dissociation constant of the Zn(II)–SOD1 complex. The dissociation constant of the complex formed, K_D , is one of the most essential parameters characterizing any biochemical interaction. Despite the obvious importance of SOD1 interaction with Zn(II) and Cu(II) ions, the affinity for the formation of zinc–SOD1 and copper–SOD1 complexes has not been thoroughly studied. We could find only one estimate for the dissociation constant of the Zn(II)–SOD1 complex under mildly denaturing conditions using 6 M guanidine-HCl in the range of 4.2×10^{-14} mM, and for the Cu(II)–SOD1 complex in the range of 6.0×10^{-18} (Crow, Sampson et al. 1997). These results cannot be used for the estimation of metal-binding affinity of Cu,Zn-SOD1 in native conditions, which is needed for the comparison of metal-binding properties of wt and mutated SOD1 forms.

1.3.3 Post-translational maturation of SOD1

The process of the maturation of human SOD1 requires three posttranslational events: acquisition of copper and zinc, formation of the intramolecular disulfide bond, and dimerization (Culotta, Yang et al. 2006; Banci, Barbieri et al. 2011). The copper chaperone for SOD1, CCS, is responsible for copper insertion and disulfide bond formation (Figure 8). CCS is also critical for regulating the localization of SOD1 in cytosol or mitochondria (Kawamata and Manfredi 2010) and is critical for enzymatic activity, folding and maintenance of the native conformation (Ahl, Lindberg et al. 2004).

The human copper chaperone for SOD1 is a three-domain cytoplasmic 29 kDa polypeptide. Two CCS domains (Atx1-like domain 1 and CCS-specific domain 3) bind Cu(I) ions and are responsible for their delivery, whereas domain 3 contributes also to the formation of an intramolecular disulfide bond between Cys57 and Cys146, which is oxygen-dependent. The presence of a disulfide bond is rare for cytosolic proteins taking into account a strongly reducing environment of the cytosol (Brown, Torres et al. 2004). Domain 2 (SOD1-like) is needed for the formation of the heterodimer with SOD1 (Furukawa and O'Halloran 2006). At the protein level, the ratio of SOD1 to CCS in the cytosol ranges between 15- and 30- fold (Rothstein, Dykes-Hoberg et al. 1999), and

because of this, CCS must cycle through the nascent SOD1 pool to activate these molecules (Furukawa and O’Halloran 2006).

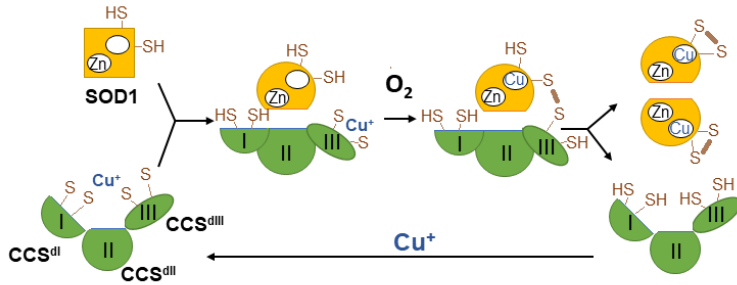


Figure 8. A proposed mechanism of SOD1 activation by CCS. A Cu(I)-bound CCS interacts with a Zn(II)-bound SOD1 lacking a copper ion and a disulfide bond, and O_2 then triggers the introduction of the copper ion and a disulfide bond into SOD1 from CCS (adapted from Furukawa, Shintani et al. 2021).

The last event of the SOD1 maturation is the homo-dimerization, which is strongly dependent on the presence of the metal ions and the disulfide bond.

1.3.4 Amyotrophic lateral sclerosis and ALS-related SOD1 mutations

Amyotrophic lateral sclerosis (ALS), also known as motor neuron disease (MND) or Lou Gehrig’s disease, is a disease that causes the death of neurons controlling voluntary muscles responsible for movement. Voluntary muscles produce movements like chewing, walking, and talking. Currently, there is no cure for ALS and no effective treatment to halt or reverse, the progression of the disease. Early symptoms of ALS usually include muscle weakness or stiffness. Gradually all muscles under voluntary control are affected, and individuals lose their muscle strength and the ability to speak, eat, move, and even breathe (Brown and Al-Chalabi 2017).

ALS is predominantly a sporadic disorder (sALS) and only 5 to 10% of all cases are genetically inherited familial forms (fALS). fALS and sALS are pathologically and clinically very similar, pointing towards a common pathogenic mechanism (Hilton, White et al. 2015) (Zelko, Mariani et al. 2002).

SOD1 has been an object of ALS research since the breakthrough in 1993 when the mutations in the SOD1 gene were found in 11 families with ALS history (Rosen 1993). Today it is known that around 12% of fALS cases are linked to the mutations in the gene encoding SOD1, which is localized to chromosome 21 (Zelko, Mariani et al. 2002). Other ALS-causing mutations are localized in genes like ALS2 (coding for alsin, a guanine nucleotide exchange factor), VAPB (coding for vesicle-associated membrane protein B), and ANG (coding for angiogenin) (Rakhit and Chakrabarty 2006). Cu,Zn-SOD1 mutations have been associated also with 5% of sALS and overall, it is the most common cause of ALS occurring in 2%–10% of all cases. SOD1 mutants are divided into two groups, called wild-type-like and metal-binding region mutants. The properties and metal content of wild-type-like mutants are quite similar to native SOD1, in contrast to the metal-binding region mutants, which are characterized by abnormal metal content (Hayward, Rodriguez et al. 2002; Anzellotti and Farrell 2008; Hilton, White et al. 2015).

The discovery that the mutations in the SOD1 gene were linked to familial ALS was a major achievement in the field of ALS research and in understanding the origin and development of the disease (Rowland and Shneider 2001; Zelko, Mariani et al. 2002;

Tokuda and Furukawa 2016; Fetherolf, Boyd et al. 2017). It has been found that ALS patients and the transgenic mice expressing ALS-related SOD1 mutants have a common feature in their spinal cord: accumulation of SOD1-rich aggregates, however, the mechanisms of SOD1 aggregation and toxicity are still not fully understood. Initially, it was suggested that mutations in the SOD1 gene might lead to a decrease in the antioxidant activity of the enzyme, which may be insufficient to get rid of the superoxide radicals and this, in turn, leads to the toxic accumulation of superoxide. This hypothesis was proven to be false in an experiment where the transgenic mice expressing human fALS mutation G93A developed motor neuron disease regardless of the elevated SOD1 activity (Gurney, Pu et al. 1994).

Later, this hypothesis has been replaced by the gain of toxic function hypothesis, suggesting that SOD1-linked ALS is caused by toxic protein aggregates (Banci, Bertini et al. 2008). This hypothesis is based on the results of studies of human ALS patients and transgenic ALS animal models, in which the accumulation of mutated SOD1-rich protein aggregates has been detected in the spinal cord (Banci, Bertini et al. 2007). Also, it has been demonstrated that different fALS-linked SOD1 mutants form aggregates *in vitro* as well as *in vivo* conditions and that abnormal metal binding plays a critical role in the aggregation of mutant SOD1 *in vivo* suggesting that ALS is a mismetallation disease (Valentine, Doucette et al. 2005; Tiwari, Liba et al. 2009; Sirangelo and Iannuzzi 2017).

The researchers have attempted to reveal the molecular mechanism of SOD1-linked ALS but so far these efforts have remained ineffective. Also, there are no comparative investigations of quantitative metal-binding properties of native SOD1 and ALS-associated mutants, which could make an important contribution to the field of ALS research.

2 Aims of the study

This study aimed to investigate the metal-binding properties of amyloidogenic proteins and in particular:

1. To study the effect of metal ions on the fibrillization of insulin.
2. To determine the affinity of Zn(II) and Cu(II) ions to insulin defined by the dissociation constant, K_D .
3. To investigate the demetallation and the metal-binding affinity of Cu,Zn-SOD1, and its ALS-related G93A mutant by LC-ICP MS.

3 Materials and methods

All used chemical reagents, peptides and proteins are described in publications I, II and III.

Protein fibrillization monitoring by ThT fluorescence (Publication I, II, III).

Calculation of kinetic parameters (Publication I, II, III).

Determination of metal binding affinity of protein (Publication I, II, III).

Determination of the oligomeric composition of protein using size-exclusion chromatography (SEC) (Publication I, III).

Equilibrium dialysis (Publication I).

Atomic absorption spectroscopy (AAS) measurements of metal binding to protein (Publication I).

TEM visualization of fibrils (Publication I).

Preparation of SOD1 protein for experiments (expression and purification) according to the protocol developed by Ahl et al. in 2004 (Publication III).

Inductively coupled plasma mass spectrometry (ICP-MS) analysis of purified proteins (Publication III).

4 Results

Publication I

- It was demonstrated that at pH 7.3 lag phase of the insulin fibrillization curve decreases whereas the fibrillization rate constant increases with rising temperature.
- Investigations of insulin at physiological pH 7.3 in the low concentration range of 2.5–10 μM showed a very slight dependence of fibrillization on the insulin concentration, while at higher protein concentrations the fibrillization rate decreases and the lag phase increases.
- The enthalpy of activation (E_a) of the insulin fibrillization was calculated equal to 84 kJ/mol at physiological pH.
- Size exclusion chromatography and electrospray ionization mass spectrometry studies demonstrated that insulin is prevalently monomeric at a concentration of 2.5 μM .
- K_D value of insulin dimers equal to 18.9 μM was calculated by electrospray ionization mass spectrometry.
- It was shown that the Zn(II) had an inhibitory effect on the monomeric insulin fibrillization at pH 7.3. This effect was achieved by the formation of a soluble Zn(II)-insulin complex with $K_D = 7.5 \mu\text{M}$.
- It was determined that the inhibitory effect of Zn(II) ($IC_{50} = 3.5 \mu\text{M}$) was very strong at pH 7.3.
- It was determined that fibrillization inhibition caused by Zn(II) was much lower at acidic pH 5.5 than at neutral pH 7.3.
- Based on the received results it was proposed the model for the fibrillization and assembling of insulin in the presence of Zn(II) ions.

Publication II

- It was calculated that the dissociation constant value of the monomeric 1 : 1 Zn–insulin complex is equal to 0.40 mM.
- It was shown that the apparent binding affinity decreases drastically at higher insulin concentrations where the peptide forms dimers.
- It was demonstrated that Cu(II) ions also bind to monomeric insulin, whereas the apparent Cu(II)-binding affinity depends on the concentration of HEPES.
- It was determined that the conditional dissociation constant of the Cu(II)–insulin complex is equal to 0.025 mM.

Publication III

- The major focus of the study was directed towards the determination of the metal-binding affinity of wt Cu,Zn-SOD1, and its mutant G93A through competition with high-affinity metal-binding ligands such as EDTA and DTPA. It was demonstrated that none of the ligands was able to demetallate these

proteins at physiological temperatures even at high millimolar concentrations indicating very high metal-binding affinity or the kinetic inertness of Cu,Zn-SOD1.

- It was shown that the release of Zn(II) and Cu(II) ions from Cu,Zn-SOD1, and Cu,Zn-SOD1 G93A mutant at elevated temperatures is cooperative – e.g. release of copper leads to a release of zinc or *vice versa*, thus, it is not possible to determine the affinity of protein towards one of these ions or establish, which ion is released first.
- It was determined that all metal-binding ligands (EDTA, DTPA) accelerated at elevated temperatures the metal release from Cu,Zn-SOD1, and Cu,Zn-SOD1 G93A mutant in a dose-dependent manner, which indicates that ligands should form a ternary complex with Cu,Zn-SOD1 in the activated intermediary state of thermal denaturation.
- It was concluded that there exists no equilibrium between SOD-1 and free metal ions, and metal removal is a part of an irreversible thermal denaturation process.
- It was confirmed that Cu,Zn-SOD1 G93A mutant has a faster metal release as compared with wild-type protein. ΔH^\ddagger values were determined from the Arrhenius plots of the de-coppering in the absence of chelators equal to 173 ± 10 kJ/mol for wt and 191 ± 23 kJ/mol for G93A mutant Cu,Zn-SOD1.
- It was shown that there is no difference in native and G93A mutant Cu,Zn-SOD1 fibrillization kinetics.

5 Discussion

Transition metal ions perform many functions in proteins. First, they act as coenzymes in a large number of biochemical reactions, however, their constitutional and stabilizing role in protein structures is also very important. It is known that some metal ions such as Zn(II) and Cu(II) have a marked effect on the fibrillization of various amyloidogenic peptides and proteins such as amyloid peptide of Alzheimer's disease (Bush, Pettingell et al. 1994), synuclein (Bharathi and Rao 2008), tau protein and prion protein, whereas metal ions can raise or inhibit fibrillization (Tougu, Karafin et al. 2009). It was demonstrated that the oligomerization of insulin is controlled by the protein concentration and strongly influenced by Zn(II), which controls aggregation (Xu, Yan et al. 2012). Fundamentally, the monomeric insulin fibrillization can be also suppressed by metal ions, and its suppression by Zn(II) that is co-secreted with insulin can be physiologically significant.

Insulin fibrillization is physiologically unwanted for many reasons. First, fibrillization excludes monomeric insulin from secretion and keeps it out from interactions with insulin receptors. Secondly, the fibrillization of insulin has an intermediate step of misfolded oligomers and prefibrillar aggregates formation (Nayak, Sorci et al. 2009; Sorci, Grassucci et al. 2009) which consist of approximately 500 or more molecules (Smith, Sharp et al. 2008). These intermediates might be cytotoxic, as demonstrated in case of Alzheimer's amyloid peptides (Walsh and Selkoe 2007) and many other peptides and proteins. If these large misfolded aggregates pass to the circulation, they can be not only cytotoxic, but also immunogenic. Such a situation is possible in the case of insulin.

Insulin fibrillization has been studied for over 60 years; however, most studies have been conducted in non-physiological conditions with Zn(II)-insulin in millimolar concentrations, under acidic conditions and at elevated temperatures where insulin forms fibrils most quickly (Ivanova, Sievers et al. 2009; Brange, Andersen et al. 1997). Zinc-free apo-insulin, which is a therapeutic form of insulin for patients with diabetes mellitus can form fibrils not only at acidic but also at physiologically relevant pH values, especially in the presence of chemical compounds such as urea, ethanol and guanidinium which are capable of dissociating insulin oligomers into monomers (Ahmad, Millett et al. 2004). According to the literature, insulin dimers begin to dissociate when diluted to concentrations below 100 μM (Jeffrey, Milthorpe et al. 1976; Roy, Lee et al. 1990) and it is assumed that insulin at a concentration of 10 μM is essentially monomeric (Nettleton, Tito et al. 2000). The K_D value for insulin dimers determined by static and dynamic laser light scattering is 12.5 μM at pH 7.3 and 25 $^\circ\text{C}$ (Kadima, Ogendal et al. 1993). Insulin is an uncommon exception among amyloidogenic peptides, as its dilution increases the tendency to fibrillate, while high concentrations of the peptide favor fibrillization of other peptides. This behavior demonstrates that oligomer formation inhibits the fibrillization of insulin (Nielsen, Khurana et al. 2001). Therefore, it can be concluded that the fibrillization of the most aggregation-prone form of insulin when the peptide is monomeric and biologically active has not been sufficiently studied.

Our results showed that there is a very weak dependence of insulin fibrillization rate on the protein concentration in the range of 2.5–10 μM , whereas the fibrillization rate decreases and the fibrillization lag time increases at higher insulin concentrations. The inhibition of fibril formation at higher insulin concentrations at physiological pH specifies that the formation of insulin oligomers is an off-pathway process for fibrillization (Noormagi, Gavrilova et al. 2010). Secondly, since the rate constant of fibril

growth at concentrations below 10 μM is constant, it can be concluded that the rate-limiting step of fibril growth is most likely associated with some intramolecular event, such as conformational change. Indeed, the fibrillization of monomeric insulin is characterized by a relatively large E_a value of 84 kJ/mol, which indicates that the formation of a fibrillization-competent structure is accompanied by significant conformational changes (Noormagi, Valmsen et al. 2015). Also, it has been demonstrated that intensive agitation of the insulin solution *in vitro* accelerates the fibrillization of the amyloidogenic peptides and proteins. In the absence of agitation, fibril formation is very slow at neutral pH, which confirms the observation that agitation is important for creating the fibrillization intermediates *in vitro* (Tiiman, Noormagi et al. 2013). This might be the reason why only small amounts of insulin fibrils have been detected after subcutaneous insulin infusion and repeated injections in mice (Storkel, Schneider et al. 1983).

Of the compounds co-released with insulin, only Zn(II) has a pronounced inhibitory effect on the fibrillization of monomeric insulin at pH 7.3. The IC_{50} of 3.5 μM indicates that Zn(II) ions inhibit fibrillization already at low micromolar concentration, and the addition of a 4-fold excess of Zn(II) almost completely suppressed the formation of insulin fibrils. However, our calculations of the Zn-insulin dissociation constant demonstrated that in circulation insulin exists as a free monomer and cannot bind Zn(II) ions due to weak affinity and low concentration of free Zn(II) ions (Gavrilova, Tougu et al. 2014).

The inhibitory effect of Zn(II) ions was much lower at acidic pH 5.5 where 20 μM Zn(II) did not affect the fibrillization rate constant and caused only a slight increase in the lag phase duration.

The pH dependence indicates the involvement of His residue(s) in the Zn(II)-induced inhibition of insulin fibrillization. It is known that the His residue at position B10 which is located in the vicinity of the six-residue B-chain segment (B12–B17), contributes to the formation of cross- β structure (Ivanova, Sievers et al. 2009) and participates in the binding of Zn(II) ions. It can be assumed that the binding of Zn(II) to His10 may prevent the formation of a β -sheet-rich conformation compatible with fibrillization. Thus, the interaction of Zn(II) with monomeric insulin inhibits its fibrillization most likely through differential stabilization of the monomeric ground state over the partially open conformation required for fibrillization.

Insulin is present in the secretory granules at very high concentration reaching 21 mM (Foster, Leapman et al. 1993). Processes, which prevent insulin from the fibrillization in secretory granules are linked to the creation of stable $\text{Zn(II)}_2\text{Insulin}_6$ complexes (in zinc-enriched granules) or formation of insulin oligomers (in zinc-depleted granules). Nevertheless, fibrillization can also occur at insulin release sites, where insulin dissociates into monomers, which are the most fibrillization-prone forms of the peptide. Based on the obtained results, we can suggest that Zn(II) ions co-secreted with insulin from pancreatic β -cells may help to avoid insulin fibrillization at its release sites after hexamer dissociation.

The biological importance of zinc–insulin interaction depends on the biological availability of zinc in pancreatic cells through the activity of the ZnT8 transporter. In secretory vesicles of pancreatic β -cells zinc and insulin concentrations are 11 and 21 mM, respectively (Foster, Leapman et al. 1993). The K_D value for the monomeric Zn(II)–insulin complex equal to 0.40 mM was calculated from our data. In secretory vesicles at high concentrations, insulin is converted into crystalline arrays of hexamers containing two zinc ions, but the main function of zinc ions is not to catalyze the

formation of hexamers, since similar hexamer structures also form in the absence of zinc ions (Lemaire, Ravier et al. 2009). Considering the affinity and content of zinc in pancreatic cells, monomeric insulin may be in the form of a zinc complex. Interestingly, the metal-binding center of insulin is not selective for Zn(II) and it can bind Cu(II) with even higher affinity, but the decisive factor here is metal availability.

The total zinc concentration in plasma is around 11 μM , but the level of labile or exchangeable zinc is much lower. Approximately 28% of the zinc pool in plasma is tightly bound to α_2 -macroglobulin (Zalewski, Truong-Tran et al. 2006). The rest of the zinc is bound to serum albumin, which is present at extremely high concentrations of 0.5–0.75 mM and has two Zn(II)-binding sites characterized by dissociation constant values of 100 nM and ~ 1 mM (Bal, Sokolowska et al. 2013). Thus, albumin can bind all of the labile zinc in serum to its high-affinity sites that are not saturated with zinc ions, and the concentration of free zinc ions is too low to bind to insulin present at subnanomolar (57–280 pM) concentrations (Suckale and Solimena 2008). Accordingly, the predominant form of insulin in circulation is free monomeric insulin interacting with the insulin receptor.

Although insulin therapy was first introduced about 100 years ago, it remains a challenge to inhibit insulin aggregation. Factors like acidic pH (Haas, Vohringer-Martinez et al. 2009), agitation (Sluzky, Tamada et al. 1991; Malik and Roy 2011), elevated temperature (Vilasi, Iannuzzi et al. 2008), contact with hydrophobic surfaces (Nault, Guo et al. 2013), or variation in ionic strength aggravate insulin aggregation (Buell, Hung et al. 2013). There have been many attempts to develop strategies to prevent insulin aggregation. The earliest strategy to inhibit the aggregation of insulin was to facilitate the self-association of insulin by the addition of Zn(II) ions (Hill, Dauter et al. 1991). The addition of Zn(II) ions stabilized the hexameric state of the protein, which had a lower aggregation propensity than the monomer. However, the promotion of the hexameric association of insulin slows down the biological activity of the protein and is undesirable (Das, Shah et al. 2022).

Later attempts to inhibit insulin fibrillization was targeted to nucleation or the elongation step of fibril formation. Recently described insulin aggregation inhibiting molecules include polycyclic aromatic compounds like curcumin and epigallocatechin gallate (EGCG) (Rabiee, Ebrahim-Habibi et al. 2013), which interact with insulin through noncovalent interactions, thereby stabilizing the protein and preventing aggregation (Wang, Dong et al. 2012).

Other insulin fibrillization inhibiting molecules include quinones (Gong, He et al. 2014; Jayamani, Shanmugam et al. 2014), synthetic peptides, KR7 (KPWWPRR-NH₂) and NK9 (NIVNVSLVK) (Banerjee, Kar et al. 2013; Ratha, Ghosh et al. 2016), the fibrillating core from human IAPP (N22FGAIL27, called NL6) and its derivative NFGAXL (NL6X, X = 2-aminobenzoic acid) (Ratha, Kar et al. 2019), supramolecular complexes like cucurbituril (Lee, Choi et al. 2014; Webber, Appel et al. 2016), calixarenes (Shinde, Barooah et al. 2016), and β -cyclodextrins (Kitagawa, Misumi et al. 2015), also a sulfobutylether- β -cyclodextrin (SBE7 β -CD) (Shinde, Khurana et al. 2017) – a water-soluble macrocycle that is capable of breaking mature fibrils to smaller non-toxic species and BSPTPE, consisting of a tetraphenylene moiety functionalized with two sulfonate groups, which inhibited insulin aggregation completely at sub-stoichiometric concentrations (Wang, Wang et al. 2011; Hong, Meng et al. 2012). Other nucleation targeting small molecules include small osmolytes, namely, betaine, citrulline, proline, and sorbitol (Choudhary, Kishore et al. 2015; Patel, Parmar et al. 2018), polyphenol called

rosmarinic acid (Zheng and Lazo 2018), glycoacridine derivatives (Van Vuong, Bednarikova et al. 2015), gelatin (Jayamani and Shanmugam 2016), gallic acid (Jayamani and Shanmugam 2014), the dye methylene blue (MB) (Mukherjee, Jana et al. 2018) and prion derived tetrapeptide, VYYR (named IS1), to effectively inhibit the heat and storage-induced fibrillization of insulin (Mukherjee, Das et al. 2021).

Although there are many small molecules that demonstrated the inhibitory effect on insulin fibrillization, they all were either nonspecific in their action, and affect the activity of other proteins (Rabiee, Ebrahim-Habibi et al. 2013) or prone to proteolytic degradation (Ratha, Kar et al. 2019) or these molecules are relatively insoluble in aqueous solution at room temperature (Wang, Dong et al. 2012; Rabiee, Ebrahim-Habibi et al. 2013) which makes them therapeutically unsuitable (Das, Shah et al. 2022).

Currently, m-cresol and phenol are used as preservatives in insulin formulations to maintain sterility as well as to stabilize the hexameric state of insulin, thereby slowing aggregation. However, prolonged exposure to phenol in insulin injections may result in phenol-based toxicity mainly affecting the central nervous system and inducing dysrhythmia, seizures, and coma (Bode 2011). An alternative to small molecule inhibitors is to generate new insulin analogs with enhanced stability and resistance to aggregation, however, the search has not yielded successful results so far (Das, Shah et al. 2022).

Another important protein whose functions and stability are tightly regulated by zinc and copper ions in human superoxide dismutase (SOD1), which is the main antioxidant defense system against the superoxide anion ($O_2^{\cdot-}$).

Fully metallated SOD1 is a very stable protein. As an enzyme it is catalytically active even at 80°C and the melting point of a protein can exceed 90°C. In the absence of both metal ions, SOD1 forms high and stable amyloid-like protein aggregates under physiological pH and temperature conditions, suggesting that metal binding may play a key protective role in the SOD1 aggregation process *in vivo* (Sirangelo and Iannuzzi 2017).

The focus of the study described in Publication III was to determine the metal-binding affinity of wild-type Cu,Zn-SOD1, and its mutant G93A. This was achieved by competition with high-affinity metal binding ligands such as EDTA and DTPA. The method chosen for protein demetallation monitoring was the LC-ICP MS, which allowed simultaneous and specific detection of the release of copper and zinc ions. It was demonstrated that metal binding affinity and kinetic inertness of Cu,Zn-SOD1 are very high as none of the ligands was able to demetallate these proteins at physiological temperatures even at high millimolar concentrations. At elevated temperatures, Cu(II) and Zn(II) ions were released from the protein simultaneously and the process followed first-order kinetics until complete demetallation.

It was indicated that the rate-limiting step in the metal release of Cu,Zn-SOD1 is the opening of the active site for the ligand as the rate of demetallation depended on the concentration of the ligand, but not on its metal-binding affinity. It was also shown that copper and zinc were released from Cu,Zn-SOD1 simultaneously, so it was not possible to determine the affinity of a protein for one of these ions or to determine which ion is released first. After calculation of activation energies (ΔH) values for Cu-WT equal to 178.2 kJ/mol and Cu-G93A equal to 248.9 kJ/mol from Arrhenius plots, it was indicated that protein conformational changes occur before demetallation, and it confirms that thermal denaturation is indeed the rate-limiting step in a metal release. The calculated activation energies fall within the range of reported values for proteins (Peterson, Eisenthal et al. 2004; Qin, Balasubramanian et al. 2014). We estimated the minimum value of the dissociation constant for Cu,Zn-SOD1, and Cu,Zn-SOD1 (G93A) mutant is in

the range of 10^{-17} M. The difference in the calculated dissociation rate constants between native and mutant Cu,Zn-SOD1 is very small, which, cannot affect the functioning of the enzyme. We also compared the fibrillization of Cu,Zn-SOD1 and its G93A mutant at 40 °C and found that fibrillization of both forms of SOD1 occurs according to a very similar sigmoidal curve, thus, there are no differences in the fibrillization propensity of these fully metallated protein forms.

Zinc-depleted SOD-1 is known to induce neurodegeneration in a transgenic mouse model with an increased propensity for fibrillization (Estevez, Spear et al. 1998; Estevez, Sampson et al. 2000). Some investigations indicate that zinc supplementation protects from ALS-associated SOD toxicity as was demonstrated in the example of transgenic mice carrying SOD with a G93A ALS mutation (Ermilova, Ermilov et al. 2005). These results together with our data allowed us to conclude that toxicity may be related to incomplete metalation of G93A SOD as compared to wild-type Cu,Zn-SOD1.

The results of this work confirm that metal binding plays a very important and protective role in the the protein aggregation process and shed some light to the details of the particular mechanisms in the case of insulin and SOD. The correct concentration of metals in the blood is very important as it is known that both excess and lack of free metals are toxic to mammalian cells and can lead to neurodegenerative diseases. It is important to conduct more research to reveal the molecular mechanisms of misfolded proteins-connected diseases and the role of metal ions in them. Further investigations about quantitative metal-binding properties of disease-associated proteins could make an important contribution to the field.

6 Conclusions

- Fibrillization of insulin at physiological pH values demonstrates an unexpected concentration dependence: it depends only slightly on the insulin concentration below 10 μM , whereas above 10 μM the fibrillization is inhibited: the fibrillization rate decreases and lag time increases. This indicates that insulin oligomers suppress fibrillization (Publication I).
- The interaction of monomeric insulin with Zn(II) causes the inhibition of its fibrillization due to differential stabilization of the monomeric ground state over the partially open conformation that is necessary for fibrillization. Zn(II) ions co-secreted with monomeric insulin might prevent its fibrillization at the release sites at physiological pH values (Publication I).
- Insulin monomers bind Zn(II) ions with a dissociation constant of 0.40 mM and Cu(II) ions with a conditional dissociation constant of 0.025 mM. In secretory granules, insulin is in complex with zinc ions, whereas in circulation it exists as a free monomer (Publication II).
- The release of metal ions from Cu,Zn-SOD1, and its G93A mutant is at elevated temperatures cooperative, which means that the release of copper leads to a release of zinc or *vice versa* (Publication III).
- There exists no equilibrium between SOD-1 and free metal ions and metal removal is a part of an irreversible thermodenaturation process (Publication III).
- Cu,Zn-SOD1 G93A mutant has slightly faster metal release as compared to the wild-type protein both in the presence and absence of metal chelators, which indicates that mutation of distant G93 residue affects metal-binding properties of the enzyme. The fibrillization of both forms of SOD1 was similar (Publication III).

References

- (2017). "IDF releases report of global survey on access to medicines and supplies for people with diabetes." *Diabetes Res Clin Pract* **129**: 224-225.
- Adams, M. J., T. L. Blundell, et al. (1969). "Structure of Rhombohedral 2 Zinc Insulin Crystals." *Nature* **224**(5218): 491-495.
- Ahl, I. M., M. J. Lindberg, et al. (2004). "Coexpression of yeast copper chaperone (yCCS) and CuZn-superoxide dismutases in Escherichia coli yields protein with high copper contents." *Protein Expr Purif* **37**(2): 311-319.
- Ahmad, A., I. S. Millett, et al. (2004). "Stimulation of insulin fibrillation by urea-induced intermediates." *J Biol Chem* **279**(15): 14999-15013.
- Ahmad, A., V. N. Uversky, et al. (2005). "Early events in the fibrillation of monomeric insulin." *J Biol Chem* **280**(52): 42669-42675.
- Akbarian, M., Y. Ghasemi, et al. (2018). "Chemical modifications of insulin: Finding a compromise between stability and pharmaceutical performance." *Int J Pharm* **547**(1-2): 450-468.
- Akbarian, M., R. Yousefi, et al. (2020). "Insulin fibrillation: toward strategies for attenuating the process." *Chem Commun (Camb)* **56**(77): 11354-11373.
- Alberti, K. G. and P. Z. Zimmet (1998). "Definition, diagnosis and classification of diabetes mellitus and its complications. Part 1: diagnosis and classification of diabetes mellitus provisional report of a WHO consultation." *Diabet Med* **15**(7): 539-553.
- Anzellotti, A. I. and N. P. Farrell (2008). "Zinc metalloproteins as medicinal targets." *Chem Soc Rev* **37**(8): 1629-1651.
- Arnesano, F., L. Banci, et al. (2004). "The unusually stable quaternary structure of human Cu,Zn-superoxide dismutase 1 is controlled by both metal occupancy and disulfide status." *J Biol Chem* **279**(46): 47998-48003.
- Bafana, A., S. Dutt, et al. (2011). "Superoxide dismutase: an industrial perspective." *Crit Rev Biotechnol* **31**(1): 65-76.
- Baker, E. N., T. L. Blundell, et al. (1988). "The structure of 2Zn pig insulin crystals at 1.5 Å resolution." *Philos Trans R Soc Lond B Biol Sci* **319**(1195): 369-456.
- Bal, W., M. Sokolowska, et al. (2013). "Binding of transition metal ions to albumin: sites, affinities and rates." *Biochim Biophys Acta* **1830**(12): 5444-5455.
- Banci, L., L. Barbieri, et al. (2011). "In-cell NMR in E. coli to monitor maturation steps of hSOD1." *PLoS One* **6**(8): e23561.
- Banci, L., I. Bertini, et al. (2008). "SOD1 and amyotrophic lateral sclerosis: mutations and oligomerization." *PLoS One* **3**(2): e1677.
- Banci, L., I. Bertini, et al. (2007). "Metal-free superoxide dismutase forms soluble oligomers under physiological conditions: a possible general mechanism for familial ALS." *Proc Natl Acad Sci U S A* **104**(27): 11263-11267.
- Banerjee, V., R. K. Kar, et al. (2013). "Use of a small peptide fragment as an inhibitor of insulin fibrillation process: a study by high and low resolution spectroscopy." *PLoS One* **8**(8): e72318.
- Beckman, J. S., A. G. Estevez, et al. (2001). "Superoxide dismutase and the death of motoneurons in ALS." *Trends Neurosci* **24**(11 Suppl): S15-20.
- Bellomo, E. A., G. Meur, et al. (2011). "Glucose regulates free cytosolic Zn(2)(+) concentration, Slc39 (ZiP), and metallothionein gene expression in primary pancreatic islet beta-cells." *J Biol Chem* **286**(29): 25778-25789.

- Berg, J. M. (1987). "Metal ions in proteins: structural and functional roles." Cold Spring Harb Symp Quant Biol **52**: 579-585.
- Berg, J. M. and Y. Shi (1996). "The galvanization of biology: a growing appreciation for the roles of zinc." Science **271**(5252): 1081-1085.
- Bharathi and K. S. Rao (2008). "Molecular understanding of copper and iron interaction with alpha-synuclein by fluorescence analysis." J Mol Neurosci **35**(3): 273-281.
- Biliaderis, C. G., R. J. Weselake, et al. (1987). "A calorimetric study of human CuZn superoxide dismutase." Biochem J **248**(3): 981-984.
- Bocian, W., J. Sitkowski, et al. (2008). "Direct insight into insulin aggregation by 2D NMR complemented by PFGSE NMR." Proteins **71**(3): 1057-1065.
- Bode, B. W. (2011). "Comparison of pharmacokinetic properties, physicochemical stability, and pump compatibility of 3 rapid-acting insulin analogues-aspart, lispro, and glulisine." Endocr Pract **17**(2): 271-280.
- Brange, J., L. Andersen, et al. (1997). "Toward understanding insulin fibrillation." J Pharm Sci **86**(5): 517-525.
- Brange, J., L. Langkjaer, et al. (1992). "Chemical stability of insulin. 1. Hydrolytic degradation during storage of pharmaceutical preparations." Pharm Res **9**(6): 715-726.
- Brange, J., D. R. Owens, et al. (1990). "Monomeric insulins and their experimental and clinical implications." Diabetes Care **13**(9): 923-954.
- Brown, R. H. and A. Al-Chalabi (2017). "Amyotrophic Lateral Sclerosis." N Engl J Med **377**(2): 162-172.
- Buell, A. K., P. Hung, et al. (2013). "Electrostatic effects in filamentous protein aggregation." Biophys J **104**(5): 1116-1126.
- Bush, A. I., W. H. Pettingell, et al. (1994). "Rapid induction of Alzheimer A beta amyloid formation by zinc." Science **265**(5177): 1464-1467.
- Chausmer, A. B. (1998). "Zinc, insulin and diabetes." J Am Coll Nutr **17**(2): 109-115.
- Chausmer, A. B. (1998). "Zinc, insulin and diabetes." Journal of the American College of Nutrition **17**(2): 109-115.
- Cherny, R. A., C. S. Atwood, et al. (2001). "Treatment with a copper-zinc chelator markedly and rapidly inhibits beta-amyloid accumulation in Alzheimer's disease transgenic mice." Neuron **30**(3): 665-676.
- Chimienti, F. (2013). "Zinc, pancreatic islet cell function and diabetes: new insights into an old story." Nutr Res Rev **26**(1): 1-11.
- Chimienti, F., S. Devergnas, et al. (2006). "In vivo expression and functional characterization of the zinc transporter ZnT8 in glucose-induced insulin secretion." J Cell Sci **119**(Pt 20): 4199-4206.
- Chimienti, F., A. Favier, et al. (2005). "ZnT-8, a pancreatic beta-cell-specific zinc transporter." Biomaterials **18**(4): 313-317.
- Choudhary, S., N. Kishore, et al. (2015). "Inhibition of insulin fibrillation by osmolytes: Mechanistic insights." Sci Rep **5**: 17599.
- Crow, J. P., J. B. Sampson, et al. (1997). "Decreased zinc affinity of amyotrophic lateral sclerosis-associated superoxide dismutase mutants leads to enhanced catalysis of tyrosine nitration by peroxynitrite." J Neurochem **69**(5): 1936-1944.
- Culotta, V. C., M. Yang, et al. (2006). "Activation of superoxide dismutases: putting the metal to the pedal." Biochim Biophys Acta **1763**(7): 747-758.
- Das, A., M. Shah, et al. (2022). "Molecular Aspects of Insulin Aggregation and Various Therapeutic Interventions." ACS Bio & Med Chem Au.

- Davidson, H. W. (2004). "(Pro)Insulin processing: a historical perspective." Cell Biochem Biophys **40**(3 Suppl): 143-158.
- del Pozo-Yauner, L., J. S. Wall, et al. (2014). "The N-terminal strand modulates immunoglobulin light chain fibrillogenesis." Biochem Biophys Res Commun **443**(2): 495-499.
- Ermilova, I. P., V. B. Ermilov, et al. (2005). "Protection by dietary zinc in ALS mutant G93A SOD transgenic mice." Neurosci Lett **379**(1): 42-46.
- Estevez, A. G., J. B. Sampson, et al. (2000). "Liposome-delivered superoxide dismutase prevents nitric oxide-dependent motor neuron death induced by trophic factor withdrawal." Free Radic Biol Med **28**(3): 437-446.
- Estevez, A. G., N. Spear, et al. (1998). „Nitric oxide and superoxide contribute to motor neuron apoptosis induced by trophic factor deprivation." J Neurosci **18**(3): 923-931.
- Fetherolf, M. M., S. D. Boyd, et al. (2017). "Copper-zinc superoxide dismutase is activated through a sulfenic acid intermediate at a copper ion entry site." J Biol Chem **292**(29): 12025-12040.
- Fodera, V., F. Librizzi, et al. (2008). "Secondary nucleation and accessible surface in insulin amyloid fibril formation." J Phys Chem B **112**(12): 3853-3858.
- Foster, M. C., R. D. Leapman, et al. (1993). "Elemental composition of secretory granules in pancreatic islets of Langerhans." Biophys J **64**(2): 525-532.
- Frankaer, C. G., M. V. Knudsen, et al. (2012). "The structures of T6, T3R3 and R6 bovine insulin: combining X-ray diffraction and absorption spectroscopy." Acta Crystallogr D Biol Crystallogr **68**(Pt 10): 1259-1271.
- Frankaer, C. G., P. Sonderby, et al. (2017). "Insulin fibrillation: The influence and coordination of Zn(2)." J Struct Biol **199**(1): 27-38.
- Frederickson, C. J., J. Y. Koh, et al. (2005). "The neurobiology of zinc in health and disease." Nat Rev Neurosci **6**(6): 449-462.
- Fukai, T. and M. Ushio-Fukai (2011). "Superoxide dismutases: role in redox signaling, vascular function, and diseases." Antioxid Redox Signal **15**(6): 1583-1606.
- Furukawa, Y. and T. V. O'Halloran (2006). "Posttranslational modifications in Cu,Zn-superoxide dismutase and mutations associated with amyotrophic lateral sclerosis." Antioxid Redox Signal **8**(5-6): 847-867.
- Furukawa, Y., A. Shintani, et al. (2021). "A dual role of cysteine residues in the maturation of prokaryotic Cu/Zn-superoxide dismutase." Metallomics **13**(9).
- Gavrilova, J., V. Tougu, et al. (2014). "Affinity of zinc and copper ions for insulin monomers." Metallomics **6**(7): 1296-1300.
- Glusker, J. P. (1991). "Structural aspects of metal liganding to functional groups in proteins." Adv Protein Chem **42**: 1-76.
- Gong, H., Z. He, et al. (2014). "Effects of several quinones on insulin aggregation." Sci Rep **4**: 5648.
- Grant, P. T., T. L. Coombs, et al. (1972). "Differences in the nature of the interaction of insulin and proinsulin with zinc." Biochem J **126**(2): 433-440.
- Grodsky, G. M. and F. Schmid-Formby (1985). "Kinetic and quantitative relationships between insulin release and 65Zn efflux from perfused islets." Endocrinology **117**(2): 704-710.
- Gupta, A. and S. Lutsenko (2009). "Human copper transporters: mechanism, role in human diseases and therapeutic potential." Future Med Chem **1**(6): 1125-1142.

- Gurney, M. E., H. Pu, et al. (1994). "Motor neuron degeneration in mice that express a human Cu,Zn superoxide dismutase mutation." Science **264**(5166): 1772-1775.
- Haas, J., E. Vohringer-Martinez, et al. (2009). "Primary steps of pH-dependent insulin aggregation kinetics are governed by conformational flexibility." Chembiochem **10**(11): 1816-1822.
- Hayward, L. J., J. A. Rodriguez, et al. (2002). "Decreased metallation and activity in subsets of mutant superoxide dismutases associated with familial amyotrophic lateral sclerosis." J Biol Chem **277**(18): 15923-15931.
- Hill, C. P., Z. Dauter, et al. (1991). "X-ray structure of an unusual Ca²⁺ site and the roles of Zn²⁺ and Ca²⁺ in the assembly, stability, and storage of the insulin hexamer." Biochemistry **30**(4): 917-924.
- Hilton, J. B., A. R. White, et al. (2015). "Metal-deficient SOD1 in amyotrophic lateral sclerosis." J Mol Med (Berl) **93**(5): 481-487.
- Hong, D. P. and A. L. Fink (2005). "Independent heterologous fibrillation of insulin and its B-chain peptide." Biochemistry **44**(50): 16701-16709.
- Hong, Y., L. Meng, et al. (2012). "Monitoring and inhibition of insulin fibrillation by a small organic fluorogen with aggregation-induced emission characteristics." J Am Chem Soc **134**(3): 1680-1689.
- Hua, Q. (2010). "Insulin: a small protein with a long journey." Protein Cell **1**(6): 537-551.
- Hutton, M. (1983). "The effects of environmental lead exposure and in vitro zinc on tissue delta-aminolevulinic acid dehydratase in urban pigeons." Comp Biochem Physiol C **74**(2): 441-446.
- Islam, M. S. and T. Loots du (2007). "Diabetes, metallothionein, and zinc interactions: a review." Biofactors **29**(4): 203-212.
- Ivanova, M. I., S. A. Sievers, et al. (2009). "Molecular basis for insulin fibril assembly." Proc Natl Acad Sci U S A **106**(45): 18990-18995.
- Jayamani, J. and G. Shanmugam (2014). "Gallic acid, one of the components in many plant tissues, is a potential inhibitor for insulin amyloid fibril formation." Eur J Med Chem **85**: 352-358.
- Jayamani, J. and G. Shanmugam (2016). "Gelatin as a Potential Inhibitor of Insulin Amyloid Fibril Formation." ChemistrySelect **1**(15): 4463-4471.
- Jayamani, J., G. Shanmugam, et al. (2014). "Inhibition of insulin amyloid fibril formation by ferulic acid, a natural compound found in many vegetables and fruits." RSC Advances **4**(107): 62326-62336.
- Jeffrey, P. D., B. K. Milthorpe, et al. (1976). "Polymerization pattern of insulin at pH 7.0." Biochemistry **15**(21): 4660-4665.
- Johnson, W. T. and C. M. Anderson (2008). "Cardiac cytochrome C oxidase activity and contents of subunits 1 and 4 are altered in offspring by low prenatal copper intake by rat dams." J Nutr **138**(7): 1269-1273.
- Kadima, W., L. Ogendal, et al. (1993). "The influence of ionic strength and pH on the aggregation properties of zinc-free insulin studied by static and dynamic laser light scattering." Biopolymers **33**(11): 1643-1657.
- Kawamata, H. and G. Manfredi (2010). "Import, maturation, and function of SOD1 and its copper chaperone CCS in the mitochondrial intermembrane space." Antioxid Redox Signal **13**(9): 1375-1384.
- Kitagawa, K., Y. Misumi, et al. (2015). "Inhibition of insulin amyloid fibril formation by cyclodextrins." Amyloid **22**(3): 181-186.

- Klostermeyer, H. and R. E. Humbel (1966). "The chemistry and biochemistry of insulin." Angew Chem Int Ed Engl **5**(9): 807-822.
- Kosinova, L., V. Veverka, et al. (2014). "Insight into the structural and biological relevance of the T/R transition of the N-terminus of the B-chain in human insulin." Biochemistry **53**(21): 3392-3402.
- Krebs, M. R., C. E. Macphee, et al. (2004). "The formation of spherulites by amyloid fibrils of bovine insulin." Proc Natl Acad Sci U S A **101**(40): 14420-14424.
- Landreh, M., G. Alvelius, et al. (2014). "Insulin, islet amyloid polypeptide and C-peptide interactions evaluated by mass spectrometric analysis." Rapid Commun Mass Spectrom **28**(2): 178-184.
- Lee, D. K., J. Geiser, et al. (2003). "Pancreatic metallothionein-I may play a role in zinc homeostasis during maternal dietary zinc deficiency in mice." J Nutr **133**(1): 45-50.
- Lee, H. H., T. S. Choi, et al. (2014). "Supramolecular inhibition of amyloid fibrillation by cucurbit[7]uril." Angew Chem Int Ed Engl **53**(29): 7461-7465.
- Lemaire, K., M. A. Ravier, et al. (2009). "Insulin crystallization depends on zinc transporter ZnT8 expression, but is not required for normal glucose homeostasis in mice." Proc Natl Acad Sci U S A **106**(35): 14872-14877.
- Lemaire, K., M. A. Ravier, et al. (2009). "Insulin crystallization depends on zinc transporter ZnT8 expression, but is not required for normal glucose homeostasis in mice." Proc Natl Acad Sci U S A.
- Lepock, J. R., L. D. Arnold, et al. (1985). "Structural analyses of various Cu²⁺, Zn²⁺-superoxide dismutases by differential scanning calorimetry and Raman spectroscopy." Arch Biochem Biophys **241**(1): 243-251.
- Levadoux, M., C. Mahon, et al. (1999). "Nuclear import of metallothionein requires its mRNA to be associated with the perinuclear cytoskeleton." J Biol Chem **274**(49): 34961-34966.
- Li, Y. V. (2013). "Zinc and insulin in pancreatic beta-cells." Endocrine **45**(2): 178-189.
- Lim, C. M., M. A. Cater, et al. (2006). "Copper-dependent interaction of dynactin subunit p62 with the N terminus of ATP7B but not ATP7A." J Biol Chem **281**(20): 14006-14014.
- Linder, M. C. and M. Hazegh-Azam (1996). "Copper biochemistry and molecular biology." Am J Clin Nutr **63**(5): 797S-811S.
- Liu, M., J. Wright, et al. (2014). "Proinsulin entry and transit through the endoplasmic reticulum in pancreatic beta cells." Vitam Horm **95**: 35-62.
- MacDonald, R. S. (2000). "The role of zinc in growth and cell proliferation." J Nutr **130**(5S Suppl): 1500S-1508S.
- Malik, R. and I. Roy (2011). "Probing the mechanism of insulin aggregation during agitation." Int J Pharm **413**(1-2): 73-80.
- Maret, W. (2011). "Redox biochemistry of mammalian metallothioneins." J Biol Inorg Chem **16**(7): 1079-1086.
- Maret, W. and H. H. Sandstead (2006). "Zinc requirements and the risks and benefits of zinc supplementation." J Trace Elem Med Biol **20**(1): 3-18.
- McCall, K. A., C. Huang, et al. (2000). "Function and mechanism of zinc metalloenzymes." J Nutr **130**(5S Suppl): 1437S-1446S.
- McCord, J. M. and I. Fridovich (1969). "Superoxide dismutase. An enzymic function for erythrocyte (hemocuprein)." J Biol Chem **244**(22): 6049-6055.

- Mondola, P., S. Damiano, et al. (2016). "The Cu, Zn Superoxide Dismutase: Not Only a Dismutase Enzyme." Front Physiol **7**: 594.
- Mounicou, S., J. Szpunar, et al. (2009). "Metalloomics: the concept and methodology." Chem Soc Rev **38**(4): 1119-1138.
- Mukherjee, M., D. Das, et al. (2021). "Prion-derived tetrapeptide stabilizes thermolabile insulin via conformational trapping." iScience **24**(6): 102573.
- Mukherjee, M., J. Jana, et al. (2018). "A Small Molecule Impedes Insulin Fibrillation: Another New Role of Phenothiazine Derivatives." ChemistryOpen **7**(1): 68-79.
- Mulligan, V. K., A. Kerman, et al. (2008). "Denaturational stress induces formation of zinc-deficient monomers of Cu,Zn superoxide dismutase: implications for pathogenesis in amyotrophic lateral sclerosis." J Mol Biol **383**(2): 424-436.
- Nault, L., P. Guo, et al. (2013). "Human insulin adsorption kinetics, conformational changes and amyloid aggregate formation on hydrophobic surfaces." Acta Biomater **9**(2): 5070-5079.
- Nayak, A., A. K. Dutta, et al. (2008). "Surface-enhanced nucleation of insulin amyloid fibrillation." Biochem Biophys Res Commun **369**(2): 303-307.
- Nayak, A., M. Sorci, et al. (2009). "A universal pathway for amyloid nucleus and precursor formation for insulin." Proteins **74**(3): 556-565.
- Nedeljkovic, Z. S., N. Gokce, et al. (2003). "Mechanisms of oxidative stress and vascular dysfunction." Postgrad Med J **79**(930): 195-199; quiz 198-200.
- Nelson, K. T. and J. R. Prohaska (2009). "Copper deficiency in rodents alters dopamine beta-mono-oxygenase activity, mRNA and protein level." Br J Nutr **102**(1): 18-28.
- Nettleton, E. J., P. Tito, et al. (2000). "Characterization of the oligomeric states of insulin in self-assembly and amyloid fibril formation by mass spectrometry." Biophys J **79**(2): 1053-1065.
- Nielsen, L., R. Khurana, et al. (2001). "Effect of environmental factors on the kinetics of insulin fibril formation: elucidation of the molecular mechanism." Biochemistry **40**(20): 6036-6046.
- Noormagi, A., J. GavriloVA, et al. (2010). "Zn(II) ions co-secreted with insulin suppress inherent amyloidogenic properties of monomeric insulin." Biochem J **430**(3): 511-518.
- Noormagi, A., K. Valmsen, et al. (2015). "Insulin Fibrillization at Acidic and Physiological pH Values is Controlled by Different Molecular Mechanisms." Protein J **34**(6): 398-403.
- Outten, C. E. and T. V. O'Halloran (2001). "Femtomolar sensitivity of metalloregulatory proteins controlling zinc homeostasis." Science **292**(5526): 2488-2492.
- Patel, P., K. Parmar, et al. (2018). "Inhibition of insulin amyloid fibrillation by Morin hydrate." Int J Biol Macromol **108**: 225-239.
- Perry, J. J., D. S. Shin, et al. (2010). "The structural biochemistry of the superoxide dismutases." Biochim Biophys Acta **1804**(2): 245-262.
- Peterson, M. E., R. Eienthal, et al. (2004). "A new intrinsic thermal parameter for enzymes reveals true temperature optima." J Biol Chem **279**(20): 20717-20722.
- Pohl, R., R. Hauser, et al. (2012). "Ultra-rapid absorption of recombinant human insulin induced by zinc chelation and surface charge masking." J Diabetes Sci Technol **6**(4): 755-763.

- Qin, Z., S. K. Balasubramanian, et al. (2014). "Correlated parameter fit of arrhenius model for thermal denaturation of proteins and cells." Ann Biomed Eng **42**(12): 2392-2404.
- Quinn, R. and J. D. Andrade (1983). "Minimizing the aggregation of neutral insulin solutions." J Pharm Sci **72**(12): 1472-1473.
- Rabiee, A., A. Ebrahim-Habibi, et al. (2013). "How curcumin affords effective protection against amyloid fibrillation in insulin." Food Funct **4**(10): 1474-1480.
- Rae, T. D., P. J. Schmidt, et al. (1999). "Undetectable intracellular free copper: the requirement of a copper chaperone for superoxide dismutase." Science **284**(5415): 805-808.
- Rakhit, R. and A. Chakrabartty (2006). "Structure, folding, and misfolding of Cu,Zn superoxide dismutase in amyotrophic lateral sclerosis." Biochim Biophys Acta **1762**(11-12): 1025-1037.
- Ratha, B. N., A. Ghosh, et al. (2016). "Inhibition of Insulin Amyloid Fibrillation by a Novel Amphipathic Heptapeptide: MECHANISTIC DETAILS STUDIED BY SPECTROSCOPY IN COMBINATION WITH MICROSCOPY." J Biol Chem **291**(45): 23545-23556.
- Ratha, B. N., R. K. Kar, et al. (2019). "Sequence specificity of amylin-insulin interaction: a fragment-based insulin fibrillation inhibition study." Biochim Biophys Acta Proteins Proteom **1867**(4): 405-415.
- Rosen, D. R. (1993). "Mutations in Cu/Zn superoxide dismutase gene are associated with familial amyotrophic lateral sclerosis." Nature **364**(6435): 362.
- Rothstein, J. D., M. Dykes-Hoberg, et al. (1999). "The copper chaperone CCS is abundant in neurons and astrocytes in human and rodent brain." J Neurochem **72**(1): 422-429.
- Rowland, L. P. and N. A. Shneider (2001). "Amyotrophic lateral sclerosis." N Engl J Med **344**(22): 1688-1700.
- Roy, M., R. W. Lee, et al. (1990). "1H NMR spectrum of the native human insulin monomer. Evidence for conformational differences between the monomer and aggregated forms." J Biol Chem **265**(10): 5448-5452.
- Rumfeldt, J. A., P. B. Stathopoulos, et al. (2006). "Mechanism and thermodynamics of guanidinium chloride-induced denaturation of ALS-associated mutant Cu,Zn superoxide dismutases." J Mol Biol **355**(1): 106-123.
- Scott, D. A. (1934). "Crystalline insulin." Biochem J **28**(4): 1592-1602 1591.
- Scott, D. A. and A. M. Fisher (1938). "The Insulin and the Zinc Content of Normal and Diabetic Pancreas." J Clin Invest **17**(6): 725-728.
- Sekler, I., S. L. Sensi, et al. (2007). "Mechanism and regulation of cellular zinc transport." Mol Med **13**(7-8): 337-343.
- Shepherd, P. R. and B. B. Kahn (1999). "Glucose transporters and insulin action--implications for insulin resistance and diabetes mellitus." N Engl J Med **341**(4): 248-257.
- Shinde, M. N., N. Barooah, et al. (2016). "Inhibition and disintegration of insulin amyloid fibrils: a facile supramolecular strategy with p-sulfonatocalixarenes." Chem Commun (Camb) **52**(14): 2992-2995.
- Shinde, M. N., R. Khurana, et al. (2017). "Sulfobutylether- β -Cyclodextrin for Inhibition and Rupture of Amyloid Fibrils." The Journal of Physical Chemistry C **121**(36): 20057-20065.

- Sirangelo, I. and C. Iannuzzi (2017). "The Role of Metal Binding in the Amyotrophic Lateral Sclerosis-Related Aggregation of Copper-Zinc Superoxide Dismutase." Molecules **22**(9).
- Slepchenko, K. G. and Y. V. Li (2012). "Rising intracellular zinc by membrane depolarization and glucose in insulin-secreting clonal HIT-T15 beta cells." Exp Diabetes Res **2012**: 190309.
- Sluzky, V., J. A. Tamada, et al. (1991). "Kinetics of insulin aggregation in aqueous solutions upon agitation in the presence of hydrophobic surfaces." Proc Natl Acad Sci U S A **88**(21): 9377-9381.
- Smith, M. I., J. S. Sharp, et al. (2008). "Insulin fibril nucleation: the role of prefibrillar aggregates." Biophys J **95**(7): 3400-3406.
- Sorci, M., R. A. Grassucci, et al. (2009). "Time-dependent insulin oligomer reaction pathway prior to fibril formation: cooling and seeding." Proteins **77**(1): 62-73.
- Steensgaard, D. B., G. Schluckebier, et al. (2013). "Ligand-controlled assembly of hexamers, dihexamers, and linear multihexamer structures by the engineered acylated insulin degludec." Biochemistry **52**(2): 295-309.
- Storkel, S., H. M. Schneider, et al. (1983). "Iatrogenic, insulin-dependent, local amyloidosis." Lab Invest **48**(1): 108-111.
- Strehlow, H. (1978). "G. Milazzo and S. Carioli: Tables of Standard Electrode Potentials. John Wiley and Sons Ltd., Chichester, New York, Brisbane, Toronto 1978. XVI + 419 Seiten. Preis: £ 17,50." Berichte der Bunsengesellschaft für physikalische Chemie **82**(10): 1114-1114.
- Suckale, J. and M. Solimena (2008). "Pancreas islets in metabolic signaling--focus on the beta-cell." Front Biosci **13**: 7156-7171.
- Swart, C. (2013). "Metrology for metalloproteins--where are we now, where are we heading?" Anal Bioanal Chem **405**(17): 5697-5723.
- Zalewski, P., A. Truong-Tran, et al. (2006). "Use of a zinc fluorophore to measure labile pools of zinc in body fluids and cell-conditioned media." Biotechniques **40**(4): 509-520.
- Zalewski, P. D., S. H. Millard, et al. (1994). "Video image analysis of labile zinc in viable pancreatic islet cells using a specific fluorescent probe for zinc." J Histochem Cytochem **42**(7): 877-884.
- Zelko, I. N., T. J. Mariani, et al. (2002). "Superoxide dismutase multigene family: a comparison of the CuZn-SOD (SOD1), Mn-SOD (SOD2), and EC-SOD (SOD3) gene structures, evolution, and expression." Free Radic Biol Med **33**(3): 337-349.
- Zheng, Q. and N. D. Lazo (2018). "Mechanistic Studies of the Inhibition of Insulin Fibril Formation by Rosmarinic Acid." J Phys Chem B **122**(8): 2323-2331.
- Zhuang, X., S. Liu, et al. (2014). "Identification of unfolding and dissociation pathways of superoxide dismutase in the gas phase by ion-mobility separation and tandem mass spectrometry." Anal Chem **86**(23): 11599-11605.
- Takahashi, A., C. Nagao, et al. (2020). "Effects of molecular crowding environment on the acquisition of toxic properties of wild-type SOD1." Biochim Biophys Acta Gen Subj **1864**(2): 129401.
- Tepaamordech, S., C. P. Kirschke, et al. (2016). "Zinc transporter 7 deficiency affects lipid synthesis in adipocytes by inhibiting insulin-dependent Akt activation and glucose uptake." FEBS J **283**(2): 378-394.

- Tiiman, A., A. Noormagi, et al. (2013). "Effect of agitation on the peptide fibrillization: Alzheimer's amyloid-beta peptide 1-42 but not amylin and insulin fibrils can grow under quiescent conditions." J Pept Sci **19**(6): 386-391.
- Tiwari, A., A. Liba, et al. (2009). "Metal deficiency increases aberrant hydrophobicity of mutant superoxide dismutases that cause amyotrophic lateral sclerosis." J Biol Chem **284**(40): 27746-27758.
- Tokuda, E. and Y. Furukawa (2016). "Copper Homeostasis as a Therapeutic Target in Amyotrophic Lateral Sclerosis with SOD1 Mutations." Int J Mol Sci **17**(5).
- Tougu, V., A. Karafin, et al. (2009). "Zn(II)- and Cu(II)-induced non-fibrillar aggregates of amyloid-beta (1-42) peptide are transformed to amyloid fibrils, both spontaneously and under the influence of metal chelators." J Neurochem **110**(6): 1784-1795.
- Valentine, J. S., P. A. Doucette, et al. (2005). "Copper-zinc superoxide dismutase and amyotrophic lateral sclerosis." Annu Rev Biochem **74**: 563-593.
- Vallee, B. L. and K. H. Falchuk (1993). "The biochemical basis of zinc physiology." Physiol Rev **73**(1): 79-118.
- Walsh, D. M. and D. J. Selkoe (2007). "A beta oligomers - a decade of discovery." J Neurochem **101**(5): 1172-1184.
- Van Vuong, Q., Z. Bednarikova, et al. (2015). "Inhibition of insulin amyloid fibrillization by glyco-acridines: an in vitro and in silico study." MedChemComm **6**(5): 810-822.
- Wang, J. B., Y. M. Wang, et al. (2011). "Quercetin inhibits amyloid fibrillation of bovine insulin and destabilizes preformed fibrils." Biochem Biophys Res Commun **415**(4): 675-679.
- Wang, S.-H., X.-Y. Dong, et al. (2012). "Effect of (-)-epigallocatechin-3-gallate on human insulin fibrillation/aggregation kinetics." Biochemical Engineering Journal **63**: 38-49.
- Webber, M. J., E. A. Appel, et al. (2016). "Supramolecular PEGylation of biopharmaceuticals." Proc Natl Acad Sci U S A **113**(50): 14189-14194.
- Weisiger, R. A. and I. Fridovich (1973). "Mitochondrial superoxide simutase. Site of synthesis and intramitochondrial localization." J Biol Chem **248**(13): 4793-4796.
- Weiss, M., D. F. Steiner, et al. (2000). *Insulin Biosynthesis, Secretion, Structure, and Structure-Activity Relationships*. Endotext. K. R. Feingold, B. Anawalt, A. Boyce et al. South Dartmouth (MA).
- Vilasi, S., C. Iannuzzi, et al. (2008). "Effect of trehalose on W7FW14F apomyoglobin and insulin fibrillization: new insight into inhibition activity." Biochemistry **47**(6): 1789-1796.
- Wittung-Stafshede, P. (2015). "Unresolved questions in human copper pump mechanisms." Q Rev Biophys **48**(4): 471-478.
- Xu, Y., Y. Yan, et al. (2012). "Multimerization and aggregation of native-state insulin: effect of zinc." Langmuir **28**(1): 579-586.
- Yamazaki, Y. and T. Takao (2008). "Metalation states versus enzyme activities of Cu, Zn-superoxide dismutase probed by electrospray ionization mass spectrometry." Anal Chem **80**(21): 8246-8252.

Acknowledgements

Firstly, I would like to express my very great appreciation to Professor Peep Palumaa for his valuable and constructive suggestions during the planning and development of this research work. His willingness to give his time so generously has been very much appreciated. Also, I would like to offer my special thanks to Dr. Vello Tõugu for his patience, valuable critics, and vast knowledge. The guidance of my supervisors helped me all time doing experiments and writing this thesis.

Besides my supervisors, I would like to thank Dr. Julia Smirnova, for her support during my PhD study. Dr. Julia Smirnova provided me with very valuable knowledge of LC-ICP MS instrument work and data analysis. Besides this, she has been a very good friend for all 8 years of my PhD studies.

My sincere thanks also go to all my colleagues in the laboratory of metalloproteomics who guided my first experiments in the lab. Without the support of all my colleagues, it would not be possible to conduct the research.

I thank my dear course mates for all the scientific discussions and great times we have had in the last 8 years, for their precious support and help. I found many good friends and like-minded people at the university.

I would like to thank all my colleagues in the Institute of Chemistry and Biotechnology for their help, advice, and friendly working atmosphere.

Special thanks should be given to the Estonian Research Council and Estonian Science Foundation, the Archimedes Foundation and DoRa program for financial support and for enabling me to introduce my results and broaden my knowledge at international conferences and seminars.

Finally, I would like to express my sincere gratitude to my family and friends who supported me in my initiatives and encouraged me to finish my studies.

Abstract

Role of metal ions in amyloidogenic properties of insulin and superoxide dismutase

Protein and peptide physical instability problems, such as the formation of amyloid fibrils are gaining much attention because it is connected to more than 40 human pathologies. It is known that proteins usually require cofactors to perform their biological functions which are often metal ions. Therefore, it is very important to investigate the physical and chemical properties of protein-metal complexes.

Zn(II) and Cu(II) metal ions have demonstrated the pronounced effects on the fibrillization of a variety of amyloidogenic peptides and proteins and the investigation of their affinity parameters in metal-protein complexes is highly important.

The aim of this study was firstly to better understand the molecular mechanisms of amyloid formation in the absence and presence of metal ions and to calculate the affinity constants of some important protein-metal ion complexes. Secondly, the goal was to investigate the demetallation of Cu,Zn-SOD1, and its ALS-related G93A mutant in the presence of different metal ion chelators at varying temperatures by using an LC-ICP MS-based method.

To achieve these goals the effect of Zn(II) and Cu(II) ions on the fibrillization of insulin was studied, the dissociation constant value for the monomeric 1 : 1 Zn(II) – insulin complex equal to 0.40 mM and Cu(II) – insulin complex equal to 0.025 mM was determined and the wt Cu,Zn-SOD1, and its mutant G93A were produced.

The obtained results demonstrated that Zn(II) inhibits the fibrillization of monomeric insulin at physiological pH values by forming a soluble Zn(II)–insulin complex. Based on the obtained results a mechanism for the assembly and fibrillization of insulin in the presence of Zn(II) ions was proposed. Also, the K_D value of insulin dimers equal to 18.9 μ M was calculated. Investigations of wt Cu,Zn-SOD1, and its mutant G93A demonstrated that none of the standard metal-binding ligands was able to remove metals from these proteins at physiological temperatures even at high millimolar concentrations which indicated very high metal-binding affinity of Cu,Zn-SOD1. To perform demetallation experiments the increased temperatures were applied, but then metal removal was a part of an irreversible thermal denaturation process. We showed that the release of Zn(II) and Cu(II) metal ions from Cu,Zn-SOD1 is cooperative and there exists no equilibrium between SOD-1 and free metal ions. Also, we concluded that it is not possible to calculate K_D for metal-protein complex as the chemical reaction does not reach equilibrium.

The obtained results provide a more detailed understanding of the molecular mechanisms of amyloid formation, reveal the affinities of many protein-metal ion complexes, and bring us to a better understanding of proteins and metal ions interactions.

Lühikokkuvõte

Metalliioonide roll insuliini ja superoksiidi dismutaasi amüloidogeensetes omadustes

Valkude ja peptiidide füüsikalise ebastabiilsuse probleemid, eelkõige amüloidsete fibrillide moodustumine, saavad palju tähelepanu, kuna need protsessid on seotud enam kui 40 erineva inimestel esineva patoloogia või haigusega. Paljud valgud vajavad oma bioloogiliste funktsioonide täitmiseks kofaktoreid, milleks on sageli metallioonid. Seetõttu on väga oluline uurida valk-metall komplekside füüsikalisi ja keemilisi omadusi. Märkimisväärset mõju mitmesuguste amüloidogeensete peptiidide ja valkude fibrillatsioonile omavad just sellised oluliste biometallide ioonid nagu Zn(II) ja Cu(II).

Käesoleva uuringu eesmärgiks oli paremini mõista amüloidide moodustumise molekulaarseid mehhanisme metallioonide puudumisel ja olemasolul ning määrata mõnede oluliste valgu-metalli ioonide komplekside afiinsuskonstandid. Nende eesmärkide saavutamiseks uurisime Zn(II) ja Cu(II) ioonide mõju insuliini fibrillatsioonile, määrasime monomeerse 1:1 Zn(II)-insuliini ja Cu(II)-insuliini kompleksi dissotsiatsioonikonstandid (K_D), mille väärtuseks saadi vastavalt 0,40 mM ja 0,025 mM. Samuti uurisime Cu,Zn-SOD1 ja selle ALS-iga seotud G93A mutandi demetalleerumist erinevate metalliioonide kelaatorite juuresolekul erinevatel temperatuuridel, kasutades LC-ICP MS-põhist meetodit.

Saadud tulemused näitasid, et Zn(II) inhibeerib monomeerse insuliini fibrillatsiooni füsioloogiliste pH väärtuste juures, moodustades lahustuva Zn(II)-insuliini kompleksi. Saadud tulemuste põhjal pakkusime välja mehhanismi insuliini oligomerisatsiooniks ja fibrilleerimiseks Zn(II) ioonide juuresolekul. Samuti arvutasime välja, et insuliini dimeeride K_D väärtus on võrdne 18,9 μ M.

Cu,Zn-SOD1 ja selle G93A mutandi uuringud näitasid, et ükski standardsetest metalli-siduvatest ligandidest ei suutnud eemaldada nendest valkudest tsink ja vaskioone füsioloogilistel temperatuuridel isegi kõrgel millimolaarsel kontsentratsioonil, mis viitas Cu,Zn-SOD1 väga kõrgele metallide sidumisafiinsusele või kineetilisele inertsusele. Ainus võimalik viis metallide eemaldamiseks oli temperatuuri märgatav tõstmine, mis viitas sellele, et metallide eemaldamine on osa pöördumatust termilise denaturatsiooni protsessist. Katsete käigus näitasime, et Zn(II) ja Cu(II) metalliioonide vabanemine Cu,Zn-SOD1-st on kooperatiivne protsess ning SOD-1 ja vabade ioonide vahel puudub tasakaal. Samuti mõistsime, et SOD-1 puhul ei ole metalli-valgu kompleksi K_D arvutamine võimalik, kuna metallide dissotsiatsioon ei saavuta tasakaaluolekut.

Kokkuvõttes võib järeldada, et teostatud uuringu tulemusel saadi üksikasjalikum ülevaate amüloidi moodustumise molekulaarsetest mehhanismidest metalliioonide juuresolekul, määrati mõnede oluliste valgu-metalli ioonide komplekside seostumisafiinsused, mis aitab meil paremini mõista valkude ja metalliioonide koostoimeid.

Appendix

Publication I

Noormägi, A., **Gavrilova, J.**, Smirnova, J., Tõugu V., Palumaa, P. “Zn(II) ions co-secreted with insulin suppress inherent amyloidogenic properties of monomeric insulin” (2010) *Biochem J.*; 430(3):511–518.

Zn(II) ions co-secreted with insulin suppress inherent amyloidogenic properties of monomeric insulin

Andra NOORMÄGI, Julia GAVRILOVA, Julia SMIRNOVA, Vello TÕUGU and Peep PALUMAA¹

Department of Gene Technology, Tallinn University of Technology, Akadeemia tee 15, Tallinn 12618, Estonia

Insulin, a 51-residue peptide hormone, is an intrinsically amyloidogenic peptide, forming amyloid fibrils *in vitro*. In the secretory granules, insulin is densely packed together with Zn(II) into crystals of Zn₂Insulin₆ hexamer, which assures osmotic stability of vesicles and prevents fibrillation of the peptide. However, after release from the pancreatic β -cells, insulin dissociates into active monomers, which tend to fibrillize not only at acidic, but also at physiological, pH values. The effect of co-secreted Zn(II) ions on the fibrillation of monomeric insulin is unknown, however, it might prevent insulin fibrillation. We showed that Zn(II) inhibits fibrillation of monomeric insulin at physiological pH values by forming a soluble Zn(II)–insulin complex. The inhibitory

effect of Zn(II) ions is very strong at pH 7.3 ($IC_{50} = 3.5 \mu M$), whereas at pH 5.5 it progressively weakens, pointing towards participation of the histidine residue(s) in complex formation. The results obtained indicate that Zn(II) ions might suppress fibrillation of insulin at its release sites and in circulation. It is hypothesized that misfolded oligomeric intermediates occurring in the insulin fibrillation pathway, especially in zinc-deficient conditions, might induce autoantibodies against insulin, which leads to β -cell damage and autoimmune Type 1 diabetes.

Key words: fibrillation, fluorescence spectroscopy, insulin, temperature dependence, thioflavin T (ThT), zinc.

INTRODUCTION

Insulin, a peptide hormone crucial for glucose metabolism, is produced in the islets of Langerhans by pancreatic β -cells. The peptide is synthesized in the endoplasmic reticulum and concentrated into secretory granules in the Golgi apparatus [1]. After processing by prohormone convertases PC1/3 and PC2 [2] insulin, with zinc, forms water-insoluble crystals of hexamer (Zn₂Insulin₆) in the slightly acidic environment (pH 5.5) of secretory granules [3,4]. Zn(II) content in the pancreatic β -cells is among the highest in the body, reaching 10 mmol per litre [5], and one third of it is localized in secretory granules together with insulin [6]. Zn(II) is uploaded to the granules with the assistance of a pancreas-specific zinc transporter ZnT8 localized on the membranes of the granules [7]. ZnT8-knockout mice, where secretory granules of insulin are zinc-depleted, show normal insulin biosynthesis, processing and release, which indicates that Zn(II) ions are not ultimately required in the processes upstream from insulin release [8].

Amyloidogenic properties of insulin have been known since the 1940s [9,10]. Fibrillation of insulin has been intensively studied at low pH values and high peptide concentration mostly as a suitable model of protein fibrillation [11]. However, insulin can also fibrillize at physiologically relevant neutral pH values [12, 13]. It is noteworthy that insulin does not form fibrils in the secretory granules, where its concentration is extremely high, reaching 21 mM [14]. Zn(II) ions, the concentration of which is approx. 11 mM in secretory granules [14], stabilize insulin at high peptide concentrations by forming crystals of Zn₂Insulin₆ [15,16]. However, insulin does not fibrillize in the Zn(II)-depleted secretory granules of transgenic ZnT8-knockout mice [8], indicating that Zn(II) is not the only factor preventing insulin fibrillation in secretory granules. In the absence of Zn(II), insulin still forms oligomeric structures, mainly hexamers, which

may prevent insulin fibrillation at high peptide concentrations. Indeed, insulin fibrillation at high peptide concentrations is slower than that at low concentrations, indicating that oligomerization inhibits insulin fibrillation [17]. Insulin is a rare exception within the amyloidogenic peptides, since the propensity for fibrillation of other peptides increases at elevated concentrations. It has also been demonstrated that insulin oligomers must dissociate to monomers before fibrillation [18]. Dissociation of insulin crystals into monomers occurs immediately after secretion of the insulin and also after its injection. Thus a question may arise as to what factors prevent the fibrillation of considerably amyloidogenic insulin monomers in the pancreatic extracellular space, at sites of the injection and also in circulation.

It is noteworthy that, despite widespread use of insulin for treatment of Type 1 diabetes, the incidence of formation of insulin fibrillar deposits at the site of repeated injections is relatively rare. Such a condition, categorized as injection amyloidosis, has been observed at the sites of repeated injection of neutral porcine insulin [19,20]. As a rule, injection solutions of insulin are supplemented with approx. 0.3 molar equivalent of Zn(II) ions [12,21]. It has been suggested that co-injected Zn(II) ions might also suppress the fibrillation of monomeric insulin and formation of insulin fibril deposits at the sites of repeated injection as well as in circulation. The influence of Zn(II) on insulin at very low concentrations of the peptide would therefore be of great interest with regard to its action and metabolism.

It is known that metal ions such as Zn(II) and Cu(II) have pronounced effects on the fibrillation of a variety of amyloidogenic peptides such as Alzheimer's amyloid peptide [22], synuclein [23,24], tau protein and prion protein, whereas metal ions can enhance [23,24] or inhibit fibrillation [25]. In principle, the fibrillation of monomeric insulin can also be suppressed by metal ions, and its suppression by Zn(II) that is co-secreted with insulin can be physiologically relevant. Moreover, fibrillation

Abbreviations used: ESI-MS, electrospray ionization MS; SEC, size-exclusion chromatography; TEM, transmission electron microscopy; ThT, thioflavin T.

¹ To whom correspondence should be addressed (email peep@staff.ttu.ee).

studies of monomeric insulin are also necessary for obtaining a better understanding about the mechanism of insulin fibrillation, as the critical amyloidogenic intermediate in fibrillation of insulin as well as other amyloidogenic peptides/proteins is a partially unfolded monomer [13,26,27]. In addition to Zn(II) ions, secretory granules of insulin also contain C-peptide [28] and amylin, which are present in equimolar and approx. 10-fold lower amounts than insulin respectively [29]. Insulin has been shown to interfere with amylin fibrillation [30], whereas C-peptide affects the pattern of insulin oligomerization [31,32] and suppresses amylin fibrillation [29]; however, the effects of the co-released peptides on the fibrillation of insulin have not been determined.

In the present work, we studied systematically the effects of Zn(II) ions, C-peptide, amylin and environmental conditions on the fibrillation of monomeric insulin at physiological pH and demonstrate that Zn(II) ions suppress fibrillation of monomeric insulin through differential stabilization of the monomeric ground state over the partially open transition state leading to amyloidogenesis. It is proposed that Zn(II) ions that are co-secreted together with insulin may prevent fibrillation of insulin at its release sites and in circulation. C-peptide and amylin did not influence the insulin fibrillation.

EXPERIMENTAL

Materials

Lyophilized insulin was purchased from Sigma–Aldrich, amylin was from rPeptide and C-peptide from Nordic BioSite. ThT (thioflavin T) and CuCl₂ · 2H₂O were from Sigma–Aldrich, and Hepes Ultrapure (molecular biology grade) was from USB Corporation. ZnCl₂ and NaCl (extra pure) were from Scharlau. All solutions were prepared in fresh Milli-Q water.

Sample preparation

A stock solution of insulin was prepared as follows. Insulin was dissolved in 20 mM Hepes, pH 7.3, and 100 mM NaCl at a concentration of 50 μM. After 30 min of incubation at 25 °C, the insulin stock solution was diluted with the same buffer and used for experiments. The oligomeric composition of insulin samples was determined by SEC (size-exclusion chromatography) on a Superdex™ 75 10/300 column (GE Healthcare) connected to an Äkta Purifier system (GE Healthcare) using 20 mM Hepes, pH 7.3, and 100 mM NaCl as the elution buffer.

Monitoring insulin fibrillation by ThT fluorescence

In a standard experiment, a freshly prepared stock solution of insulin was diluted to a final concentration of 2.5 μM in 20 mM Hepes, pH 7.3, and 100 mM NaCl containing 2.5 μM ThT and an appropriate amount of ZnCl₂. A 450-μl portion of each sample was incubated in a 0.5-cm-path-length quartz cell, equilibrated at 50 °C and agitated with a magnetic stirrer at 250 rev./min. The increase in ThT fluorescence was measured at 480 nm using a λ_{ex} of 440 nm on a PerkinElmer LS-45 fluorescence spectrophotometer equipped with a magnetic stirrer. When insulin was incubated without agitation under similar conditions, the fibrillation process was extremely slow and only a slight increase in ThT fluorescence was observed during prolonged incubation (5 days). Agitation at 250 rev./min was found to be optimal for monitoring the insulin fibrillation, and the effect of agitation was similar to that observed for Alzheimer's amyloid peptide fibrillation [25]. In temperature-dependence studies, temperature was varied from 35 °C to 50 °C. In a second series of experiments, the concentration of insulin was varied from 2.5 to 30 μM.

The kinetic curves of fibrillation were fitted to several sigmoidal functions including Avrami, Gompertz and Boltzmann using the Origin program (OriginLab) and it was found that the Boltzmann equation (eqn 1) provides the best fit of the experimental data and allows calculation of the kinetic parameters of fibrillation:

$$y = \frac{A_2 - A_1}{1 + e^{-(t-t_0)/\tau}} + A_1 \quad (1)$$

where A₁ is the initial fluorescence level, A₂ is the maximum fluorescence and t₀ is the time when fluorescence has reached half-maximum; 1/τ is the apparent rate constant (k) of the fibril growth and lag time is approximated by t₀ - 2τ as suggested previously [33]. IC₅₀ values were calculated according to hyperbolic dose-response curves as described in [25].

TEM (transmission electron microscopy)

TEM grids were placed on an adhesive solid surface and 3 μl of previously centrifuged (30 min, 12000 g) peptide solution was pipetted on to each grid and allowed to air dry. Then, drops of 2% uranylacetate were spotted on to a Parafilm plate and grids were placed on them with the upper side down (to bring the probe and the contrast solution in contact). Probes were kept in uranylacetate for 10 min, then removed and washed with Milli-Q water. After that, excess water was removed with a filter paper and the grids were placed into a special carrier. TEM images from the samples were created on a Selmi EM-125 instrument at 75 kV accelerating voltage and recorded on to high-resolution 60 × 90-mm negative film.

ESI-MS (electrospray ionization MS) measurements

Samples of 1–50 μM insulin in 100 mM ammonium acetate, pH 7.3, incubated for 10 min within a gas-tight syringe at 50 °C, were injected into the electrospray ion source of a QSTAR Elite ESI-Q-TOF (time-of-flight) MS instrument (Applied Biosystems) by a syringe pump at 10 μl/min, and ESI-MS spectra were recorded for up to 5 min in the m/z region 500–3000 Da using the following instrument parameters: ion-spray voltage, 5500 V; source gas, 45 litres/min; curtain gas, 20 litres/min; declustering potential, 60 V; focusing potential, 320 V; and detector voltage, 2300 V. ESI-MS spectra were analysed with the Bioanalyst program (Applied Biosystems).

Equilibrium dialysis

A dialysis experiment was performed with cellulose ester Spectra/Por dialysis-membrane tubing with a molecular-mass cut-off of 1000 Da (Spectrum Laboratories) containing 1.5 ml of 10 μM insulin dissolved in 20 mM Hepes, pH 7.3, and 100 mM NaCl. Dialysis tubing was equilibrated with 500 ml of dialysate solution containing 20 mM Hepes, pH 7.3, 100 mM NaCl and 5 μM ZnCl₂, under agitation for 24 h at 4 °C until equilibrium was achieved. At the end of the experiment, samples were taken from both the inside and outside solutions, acidified with 1 M HCl and analysed for zinc content by atomic absorption spectroscopy on a PerkinElmer 3100 instrument

RESULTS

Monitoring the *in vitro* formation of insulin fibrils

Insulin fibrillation experiments were performed with freshly solubilized peptide under continuous agitation by monitoring an increase in the fluorescence of the fibril-reactive dye ThT *in situ*. Under these conditions, a relatively fast increase in

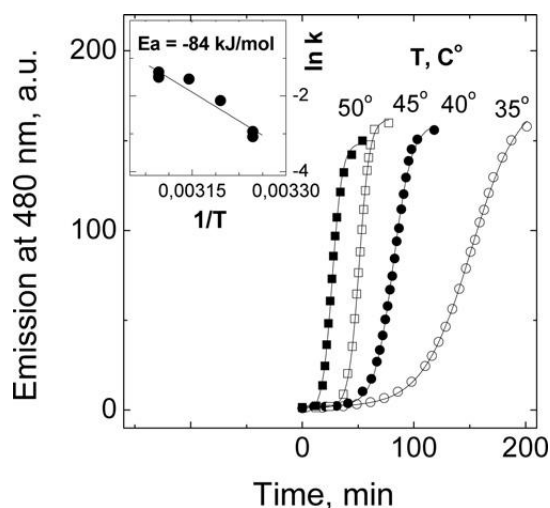


Figure 1 Temperature dependence of insulin fibrillation as followed by ThT fluorescence

Conditions: 2.5 μM insulin in 20 mM Hepes, pH 7.3, and 100 mM NaCl. Insulin was incubated at 50 $^{\circ}\text{C}$ (black squares), 45 $^{\circ}\text{C}$ (white squares), 40 $^{\circ}\text{C}$ (black circles) and 35 $^{\circ}\text{C}$ (white circles) in a quartz cell with continuous agitation in the presence of 2.5 μM ThT. Solid lines correspond to fits of the data to the Boltzmann equation (eqn 1). Inset: temperature dependence shown as Arrhenius coordinates. a.u., arbitrary units.

ThT fluorescence was observed in accordance with a typical two-phase growth curve (Figure 1). The kinetic curves of fibrillation fitted well to the Boltzmann equation (eqn 1), and the midpoint of fibril formation (t_m) and the rate constants for the fibrillation process were calculated. Fibrillation was monitored in the presence of 2.5 μM or 10 μM ThT. In a separate experiment, we demonstrated that ThT inhibits insulin fibrillation at concentrations higher than 10 μM . Experiments conducted with 2.5 μM insulin showed that the fibrillation rate constant increased and the duration of the lag phase decreased with increasing temperature (Figure 1). The enthalpy of activation E_a (-84 kJ/mol) was found from the slope in the Arrhenius plot (Figure 1, inset). In further experiments, insulin fibrillation was carried out at 50 $^{\circ}\text{C}$ for practical reasons. Fibrillation curves at 2.5 and 5 μM insulin exposed similar kinetics and lag phases, whereas at concentrations above 10 μM the lag phase increased and the values of the rate constant for fibril growth decreased (Figure 2).

Monomer–dimer equilibrium of insulin studied by ESI–MS

The ESI–MS spectrum of 2 μM insulin exposed +4 and +5 peaks of monomeric insulin (Figure 3a), whereas at higher peptide concentrations +6 and +7 peaks of dimeric insulin started increasing in the spectra (Figures 3b and 3c). Monomeric insulin was also the major peak in the spectrum at 50 μM insulin (Figure 3c), when a substantial proportion of the insulin is supposed to be dimeric. Such a behaviour is indicative of partial dissociation of insulin dimers to monomers during ESI. Moreover, in calculating the K_d for insulin dimers it should also be considered that the ionization efficiency of monomers and dimers is not equal in ESI–MS. To obtain the binding isotherm, the fractional content of insulin-dimer peaks was calculated by dividing the summarized area of all insulin-dimer peaks to the summarized

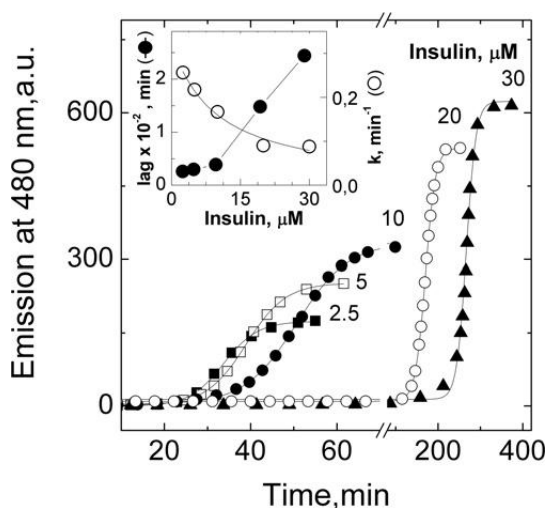


Figure 2 Effect of insulin concentration on its fibrillation

Conditions: 2.5 μM (black squares), 5 μM (white squares), 10 μM (black circles), 20 μM (white circles) and 30 μM (black triangles) insulin in 20 mM Hepes, pH 7.3, and 100 mM NaCl were incubated at 50 $^{\circ}\text{C}$ in a quartz cell with continuous agitation in the presence of 2.5 μM ThT. Solid lines correspond to fits of the data to the Boltzmann equation (eqn 1). Inset: dependence of the fibrillation rate constant on the insulin concentration. a.u., arbitrary units.

areas of all insulin peaks in ESI–MS spectra, and the latter parameter was plotted against insulin concentration (Figure 3d). The curve obtained was fitted to the equation of the hyperbola and the maximal fractional content F_{max} (0.18 ± 0.03) indicated that 80% of the insulin dissociated to monomers during ESI, which was expected as the insulin-dimer K_d is relatively high. The obtained K_d (18.9 ± 0.6 μM) describes the equilibrium of insulin-dimer dissociation. Our ESI–MS results at pH 7.3 are similar to previous nanospray ESI–MS studies; however, slightly different charge states for different species were observed at pH 3.3 [21]. On the basis of SEC and ESI–MS studies, we can conclude that at 2.5 μM insulin is prevalently monomeric and the effects of insulin oligomerization on the fibrillation kinetics are negligible.

Effects of Zn(II) on the fibrillation of insulin

The effect of Zn(II) on the fibrillation of 2.5 μM insulin was studied at pH 7.3 and 5.5. At pH 7.3, Zn(II) ions decreased the fibrillation rate constant and increased the lag phase of the process in a concentration-dependent manner, whereas the maximal level of ThT fluorescence was not affected (Figure 4a). The inhibitory effect of Zn(II) characterized by the IC_{50} [defined as the Zn(II) concentration at which a halving of the fibrillation rate constant was observed] was equal to 3.5 ± 0.9 μM (Figure 4a). At pH 5.5, the effect of Zn(II) was much weaker and only an insignificant (10%) decrease in fibrillation rate was observed in the presence of 20 μM Zn(II) (Figure 4b).

Effects of C-peptide and amylin on the fibrillation of insulin

Fibrillation of 2.5 μM insulin at pH 7.3 and 50 $^{\circ}\text{C}$ was not affected by 2.5 and 5 μM C-peptide or by 1 μM amylin (Figure 5), indicating that micromolar concentrations of these peptides do not affect fibrillation of monomeric insulin.

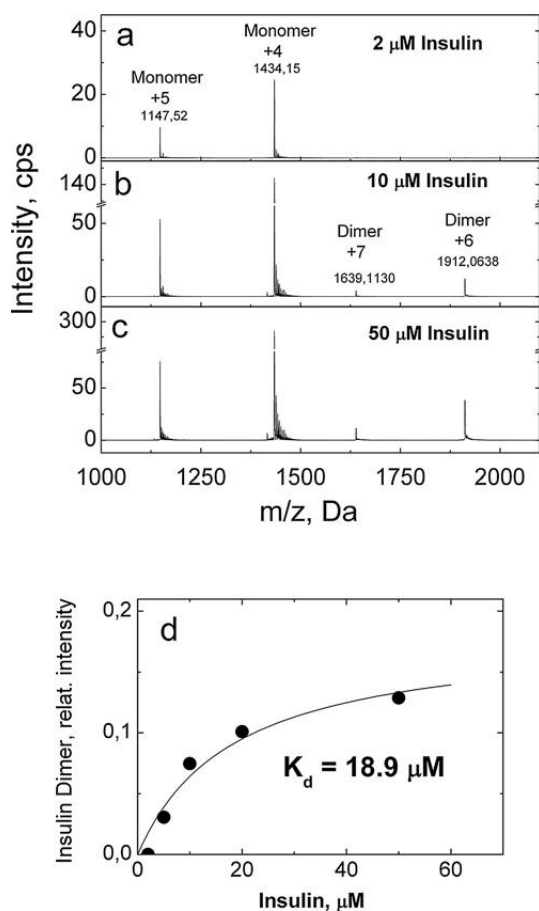


Figure 3 Determination of the apparent K_d for insulin dimers by ESI-MS

ESI-MS spectra of (a) 2 μM , (b) 10 μM and (c) 50 μM insulin in 100 mM ammonium acetate, pH 7.3; $T = 50^\circ\text{C}$. Monomeric insulin exposes charge states +4 and +5, and dimeric insulin exposes charge states +6 and +7. (d) Dependence of the relative intensity of insulin dimer peaks on the insulin concentration. The solid line shows the curve fitted for $K_d = 18.9 \mu\text{M}$. cps, c.p.s.; relat., relative.

SEC of insulin

SEC analysis showed that injection of 10 μM insulin exposed one peak with an elution volume of 14.5 ml (Figure 6a), whereas increasing the insulin concentration to 100 μM decreased the elution volume (Figure 6b), indicative of peptide oligomerization at higher concentrations in agreement with results in the literature [21,33]. SEC of aliquots of the fibrillation mixture showed that fibrillation is accompanied by the loss of insulin from the solution (Figure 6c). Fibrillation of 10 μM insulin is completely suppressed in the presence of 5 μM Zn(II) (Figure 4a) and SEC analysis of the fibrillation mixture in these conditions indicates that the peptide exposes a similar SEC peak as that for the initial solution of 10 μM insulin (Figure 6d). Moreover, the presence of 5 μM Zn(II) in elution buffer did not cause a shift of the insulin peak in SEC, confirming that 5 μM Zn(II) keeps insulin in a soluble state and does not induce changes in oligomers of insulin under our experimental conditions.

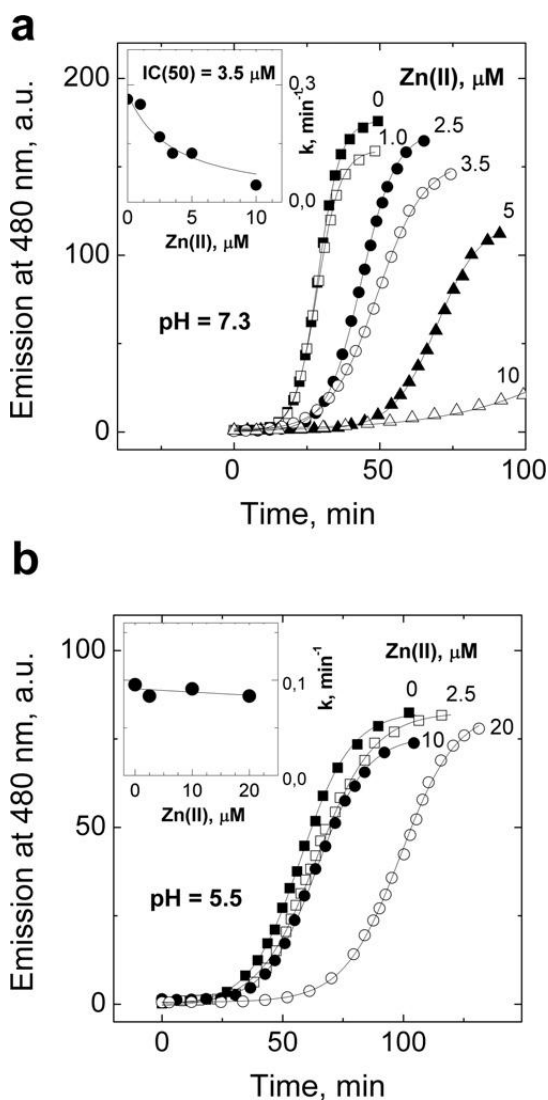


Figure 4 Effect of Zn(II) on fibrillation of insulin

Conditions: 2.5 μM of insulin in 20 mM HEPES and 100 mM NaCl at (a) pH 7.3 and (b) pH 5.5 was incubated at 50°C in a quartz cell with continuous agitation in the presence of 2.5 μM ThT and various concentrations of Zn(II) as shown in the Figure. Solid lines correspond to fits of the data to the Boltzmann equation (eqn 1). Insets: dependence of the fibrillation rate constant on the concentration of Zn(II). a.u., arbitrary units.

Equilibrium dialysis

Equilibrium dialysis of 10 μM insulin solution against 5 μM Zn(II) showed that in these conditions insulin binds 0.4 mol of Zn(II) per mol, which corresponds to the value of the K_{Zn} dissociation constant (7.5 μM).

Characterization of insulin fibrils by TEM

Insulin samples showing high ThT fluorescence (agitated for more than 30 min) showed the presence of fibrils in TEM, confirming

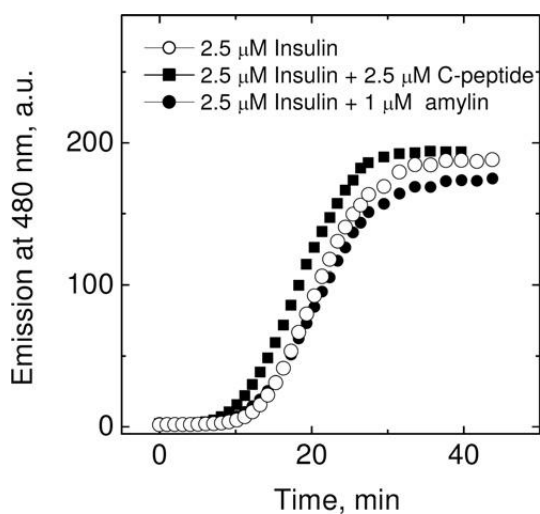


Figure 5 Effects of C-peptide and amylin on the fibrillation of insulin

Conditions: $2.5 \mu\text{M}$ insulin in 20 mM Hepes, $\text{pH } 7.3$, 100 mM NaCl and $2.5 \mu\text{M}$ ThT was incubated at 50°C in a quartz cell with continuous agitation in the absence of other peptides (white circles) and in the presence of $2.5 \mu\text{M}$ C-peptide (black squares) or $1 \mu\text{M}$ amylin (black circles). a.u., arbitrary units.

that the increase of ThT fluorescence reflects peptide fibrillation in our assay. In the samples of $10 \mu\text{M}$ insulin with added $5 \mu\text{M}$ Zn(II), almost no aggregates were detected at $\text{pH } 7.3$ after 30 min of agitation; however, at $\text{pH } 5.5$, insulin fibrils were observed

(Figure 6e), which confirms that $5 \mu\text{M}$ Zn(II) protects insulin from fibrillation at $\text{pH } 7.3$, but not at acidic pH values.

DISCUSSION

The fibrillation of insulin has been studied thoroughly for more than 60 years; however, the majority of studies have been performed with millimolar concentrations of Zn(II)–insulin, which fibrillizes at elevated temperatures and in acidic conditions [12]. Low pH is necessary for fibrillation since, at high millimolar concentrations and neutral pH, Zn(II)–insulin is predominantly in the form of hexamers resistant to fibrillation [18]. The addition of Zn(II) ions that stabilize the hexameric form is commonly used in injection solutions of insulin [12,21].

Zinc-free apo-insulin can fibrillize not only at acidic, but also at physiologically relevant, pH values, especially in the presence of chemical compounds such as ethanol, urea and guanidinium that are able to dissociate insulin to monomers [12,13]. Insulin is a rare exception within the amyloidogenic peptides since its dilution increases the propensity for fibrillation, whereas the fibrillation of other peptides is favoured at high peptide concentrations. Such a behaviour indicates that oligomerization inhibits insulin fibrillation [17]. Thus it follows that the fibrillation of the monomeric biologically active form of insulin, which is the most aggregation-prone form of the peptide, is insufficiently studied.

The behaviour of monomeric insulin can be studied at low peptide concentrations. According to the literature, insulin dimers begin to dissociate when diluted to concentrations below $100 \mu\text{M}$ [34,35] and $10 \mu\text{M}$ insulin is assumed to be essentially monomeric [21]. The K_d value for insulin dimers determined by static and dynamic laser light scattering is $12.5 \mu\text{M}$ at $\text{pH } 7.3$ and 25°C [36]. Our present ESI–MS studies at 50°C and $\text{pH } 7.3$ yielded a K_d of $18.9 \mu\text{M}$, which is in good agreement with the literature.

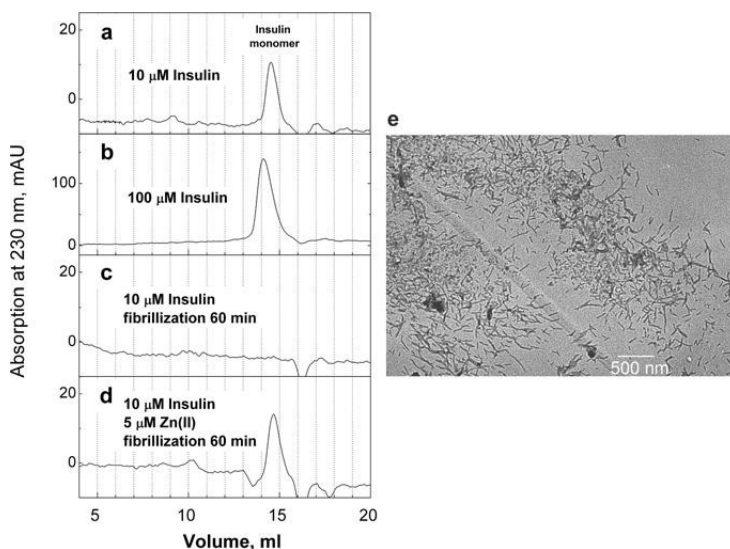
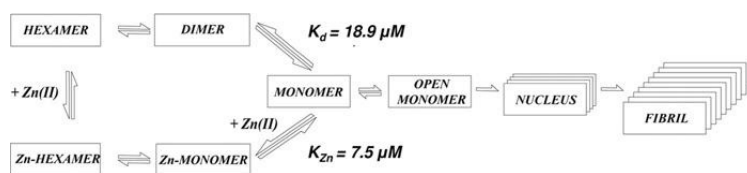


Figure 6 SEC of insulin samples and TEM image of insulin fibrils

(a) $10 \mu\text{M}$ insulin; (b) $100 \mu\text{M}$ insulin; (c) $10 \mu\text{M}$ insulin agitated at 50°C for 60 min; and (d) $10 \mu\text{M}$ insulin agitated in the presence of $5 \mu\text{M}$ Zn(II) for 60 min; Superdex™ 75 column; incubation and elution buffer, 20 mM Hepes, $\text{pH } 7.3$, and 100 mM NaCl; 25°C . (e) TEM image of fibrils formed by agitation of $10 \mu\text{M}$ insulin in the presence of $5 \mu\text{M}$ Zn(II) for 60 min at $\text{pH } 5.5$. Scale bar, 500 nm . mAU, milli absorbance units.



Scheme 1 Mechanism for assembly and fibrillogenesis of insulin in the presence of Zn(II) ions

Insulin is hexameric at high peptide concentrations both in the presence and absence of Zn(II). Insulin hexamers dissociate to dimers and monomers at low peptide concentrations, whereas peptide monomers can also bind Zn(II) ions. Monomeric insulin tends to fibrillize via a partially unfolded intermediate that is also assumed to be important for receptor binding. Zn(II)-insulin-monomer formation is off-pathway for fibrillation as it prevents opening of the conformation of monomeric insulin.

Accordingly, at $2.5 \mu\text{M}$, insulin is prevalently monomeric and the equilibrium concentration of dimers is approx. $0.22 \mu\text{M}$.

Our results demonstrated that fibrillation of insulin depends only slightly on the insulin concentration in the range 2.5 – $10 \mu\text{M}$, whereas at higher concentrations the fibrillation lag time increases and the fibrillation rate decreases. The inhibition of fibril formation at higher insulin concentrations indicates that the formation of insulin oligomers is an off-pathway process for fibrillation. Secondly, as the rate constant for fibril growth at concentrations below $10 \mu\text{M}$ is constant, we can conclude that the rate-limiting step of fibril growth is most probably connected with some intramolecular event such as conformational change. Indeed, the fibrillation of monomeric insulin is characterized by a relatively large E_a value of -84 kJ/mol , indicating that the formation of a fibrillation-competent structure is accompanied by substantial conformational changes. The native conformation of insulin in Zn(II)₂Insulin₆ hexamers [37] as well as its monomers is essentially α -helical [38]. Multiple techniques including FTIR (Fourier-transform infrared) and CD demonstrate that insulin fibril formation is accompanied by extensive unfolding of the molecule to allow conversion from an α -helical into a β -sheet conformation [11,21], necessary to build up the cross- β framework of insulin fibrils [39]. Apparently, such a conformational change in disulfide-linked native insulin is causing the observed large E_a .

From the compounds co-released with insulin, only Zn(II) exposed a pronounced inhibitory effect upon the fibrillation of monomeric insulin at pH 7.3. An IC_{50} of $3.5 \mu\text{M}$ indicates that Zn(II) ions already inhibit fibrillation at a low micromolar concentration and the addition of a 4-fold excess of Zn(II) almost completely suppressed the formation of insulin fibrils. Equilibrium dialysis of insulin against $5 \mu\text{M}$ Zn(II) confirmed that the inhibitory effect is in the same range as the Zn(II) binding affinity of insulin, K_{Zn} ($7.5 \mu\text{M}$) at low concentrations. At pH 5.5, the inhibitory effect of Zn(II) was much weaker as $20 \mu\text{M}$ Zn(II) did not affect the fibrillation rate constant and caused only a slight increase of the lag phase. The pH-dependence points towards participation of histidine residue(s) in the Zn(II)-induced inhibition of insulin fibrillation. It is known that the histidine residue at position B10 that is located in the vicinity of the six-residue B-chain segment (B12–B17) contributing to the formation of cross- β structure [40] participates in the binding of Zn(II) ions. It could be suggested that binding of Zn(II) to His¹⁰ may hinder the formation of a β -sheet-rich conformation compatible for fibrillation nearby. Thus the interaction of Zn(II) with the monomeric insulin inhibits its fibrillation most probably through differential stabilization of the monomeric ground state over the partially open conformation that is necessary for fibrillation. A schematic model describing the

effect of Zn(II) ions on the fibrillation of insulin is presented in Scheme 1.

Biological context

Insulin is present in the secretory granules at a extremely high concentration reaching 21 mM [14]. The main factor preventing insulin fibrillation in secretory granules is the formation of stable Zn(II)₂Insulin₆ hexamers (in zinc-enriched granules) or insulin oligomers (in zinc-depleted granules). Nevertheless, the fibrillation may also occur at the sites of its release, where insulin dissociates to monomers, which are the most fibrillation-prone form of the peptide. Based on the present results, we suggest that Zn(II) ions that are co-secreted with insulin from pancreatic β -cells might help insulin to avoid fibrillation at its release sites after dissociation of hexamers. Insulin fibrillation is a physiologically undesirable process for many reasons. First, fibrillation removes monomeric insulin out of secretion and prevents its interaction with insulin receptors. Secondly, insulin fibrillation occurs via intermediate misfolded oligomers [41,42] and prefibrillar aggregates, composed of 500 or more monomers and the dimensions of which might reach 14 \AA ($1 \text{ \AA} = 0.1 \text{ nm}$) [43]. These intermediates might be cytotoxic, as demonstrated in the case of Alzheimer's amyloid peptides [44] and also in the case of many other peptides and proteins. Besides being cytotoxic, these large misfolded oligomeric intermediates can also be immunogenic if they occur in the circulation. Such a scenario is feasible in the case of insulin.

Type 1 diabetes is an autoimmune disease that is characterized by the presence of autoantibodies against insulin and some other pancreatic proteins. These diabetes-related autoantibodies are present already in the preclinical asymptomatic latent period of the disease, and several studies have shown that insulin autoantibodies are the first to appear in young children, implying that insulin may be the primary autoantigen in most cases of childhood Type 1 diabetes [45]. The reason why autoantibodies that attack and destroy pancreatic β -cells are generated is currently largely unknown. It cannot be ruled out that the pathology is related to the generation of antibodies against misfolded insulin oligomers occurring as on-pathway intermediates during insulin fibrillation. Based on the present results, it can be hypothesized that Zn(II) ions co-secreted from pancreatic β -cells protect the organism from insulin fibrillation and formation of intermediary non-native insulin oligomers/aggregates. It can also be hypothesized that disturbances in zinc metabolism and especially zinc deficiency might enhance insulin fibrillation with intermediary formation of misfolded oligomers, which are immunogenic and might induce the generation of insulin autoantibodies. Currently, there is no direct evidence confirming the suggested hypothesis;

however, epidemiological studies associate diabetes with zinc deficiencies, which is in good agreement with the suggested hypothesis.

AUTHOR CONTRIBUTION

Peep Palumaa and Vello Tõugu designed experiments, analysed data and wrote the paper, Andra Noormägi designed and performed experiments, analysed data and wrote the paper, and Julia Gavrilova and Julia Smirnova performed experiments and analysed data.

ACKNOWLEDGEMENTS

We thank Dr Valdek Mikli and Kairit Zovo for help with TEM experiments.

FUNDING

This work was supported by the Estonian Ministry of Education and Research [grant number SF0140055s08 (to P.P.)]; the Estonian Science Foundation [grant numbers 6840 (to V.T.) and 7191 (to P.P.)]; and a World Federation of Scientists scholarship (to A.N.).

REFERENCES

- Orci, L., Ravazzola, M., Amherdt, M., Madsen, O., Vassalli, J. D. and Perrelet, A. (1985) Direct identification of prohormone conversion site in insulin-secreting cells. *Cell* **42**, 671–681
- Creemers, J. W., Jackson, R. S. and Hutton, J. C. (1998) Molecular and cellular regulation of prohormone processing. *Semin. Cell Dev. Biol.* **9**, 3–10
- Orci, L., Ravazzola, M., Storch, M. J., Anderson, R. G., Vassalli, J. D. and Perrelet, A. (1987) Proteolytic maturation of insulin is a post-Golgi event which occurs in acidifying clathrin-coated secretory vesicles. *Cell* **49**, 865–868
- Dodson, G. and Steiner, D. (1998) The role of assembly in insulin's biosynthesis. *Curr. Opin. Struct. Biol.* **8**, 189–194
- Clifford, K. S. and MacDonald, M. J. (2000) Survey of mRNAs encoding zinc transporters and other metal complexing proteins in pancreatic islets of rats from birth to adulthood: similar patterns in the Sprague–Dawley and Wistar BB strains. *Diabetes Res. Clin. Pract.* **49**, 77–85
- Figlewicz, D. P., Forhan, S. E., Hodgson, A. T. and Grodsky, G. M. (1984) ⁶⁵Zinc and endogenous zinc content and distribution in islets in relationship to insulin content. *Endocrinology* **115**, 877–881
- Chimienti, F., Devergnas, S., Pattou, F., Schuit, F., Garcia-Cuenca, R., Vandewalle, B., Kerr-Conte, J., Van Lommel, L., Grunwald, D., Favier, A. and Seve, M. (2006) *In vivo* expression and functional characterization of the zinc transporter ZnT8 in glucose-induced insulin secretion. *J. Cell Sci.* **119**, 4199–4206
- Lemaire, K., Ravier, M. A., Schraenen, A., Creemers, J. W., Van de Plas, R., Granvik, M., Van Lommel, L., Waelkens, E., Chimienti, F., Rutter, G. A. et al. (2009) Insulin crystallization depends on zinc transporter ZnT8 expression, but is not required for normal glucose homeostasis in mice. *Proc. Natl. Acad. Sci. U.S.A.* **106**, 14872–14877
- Waugh, D. F. (1946) A fibrous modification of insulin. I. The heat precipitate of insulin. *J. Am. Chem. Soc.* **68**, 247–250
- Langmuir, I. and Waugh, D. F. (1940) Pressure-soluble and pressure displaceable components of monolayers of native and denatured proteins. *J. Am. Chem. Soc.* **62**, 2771–2793
- Bouchard, M., Zurdo, J., Nettleton, E. J., Dobson, C. M. and Robinson, C. V. (2000) Formation of insulin amyloid fibrils followed by FTIR simultaneously with CD and electron microscopy. *Protein Sci.* **9**, 1960–1967
- Brange, J., Andersen, L., Laursen, E. D., Meyn, G. and Rasmussen, E. (1997) Toward understanding insulin fibrillation. *J. Pharm. Sci.* **86**, 517–525
- Ahmad, A., Millett, I. S., Doniach, S., Uversky, V. N. and Fink, A. L. (2004) Stimulation of insulin fibrillation by urea-induced intermediates. *J. Biol. Chem.* **279**, 14999–15013
- Foster, M. C., Leapman, R. D., Li, M. X. and Atwater, I. (1993) Elemental composition of secretory granules in pancreatic islets of Langerhans. *Biophys. J.* **64**, 525–532
- Brange, J., Havelund, S., Hommel, E., Sorensen, E. and Kuhl, C. (1986) Neutral insulin solutions physically stabilized by addition of Zn²⁺. *Diabet. Med.* **3**, 532–536
- Rasmussen, T., Kasimova, M. R., Jiskoot, W. and van de Weert, M. (2009) The chaperone-like protein α -crystallin dissociates insulin dimers and hexamers. *Biochemistry* **48**, 9313–9320
- Nielsen, L., Khurana, R., Coats, A., Frokjaer, S., Brange, J., Vyas, S., Uversky, V. N. and Fink, A. L. (2001) Effect of environmental factors on the kinetics of insulin fibril formation: elucidation of the molecular mechanism. *Biochemistry* **40**, 6036–6046
- Ahmad, A., Millett, I. S., Doniach, S., Uversky, V. N. and Fink, A. L. (2003) Partially folded intermediates in insulin fibrillation. *Biochemistry* **42**, 11404–11416
- Dische, F. E., Wernstedt, C., Westermark, G. T., Westermark, P., Pepsys, M. B., Rennie, J. A., Gilbey, S. G. and Watkins, P. J. (1988) Insulin as an amyloid-fibril protein at sites of repeated insulin injections in a diabetic patient. *Diabetologia* **31**, 158–161
- Storkel, S., Schneider, H. M., Muntefering, H. and Kashiwagi, S. (1983) Iatrogenic, insulin-dependent, local amyloidosis. *Lab. Invest.* **48**, 108–111
- Nettleton, E. J., Tito, P., Sunde, M., Bouchard, M., Dobson, C. M. and Robinson, C. V. (2000) Characterization of the oligomeric states of insulin in self-assembly and amyloid fibril formation by mass spectrometry. *Biophys. J.* **79**, 1053–1065
- Bush, A. I., Pettingell, W. H., Multhaup, G., d Paradis, M., Vonsattel, J. P., Gusella, J. F., Beyreuther, K., Masters, C. L. and Tanzi, R. E. (1994) Rapid induction of Alzheimer A β amyloid formation by zinc. *Science* **265**, 1464–1467
- Bharathi, Indi, S. S. and Rao, K. S. (2007) Copper- and iron-induced differential fibril formation in α -synuclein: TEM study. *Neurosci. Lett.* **424**, 78–82
- Bharathi, K. S. and Rao, K. S. (2008) Molecular understanding of copper and iron interaction with α -synuclein by fluorescence analysis. *J. Mol. Neurosci.* **35**, 273–281
- Tõugu, V., Karafin, A., Zovo, K., Chung, R. S., Howells, C., West, A. K. and Palumaa, P. (2009) Zn(II)- and Cu(II)-induced nonfibrillar aggregates of amyloid- β (1–42) are transformed to amyloid fibrils, both spontaneously and under the influence of metal chelators. *J. Neurochem.* **110**, 1784–1795
- Nielsen, L., Frokjaer, S., Brange, J., Uversky, V. N. and Fink, A. L. (2001) Probing the mechanism of insulin fibril formation with insulin mutants. *Biochemistry* **40**, 8397–8409
- Ahmad, A., Uversky, V. N., Hong, D. and Fink, A. L. (2005) Early events in the fibrillation of monomeric insulin. *J. Biol. Chem.* **280**, 42669–42675
- Steiner, D. F. (2004) The proinsulin C-peptide – a multitrope model. *Exp. Diabetes Res.* **5**, 7–14
- Westermark, P., Li, Z. C., Westermark, G. T., Leckstrom, A. and Steiner, D. F. (1996) Effects of beta cell granule components on human islet amyloid polypeptide fibril formation. *FEBS Lett.* **379**, 203–206
- Cui, W., Ma, J. W., Lei, P., Wu, W. H., Yu, Y. P., Xiang, Y., Tong, A. J., Zhao, Y. F. and Li, Y. M. (2009) Insulin is a kinetic but not a thermodynamic inhibitor of amylin aggregation. *FEBS J.* **276**, 3365–3371
- Shafiq, J., Melles, E., Sigmundsson, K., Johansson, B. L., Ekberg, K., Alvelius, G., Henriksson, M., Johansson, J., Wahren, J. and Jornvall, H. (2006) Proinsulin C-peptide elicits disaggregation of insulin resulting in enhanced physiological insulin effects. *Cell. Mol. Life Sci.* **63**, 1805–1811
- Jornvall, H., Lindahl, E., Astorga-Wells, J., Lind, J., Holmlund, A., Melles, E., Alvelius, G., Nerelius, C., Maler, L. and Johansson, J. (2010) Oligomerization and insulin interactions of proinsulin C-peptide: threefold relationships to properties of insulin. *Biochem. Biophys. Res. Commun.* **391**, 1561–1566
- Jeffrey, P. D. and Coates, J. H. (1966) An equilibrium ultracentrifuge study of the self-association of bovine insulin. *Biochemistry* **5**, 489–498
- Jeffrey, P. D., Milthorpe, B. K. and Nichol, L. W. (1976) Polymerization pattern of insulin at pH 7.0. *Biochemistry* **15**, 4660–4665
- Roy, M., Lee, R. W., Brange, J. and Dunn, M. F. (1990) ¹H NMR spectrum of the native human insulin monomer. Evidence for conformational differences between the monomer and aggregated forms. *J. Biol. Chem.* **265**, 5448–5452
- Kadima, W., Ogdal, L., Bauer, R., Kaarsholm, N., Brodersen, K., Hansen, J. F. and Porting, P. (1993) The influence of ionic strength and pH on the aggregation properties of zinc-free insulin studied by static and dynamic laser light scattering. *Biopolymers* **33**, 1643–1657
- Adam, M. G., Collier, L., Hodgkin, D. C. and Dodson, G. G. (1966) X-ray crystallographic studies on zinc insulin crystals. *Am. J. Med.* **40**, 667–671
- Bocian, W., Silkowski, J., Bednarek, E., Tarnowska, A., Kawecki, R. and Kozerski, L. (2008) Structure of human insulin monomer in water/acetonitrile solution. *J. Biomol. NMR* **40**, 55–64
- Burke, M. J. and Rougvie, M. A. (1972) Cross-protein structures. I. Insulin fibrils. *Biochemistry* **11**, 2435–2439
- Ivanova, M. I., Sievers, S. A., Sawaya, M. R., Wall, J. S. and Eisenberg, D. (2009) Molecular basis for insulin fibril assembly. *Proc. Natl. Acad. Sci. U.S.A.* **106**, 18990–18995
- Sorci, M., Grassucci, R. A., Hahn, I., Frank, J. and Belfort, G. (2009) Time-dependent insulin oligomer reaction pathway prior to fibril formation: cooling and seeding. *Proteins* **77**, 62–73

- 42 Nayak, A., Sorci, M., Krueger, S. and Belfort, G. (2009) A universal pathway for amyloid nucleus and precursor formation for insulin. *Proteins* **74**, 556–565
- 43 Smith, M. I., Sharp, J. S. and Roberts, C. J. (2008) Insulin fibril nucleation: the role of prefibrillar aggregates. *Biophys. J.* **95**, 3400–3406
- 44 Walsh, D. M. and Selkoe, D. J. (2007) $A\beta$ oligomers – a decade of discovery. *J. Neurochem.* **101**, 1172–1184
- 45 Knip, M. (2002) Natural course of preclinical Type 1 diabetes. *Horm. Res.* **57** (Suppl. 1), 6–11
-

Received 22 April 2010/8 July 2010; accepted 15 July 2010

Published as BJ Immediate Publication 15 July 2010, doi:10.1042/BJ20100627

Publication II

Gavrilova, J., Tõugu V., Palumaa, P. “Affinity of zinc and copper ions for insulin Monomers” (2014) *Metallomics*; (6) 1296–1300.

Affinity of zinc and copper ions for insulin monomers†

Cite this: *Metallomics*, 2014, 6, 1296

Julia Gavrilova, Vello Tõugu and Peep Palumaa*

Received 27th February 2014,
Accepted 22nd May 2014

DOI: 10.1039/c4mt00059e

www.rsc.org/metallomics

Zinc is an essential trace element involved in the correct packing and storage of insulin. Total zinc content in the pancreatic β -cells is among the highest in the body and changes in the Zn^{2+} levels have been found to be associated with diabetes. The most common form of the Zn–insulin complex is a hexamer containing two zinc ions. However, zinc can also form other complexes with insulin, whereas dissociation constants of these complexes are not known. We have determined that the dissociation constant value of the monomeric 1:1 Zn–insulin complex is equal to 0.40 μ M. The apparent binding affinity decreases drastically at higher insulin concentrations where the peptide forms dimers. Cu^{2+} ions also bind to monomeric insulin, whereas the apparent Cu^{2+} -binding affinity depends on HEPES concentration. The conditional dissociation constant of the Cu^{2+} –insulin complex is equal to 0.025 μ M. The analysis demonstrates that insulin cannot form complexes with zinc ions in circulation due to the low concentration of free Zn^{2+} in this environment.

Introduction

Insulin is the main peptide hormone involved in glucose metabolism and universally used in the treatment of type I diabetes. Insulin is produced by β -cells of the pancreas and its secretion into circulation is influenced by different stimuli, including an increased blood glucose level. The insulin molecule consists of a 21-residue A chain and a 30-residue B chain connected by two interchain disulfide bonds. At micromolar concentrations insulin self-associates into dimers¹ and at millimolar concentrations it readily forms globular hexamers that normally contain two zinc ions.^{2,3}

Insulin has inherent properties for interaction with zinc ions and this transient metal plays an essential role in all stages of insulin metabolism, from production and storage to secretion and utilization.⁴ The zinc content of pancreatic β -cells is among the highest in the body. Zinc ions are actively transported into secretory vesicles inside the β -cells by the help of pancreas-specific zinc transporter ZnT8.⁵ Inside the secretory granules insulin forms crystalline arrays of hexamers that contain two Zn^{2+} ions per hexameric unit. Thus, a substantial amount of Zn^{2+} is co-secreted with insulin. Additionally, the secretory granules of β -cells may contain Zn^{2+} in excess to what is necessary to form Zn–insulin hexamers, which results in an even greater yield of free Zn^{2+} during exocytosis.⁶ Co-secreted

zinc can act as an autocrine inhibitory modulator of insulin secretion,⁷ however, it is not known whether zinc can modulate the action of insulin.

Once in the extracellular microenvironment, the Zn^{2+} –insulin complex dissociates. It is mentioned that timely removal of secreted free Zn^{2+} from the extracellular space is critical in order to maintain the normal function of insulin⁶ because monomeric insulin is the active form recognized by receptors. During transfer from vesicles to the portal vein, insulin is diluted approximately 10⁷-fold; at this dilution the Zn^{2+} –insulin complexes dissociate within seconds,⁸ however, the final level of dissociation depends on the concentration of free zinc ions in the serum and the affinity constant of the Zn^{2+} –insulin complex.

The dissociation constant of the complex formed, K_D , is one of the most essential parameters characterizing any biochemical interaction. Both the amount of the complex formed under physiological conditions as well as the putative effects of the dyshomeostasis of interacting partners on the balance of the complex formation depend directly on the K_D value. Despite the obvious importance of insulin interaction with Zn^{2+} ions, the affinity for the formation of zinc–insulin complexes has not been thoroughly studied. We could find only one estimate for the dissociation constant of the Zn^{2+} –insulin complex in the range of 2 μ M,⁹ which, unfortunately, is determined in the presence of Tris buffer that has very complex interactions with transition metal ions. The insulin hexamer can exist in three different allosteric forms: T6 (tense), R3T3, and R6 (relaxed). R6 is the most stable form of hexameric insulin (For a review on the allosteric properties of insulin see ref. 4). It is known that the rate of 2,2',2''-terpyridine assisted Zn^{2+} release from the R6

Department of Gene Technology, Tallinn University of Technology,

Akadeemia tee 15, 12618 Tallinn, Estonia. E-mail: peep.palumaa@ttu.ee

† Electronic supplementary information (ESI) available. See DOI: 10.1039/c4mt00059e

conformation of hexameric insulin is 70 000 fold slower than that from the T6 state which most probably also means higher affinity of zinc for the R6 state.¹⁰

In the present study, we determined the dissociation constants for reversible insulin–zinc and insulin–copper complex formation using the changes in the intrinsic fluorescence of insulin. Copper does not associate with insulin under physiological conditions and we studied its interactions with insulin only because of its similarity to Zn²⁺. We show that the metal-binding center of insulin is not selective for Zn²⁺ and it can bind Cu²⁺ with increased affinity. Some peptide aggregation occurred during the zinc-binding experiments at higher insulin concentrations which resulted in drastically decreased metal-binding affinity. In the case of copper we demonstrated that the concentration of buffer has an influence on the apparent

constant for at least 1 hour confirming the stability of the peptide solution. The fluorescence of the amyloid dye used, ThT, was measured at 480 nm using excitation at 440 nm.

Size-exclusion chromatography

The oligomeric composition of insulin samples was determined by SEC on a Superdex 75 10/300 column (GE Healthcare, Giles, United Kingdom) connected to an Äkta Purifier system (GE Healthcare, Giles, United Kingdom). 0.02 M HEPES pH 7.3 containing 0.1 M NaCl was used as an elution buffer.

Calculation of dissociation constants

The values of the dissociation constants and the stoichiometries of the Zn²⁺–insulin and Cu²⁺–insulin complexes were calculated by fitting the titration data to the following quadric equation:

$$I = \frac{I_{\infty} + (I_0 - I_{\infty})}{[L]} \times \left(\frac{([L] + [Me^{2+}] + K_D^{app}) - \sqrt{(K_D + [L] + [Me^{2+}])^2 - 4 \times [Me^{2+}] \times [L]}}{2} \right), \quad (1)$$

affinity of insulin for Cu²⁺ ions and derived the value for the conditional (buffer independent) dissociation constant of the Cu²⁺–insulin complex.

Experimental

Materials

Lyophilized bovine insulin, CuCl₂ and Thioflavin T (ThT) were from Sigma-Aldrich (St. Louis, MO, USA); 2-[4-(2-hydroxyethyl)-piperazin-1-yl]ethane-1-sulfonic acid (HEPES) ultrapure from USB Corporation (Cleveland, OH, USA). ZnCl₂ and NaCl were extra pure from Scharlau (Barcelona, Spain). All solutions were prepared in fresh Millipore Q water.

Sample preparation

Stock solutions of insulin (50 μM) were prepared by dissolving an appropriate amount of the lyophilized peptide in 0.02 M HEPES and 0.1 M NaCl, pH 7.3. The insulin solution contained traces of zinc in the molar ratio less than 1 : 10 as determined by AAS. After 30 minutes incubation the stock solution was diluted with buffer to the appropriate concentration and used for experiments.

Fluorescence spectroscopy

Fluorescence spectra were collected on a Perkin–Elmer LS-55 fluorescence spectrophotometer (Perkin Elmer, Waltham, MA, USA). For the detection of intrinsic tyrosine fluorescence of insulin, excitation at 270 nm was used and the emission was recorded at 305 nm. The titration of insulin with metal ions was carried out in a 0.5 cm path length quartz cuvette by adding 1–10 μL aliquots of the stock solutions of the respective metal salt to the insulin solution. After each addition the solution was stirred for 10 seconds and the average fluorescence intensity was measured over a 30 s period. In the control experiment without salts added the intrinsic fluorescence of insulin was

where [Me²⁺] is the total concentrations of metal ions, [L] is the concentration of metal binding sites and K_D is the dissociation constant of the metal–insulin complex. I₀, I and I_∞ are the fluorescence intensities of the peptide sample in the absence, the presence, and the saturation of metal ions.

Non-linear least-square fitting and statistical analysis of the data were performed using the Origin 6.1 program (OriginLab Corporation, USA).

Results and discussion

Binding of Zn²⁺ ions to insulin

The intrinsic fluorescence of the tyrosine residues in the insulin molecule was sensitive to the binding of zinc (and also copper) ions to the peptide. Fig. 1 shows that the fluorescence intensity of insulin decreases during titration with Zn²⁺ ions. The effect of Zn²⁺ was reversible: addition of 10 mM of EDTA restored 90% of the initial fluorescence intensity (see Fig. S1, ESI[†]). The binding curves can be quantitatively described by eqn (1) and the K_D^{app} values and the number of binding centers can be determined. The superscript “app” denotes the dependence of the dissociation constant on the composition of the solution; in the case of Zn²⁺ ions the K_D values were independent of the buffer concentration and depended on the insulin concentration (Fig. S2, ESI[†]). The binding stoichiometry was shown to be equal to 1 : 1 at low insulin concentrations, where the L values found in the result of fitting were close to the insulin concentration. Due to the increase in K_D values the L could not be treated as a variable at high insulin concentrations and we used insulin concentration as L in data fitting suggesting the same stoichiometry at all insulin concentrations.

The K_D^{app} values increased with increasing insulin concentration, indicating better binding at low insulin concentrations. The semilogarithmic plot of K_D versus insulin concentration (Fig. 2) shows a sharp threshold in the apparent affinity at

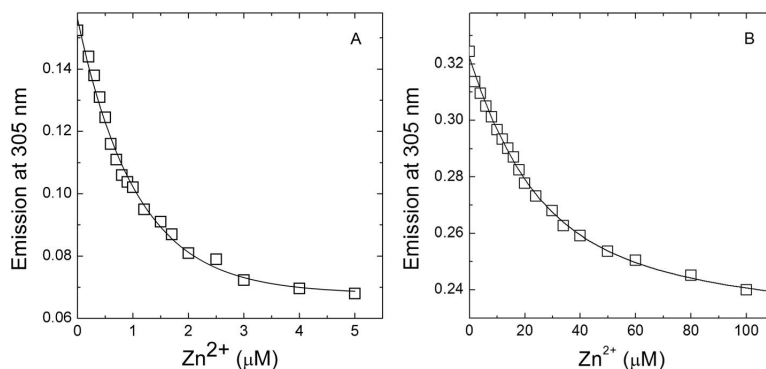


Fig. 1 Binding of Zn^{2+} ions to insulin. Decrease of the intrinsic tyrosine fluorescence of insulin with increasing concentration of Zn^{2+} . (A) 1 μM insulin, the solid line corresponds to eqn (1), $K_{\text{D}}^{\text{app}} = 0.40$, 0.11 μM and binding stoichiometry 0.93 ± 0.17 ; (B) 20 μM insulin, the solid line corresponds to $K_{\text{D}}^{\text{app}} = 12.8$, 3.8 μM and binding stoichiometry 0.97 ± 0.29 . Titration was carried out at pH 7.4 in 0.02 M HEPES buffer containing 0.1 M NaCl.

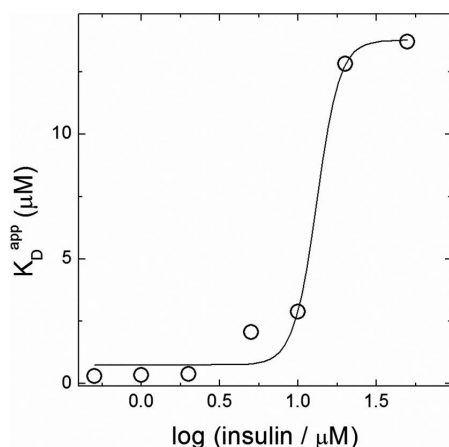


Fig. 2 Dependence of the apparent dissociation constant values of the Zn^{2+} -insulin complex on the insulin concentration.

concentrations between 10 and 20 μM . We suggest that the observed decrease in the Zn^{2+} binding affinity at higher insulin concentrations may be associated with insulin dimerization, since the K_{D} value for dimerization is in the same concentration range.^{11,12} Size-exclusion chromatography (SEC) analysis showed that the injection of 2 μM insulin exposed one peak with an elution volume of 15.04 mL, which corresponds to the monomeric state of protein. At the same time, injection of 50 μM insulin decreased the elution volume to 13.79 mL indicative of peptide oligomerization (Fig. S3, ESI[†]). An elution volume of 50 μM insulin corresponds to the molecular mass of 10 kDa, which is consistent with the dimeric state of insulin. The presence of 200 μM Zn^{2+} in the probe did not cause any shift of the insulin peak in SEC confirming that Zn^{2+} keeps insulin in a soluble state and does not induce oligomerization.

The dissociation constant value at low insulin concentrations (≤ 2 μM), $K_{\text{D}} = 0.40$ μM , corresponds to the binding of an

equimolar amount of Zn^{2+} ions to monomeric insulin. However, we cannot draw a conclusion that the K_{D} value at high insulin concentrations corresponds to low affinity of insulin dimers for zinc ions. First, the intensity of the intrinsic fluorescence of the tyrosine residues in insulin showed slow equilibration after adding each new portion of Zn^{2+} into the solution. Aggregation of the peptide was apparent due to an increase in the turbidity of the solution, thus the process of Zn^{2+} binding may be more complex at high insulin concentrations. In principle Zn^{2+} -insulin complexes with different stoichiometry can form at higher insulin concentrations and as long as we do not know their fluorescent characteristics or cannot determine their presence using some other method we cannot exclude the possibility that the decrease in affinity is not due to precipitation. The nature of aggregates formed at high insulin concentrations was tested with the well-known amyloid dye ThT. Insulin can form amyloid aggregates also at neutral pH,^{12,13} however, amyloid formation was suppressed by Zn^{2+} ions.¹² ThT fluorescence did not increase in the presence of insulin aggregates, which indicated that no insulin fibrils were formed during metal ion titration experiments. The $K_{\text{D}}^{\text{app}}$ value of the monomeric Zn^{2+} -insulin complex was considerably smaller than the IC_{50} value estimated from the inhibition curves of insulin fibrillization by Zn^{2+} .¹²

As the oligomeric insulin binds calcium ions besides Zn^{2+} , we also examined the effects of calcium ions on the insulin intrinsic fluorescence and zinc binding properties. Ca^{2+} had no effect on either the intrinsic fluorescence of insulin or on its Zn^{2+} binding affinity.

Affinity of insulin for Cu^{2+} ions

Addition of Cu^{2+} leads to the decrease in the intrinsic fluorescence of the molecule (Fig. 3). The $K_{\text{D}}^{\text{app}}$ values were calculated from the respective titration curves according to eqn (1). The K_{D} values show that insulin is not selective to zinc, suggesting that most likely the molecular basis for the interaction of insulin with zinc and copper ions is similar.

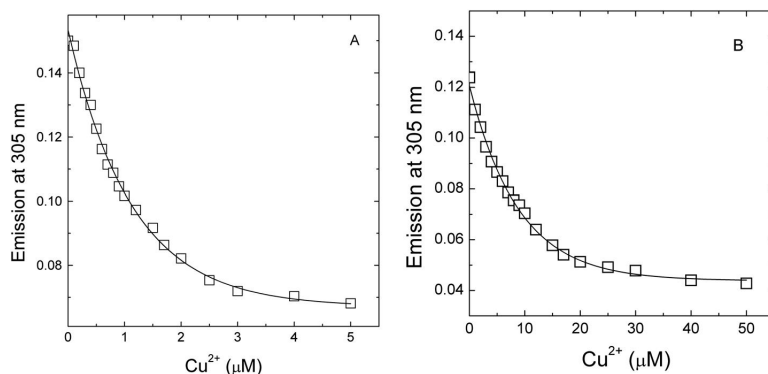


Fig. 3 Binding of Cu^{2+} ions to insulin. Decrease of intrinsic tyrosine fluorescence with increasing concentration of Cu^{2+} . (A) $1 \mu\text{M}$ insulin, $K_D = 0.40 \pm 0.09 \mu\text{M}$ and stoichiometry 0.97 ± 0.14 ; (B) $10 \mu\text{M}$ insulin, $K_D = 2.21 \pm 0.38 \mu\text{M}$. Titration was carried out at pH 7.4 in 20 mM HEPES buffer, 0.1 M NaCl; excitation at 270 nm.

Table 1 Effect of HEPES on the Cu^{2+} binding to insulin. The dependence of apparent dissociation constants K_D^{app} of the Cu–insulin complexes on the HEPES concentrations and the conditional dissociation constant (K_D) values calculated according to eqn (2) and (3)

Concentration of HEPES (mM)	C^a	K_D^{app} (μM), SD	K_D (μM)
5	0.67	0.10, 0.03	0.021
20	1.19	0.40, 0.08	0.026
50	1.57	1.00, 0.20	0.027

^a Correction function values calculated according to eqn (3).

In contrast to the Zn^{2+} –insulin complex, the fluorescence intensity of insulin in the presence of Cu^{2+} ions stabilized quickly also at high peptide concentrations. It is known that HEPES buffer used in this study forms a complex with Cu^{2+} ions and affects the corresponding apparent dissociation constant.¹⁴ We found that K_D^{app} values vary when different concentrations of HEPES buffer are used (Table 1 and Fig. 4). In the same experiment with Zn^{2+} ions no significant difference between binding constants was observed (Fig. S2, ESI[†]), indicating that HEPES does not form detectable complexes with Zn^{2+} .

Although HEPES does not form ternary complexes with metal ions,¹⁴ it is still recommended for copper binding studies; however, its influence on the binding equilibrium is taken into account by calculating the dissociation constants at zero buffer concentration (conditional dissociation constant).

Conditional constants K_D in HEPES were calculated from the apparent dissociation constants using the appropriate correction functions:¹⁴

$$\log K_D = \log K_D^{\text{app}} - C \quad (2)$$

$$C = \log \left(1 + \beta_{\text{MeL}} \times \frac{C_L}{1 + 10^{-\text{pH} + \text{p}K_a}} \right) \quad (3)$$

where C_L is the buffer concentration, K_a is the deprotonation constant of the buffer, and β_{MeL} is the dissociation constant of the metal²⁺–HEPES complex. The conditional dissociation constants for Cu^{2+} –insulin complexes (Table 1) and the K_D

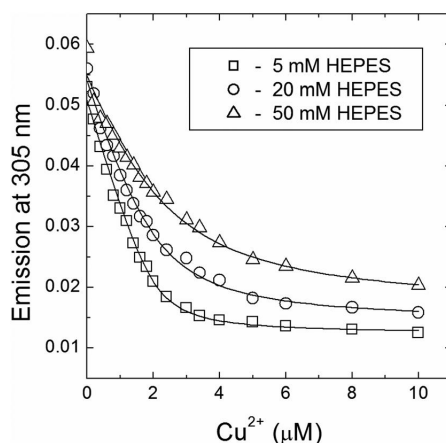


Fig. 4 The effect of HEPES buffer concentration on the binding of Cu^{2+} ions to insulin. pH 7.4, 0.1 M NaCl, buffer concentrations are shown in the legend.

value $0.025 \mu\text{M}$ were obtained. Thus, the metal-binding site of insulin is not selective for Zn^{2+} and it can bind Cu^{2+} with even better affinity. The semilogarithmic plot of the dependence of insulin affinity on the insulin concentration, shown in Fig. 5, was also similar to the one obtained with zinc ions.

Biological relevance

The biological significance of zinc–insulin interaction relies clearly on the biological availability of zinc in the pancreatic cells due to ZnT8 transporter activity. Zinc ions are related to several aspects of insulin metabolism. First, zinc co-crystallizes with insulin into dense secretory granules, second, zinc-ions co-secreted with insulin are involved in the regulation of the response to glucose levels.^{7,15,16} In principle, the monomeric insulin can interact with zinc ions in pancreatic β -cells as well

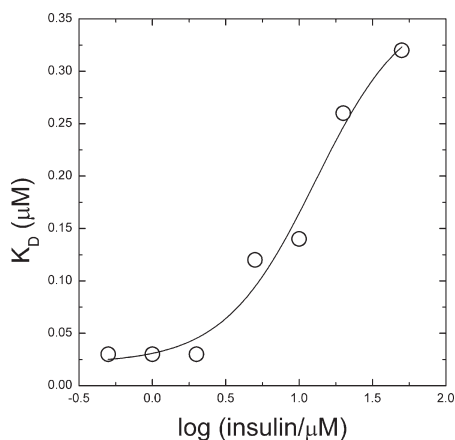


Fig. 5 Dependence of the apparent dissociation constant values of the Cu^{2+} –insulin complex on the insulin concentration.

as in circulation. In the secretory vesicles of pancreatic β -cells the concentrations of zinc and insulin are 11 and 21 mM, respectively.¹⁷ The K_D value for the monomeric Zn^{2+} –insulin complex equal to 0.40 μM was calculated from our data. In secretory vesicles at high concentrations insulin ends up in crystalline arrays of hexamers containing two zinc ions, but the primary function of zinc ions is not to catalyze the hexamer formation since similar hexameric structures are also formed in the absence of zinc ions.¹⁵ Considering the affinity and zinc content in pancreatic cells, monomeric insulin can be present in the form of a zinc complex.

The total concentration of zinc in the plasma is around 11 μM , however, the level of labile or exchangeable zinc is considerably lower. Approximately 28% of the zinc pool in plasma is tightly bound to α_2 -macroglobulin.¹⁸ The rest of the zinc is bound to serum albumin, which is present at extremely high 0.5–0.75 mM concentrations and has two Zn^{2+} -binding sites characterized with dissociation constant values 100 nM and $\sim 1 \mu\text{M}$.¹⁹ Thus, albumin can bind all labile zinc in serum to its high-affinity sites which are not saturated with zinc ions and the concentration of free zinc ions is too low for binding to insulin that is present at subnanomolar (57–280 pM) concentrations.²⁰ Accordingly, the prevalent form of insulin in circulation is free monomeric insulin that interacts with the insulin receptor.

Conclusions

Insulin monomers bind zinc ions with a dissociation constant of 0.40 μM and copper(II) ions with a conditional dissociation constant of 0.025 μM . In secretory granules insulin is in complex with zinc ions, whereas in circulation it exists as a free monomer.

Acknowledgements

This work was supported by the Estonian Ministry of Education and Research (grant IUT 19-8), Estonian Science Foundation grants no. 9318 (V.T.) and no. 8811 (P.P.).

References

- 1 T. N. Vinther, M. Norrman, H. M. Strauss, K. Huus, M. Schlein, T. A. Pedersen, T. Kjeldsen, K. J. Jensen and F. Hubalek, *PLoS One*, 2012, **7**, e30882.
- 2 G. Dodson and D. Steiner, *Curr. Opin. Struct. Biol.*, 1998, **8**, 189–194.
- 3 U. Derewenda, Z. Derewenda, G. G. Dodson, R. E. Hubbard and F. Korber, *Br. Med. Bull.*, 1989, **45**, 4–18.
- 4 M. F. Dunn, *BioMetals*, 2005, **18**, 295–303.
- 5 F. Chimienti, S. Devergnas, F. Pattou, F. Schuit, R. Garcia-Cuenca, B. Vandewalle, J. Kerr-Conte, L. Van Lommel, D. Grunwald, A. Favier and M. Seve, *J. Cell Sci.*, 2006, **119**, 4199–4206.
- 6 Y. V. Li, *Endocrine*, 2013, **45**, 178–189.
- 7 K. G. Slepchenko, C. B. James and Y. V. Li, *Exp. Physiol.*, 2013, **98**, 1301–1311.
- 8 G. Gold and G. M. Grodsky, *Experientia*, 1984, **40**, 1105–1114.
- 9 T. L. Coombs, P. T. Grant and B. H. Frank, *Biochem. J.*, 1971, **125**, 62P–63P.
- 10 S. Rahuel-Clermont, C. A. French, N. C. Kaarsholm, M. F. Dunn and C. I. Chou, *Biochemistry*, 1997, **36**, 5837–5845.
- 11 W. Kadima, L. Ogdal, R. Bauer, N. Kaarsholm, K. Brodersen, J. F. Hansen and P. Porting, *Biopolymers*, 1993, **33**, 1643–1657.
- 12 A. Noormägi, J. Gavrilova, J. Smirnova, V. Tõugu and P. Palumaa, *Biochem. J.*, 2010, **430**, 511–518.
- 13 L. Nielsen, R. Khurana, A. Coats, S. Frokjaer, J. Brange, S. Vyas, V. N. Uversky and A. L. Fink, *Biochemistry*, 2001, **40**, 6036–6046.
- 14 M. Sokolowska and W. Bal, *J. Inorg. Biochem.*, 2005, **99**, 1653–1660.
- 15 K. Lemaire, M. A. Ravier, A. Schraenen, J. W. Creemers, R. Van de Plas, M. Granvik, L. Van Lommel, E. Waelkens, F. Chimienti, G. A. Rutter, P. Gilon, P. A. In't Veld and F. C. Schuit, *Proc. Natl. Acad. Sci. U. S. A.*, 2009, **106**, 14872–14877.
- 16 F. Chimienti, *Nutr. Res. Rev.*, 2013, **26**, 1–11.
- 17 M. C. Foster, R. D. Leapman, M. X. Li and I. Atwater, *Biophys. J.*, 1993, **64**, 525–532.
- 18 P. Zalewski, A. Truong-Tran, S. Lincoln, D. Ward, A. Shankar, P. Coyle, L. Jayaram, A. Copley, D. Grosser, C. Murgia, C. Lang and R. Ruffin, *Biotechniques*, 2006, **40**, 509–520.
- 19 W. Bal, M. Sokolowska, E. Kurowska and P. Faller, *Biochim. Biophys. Acta*, 2013, **1830**, 5444–5455.
- 20 J. Suckale and M. Solimena, *Front. Biosci.*, 2008, **13**, 7156–7171.

Publication III

Smirnova, J., **Gavrilova, J.**, Noormägi, A., Valmsen, K., Pupart H., Luo, J., Tõugu, V., Palumaa, P. "Evaluation of Zn²⁺- and Cu²⁺-binding affinities of native Cu,Zn-SOD1 and its G93A mutant by LC ICP MS" (2022) *Molecules*; (27) 3160.

Article

Evaluation of Zn²⁺- and Cu²⁺-Binding Affinities of Native Cu,Zn-SOD1 and its G93A Mutant by LC-ICP MS

Julia Smirnova ¹, Julia Gavrilova ¹, Andra Noormägi ¹, Karin Valmsen ¹, Hegne Pupart ¹, Jinghui Luo ², Vello Tõugu ¹ and Peep Palumaa ^{1,*}

¹ Department of Chemistry and Biotechnology, Tallinn University of Technology, Akadeemia tee 15, 12618 Tallinn, Estonia; julia.smirnova@taltech.ee (J.S.); julia.smirnova@taltech.ee (J.G.); andra.noormagi@gmail.com (A.N.); karin.valmsen@gmail.com (K.V.); hegne.pupart@gmail.com (H.P.); vello.tougu@taltech.ee (V.T.)

² Paul Scherrer Institute, Forschungsstrasse 111, 5232 Villigen, Switzerland; jinghui.luo@psi.ch

* Correspondence: peep.palumaa@ttu.ee; Tel.: +372 5025559

Abstract: The tight binding of Cu and Zn ions to superoxide dismutase 1 (SOD1) maintains the protein stability, associated with amyotrophic lateral sclerosis (ALS). Yet, the quantitative studies remain to be explored for the metal-binding affinity of wild-type SOD1 and its mutants. We have investigated the demetallation of Cu,Zn-SOD1 and its ALS-related G93A mutant in the presence of different standard metal ion chelators at varying temperatures by using an LC-ICP MS-based approach and fast size-exclusion chromatography. Our results showed that from the slow first-order kinetics both metal ions Zn²⁺ and Cu²⁺ were released simultaneously from the protein at elevated temperatures. The rate of the release depends on the concentration of chelating ligands but is almost independent of their metal-binding affinities. Similar studies with the G93A mutant of Cu,Zn-SOD1 revealed slightly faster metal-release. The demetallation of Cu,Zn-SOD1 comes always to completion, which hindered the calculation of the K_D values. From the Arrhenius plots of the demetallation in the absence of chelators $\Delta H^\ddagger = 173$ kJ/mol for wt and 191 kJ/mol for G93A mutant Cu,Zn-SOD1 was estimated. Obtained high ΔH values are indicative of the occurrence of protein conformational changes before demetallation and we concluded that Cu,Zn-SOD1 complex is in native conditions kinetically inert. The fibrillization of both forms of SOD1 was similar.

Keywords: Cu,Zn-SOD1; ALS; metal-binding affinity; LC-ICP MS

Citation: Smirnova, J.; Gavrilova, J.; Noorm, A.; Valmsen, K.; Pupart, H.; Luo, J.; Vello Tõugu; Palumaa, P. Evaluation of Zn²⁺- and Cu²⁺-Binding Affinities of Native Cu,Zn-SOD1 and its G93A Mutant by LC-ICP MS. *Molecules* **2022**, *26*, x. <https://doi.org/10.3390/xxxxx>

Received: 14 April 2022

Accepted: 13 May 2022

Published: date

Publisher's Note: MDPI stays neutral with regard to jurisdictional claims in published maps and institutional affiliations.



Copyright: © 2022 by the authors. Licensee MDPI, Basel, Switzerland. This article is an open access article distributed under the terms and conditions of the Creative Commons Attribution (CC BY) license (<http://creativecommons.org/licenses/by/4.0/>).

1. Introduction

Cu,Zn-superoxide dismutase 1 (SOD1) is a cytoplasmic antioxidant enzyme, important for defense against potentially toxic superoxide radicals [1], produced as natural by-products in aerobic respiration [2]. SOD1 is expressed as a 16 kDa polypeptide chain, whose maturation into an enzymatically active protein involves metalation by Zn²⁺- and Cu⁺ ions, the formation of a conserved intra-subunit disulfide bond between Cys-57 and Cys-146, and subsequent dimerization [1]. Metalation of SOD1 with a copper ion is assisted by a copper chaperone for SOD-CCS, which also participates in the formation of a disulphide bond, uncommon for cytosolic proteins [3,4]. The redox-active copper ion is responsible for the catalytic activity in the conversion of superoxide radicals to hydrogen peroxide and dioxygen [5,6]. It is suggested that Zn²⁺ ion contributes to the formation and persistence of the native structure as its removal leads to immediate inactivation of SOD1 [7]. The major structural motif of SOD1 is β -barrel, whereas the metal-binding site is composed of loop regions located at the bottom of the active site channel [8].

SOD1 is characterized by extreme thermal stability and resistance to chemical denaturation. The melting temperature of natively folded Cu,Zn-SOD1, as measured by differ-

ential scanning calorimetry (DSC), is between 92° and 101° C [5,9,10]. The remarkable stability of SOD1 is supported by several factors. The main contribution comes from the binding of metal ions, as apo-protein has substantially lower stability [9,11,12]. The redox state of copper is also important: the reduction of Cu²⁺ ions to Cu⁺ with dithionite increases the thermal stability of bovine Cu,Zn-SOD1 protein by four degrees [13]. The protein is further stabilized by a conserved intra-subunit disulfide bond anchoring the loop that forms part of the dimer interface to the β-barrel [5]. The dimerization also greatly increases the stability of Cu,Zn-SOD1 by reducing the solvent-accessible surface area [14].

SOD1 is involved in the pathogenesis of amyotrophic lateral sclerosis (ALS), as in the case of 20-25 % of the familial ALS (fALS) patients the SOD1 protein is mutated [5]. According to The Human Gene Mutation Database, 209 mutations of SOD1 were identified, both inside and outside of the active site. Accordingly, based on SOD activities and metal-binding properties, two groups of fALS SOD1 mutants were distinguished: the metal-binding region (MBR) mutants and the wild-type-like (WTL) mutants [5]. In the case of the MBR mutants of SOD1, abolished or distorted binding of metal ions leads to the loss of native catalytic activity. Moreover, misbound copper ions can catalytically generate reactive oxygen species (ROS) through Fenton or Haber–Weiss chemistry, thus gaining a toxic function. Besides catalytic incompetence, it is known that the ALS mutants of SOD1 can distort the structure of SOD1 into conformations prone to aggregation and fibrillization, which is also observed in the case of ALS [1,15]. Those SOD1 aggregates can also bind copper ions and gain toxic function, as described above. The WTL mutants of SOD1 are remarkably similar to wild-type SOD1 in most of their physico-chemical properties, nonetheless, often these variants were shown to aggregate more readily [16].

Pathogenic WTL mutation G93A is located in loop V where it is distant from the metal binding region, disulfide, and dimer interface regions, but is conserved in 90% of SOD1 sequences. Mutation retains metal binding and catalytic activity, but rotates the peptide bond carbonyls of residues 92 and 93 away from the core and shifts the overall position of loop V away from loop III [17]. Based on NMR data, it is demonstrated that the remote metal-binding region is also selectively destabilized by G93A mutation [18], which should reflect in the changes of the metal-binding properties of the protein. The transgenic mice expressing human G93A Cu,Zn-SOD1 show progressive aggregation of the G93A Cu,Zn-SOD1 and ubiquitin in the spinal cord motor neurons [19,20], which points towards an increased propensity to aggregation for the G93A mutant. Thus, it is possible to explain the pathogenicity of the G93A mutation by changed metal-binding properties or increased propensity to aggregation.

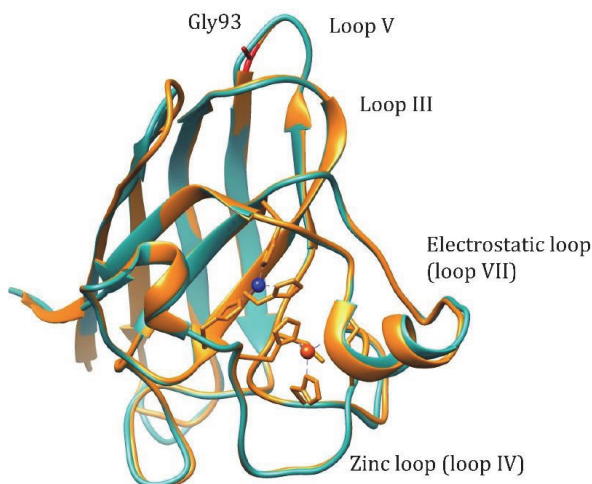


Figure 1. Structure alignment of the human wt Cu,Zn-SOD1 (light-blue, PDB: 2C9V) and G93A mutant (yellow, PDB: 2WKO). Cu²⁺ ion: blue, Zn²⁺ ion: orange.

Discrimination between these two possibilities could be realized by *in vitro* studies of the metal-binding properties and fibrillization of wt Cu,Zn-SOD1 and its G93A mutant. Despite the obvious importance of SOD1 interaction with metal ions, there are still no reliable quantitative data about the metal-binding affinity of wt Cu,Zn-SOD1. It is known that the metal-binding affinity of SOD-1 is very high in the native conditions, which is common for the binding sites buried in the protein interior. There is also evidence that the metal release from wt Cu,Zn-SOD1 might be connected with the unfolding of the protein [21]. So far there are attempts to estimate the K_D values for the metal-SOD1 complexes only under mildly denaturing conditions. In these studies, the competition of the partially denatured protein with the metal chelators of known metal-binding affinity was studied [22]. These results cannot be used for the estimation of the metal-binding affinity of SOD1 in native conditions, which is needed for the comparison with the metal-binding properties of wt and mutated SOD1 forms.

To get quantitative information about the metal-binding affinities of wt and G93A mutant SOD1, we have investigated the demetallation of corresponding proteins at elevated temperatures in the presence of different standard metal ion chelators by using an LC-ICP MS-based approach, elaborated in our previous study [23]. Size exclusion chromatography was used to separate high molecular weight (HMW) SOD1 fraction from low molecular weight (LMW) metal complexes, which gives an adequate reflection of metal ion release. Such a direct approach showed that both metal ions Zn²⁺ and Cu²⁺ are released simultaneously at elevated temperatures from the protein, according to slow first-order kinetics. The rate of the release depends on the concentration of chelating ligands, but is almost independent of their metal-binding affinities. The obtained results demonstrate that the metal ion release from the wt Cu,Zn-SOD1 is dependent on the rate-limiting opening of the native protein conformation, where chelating ligands can form ligand-exchange complexes for the release of metal ions without preference. As the demetallation of Cu,Zn-SOD1 always comes to completion, it is impossible to calculate the metal-binding affinities of native SOD1 for Zn²⁺ and Cu²⁺ ions and we have to conclude that the Cu,Zn-SOD1 complex is kinetically inert in native conditions. By using concentration dependences and Arrhenius plots, we estimated that the half-life for the dissociation of metal ions from native Cu,Zn-SOD1 at 40° C is approximately 3.5 months. Similar studies with the G93A mutant of Cu,Zn-SOD1 revealed slower metal-release and higher thermodynamic stability of mutant SOD1 at physiological temperatures, whereas the fibrillization of both forms of SOD1 was similar.

2. Results

2.1. Preparation of Cu,Zn-SOD1

After expression and purification, the human SOD1 protein with MW of 15805.2 Da determined by MALDI TOF MS (theoretical molecular weight 15804.5 Da) and the G93A mutant with MW of 15817.6 Da were obtained. ICP-MS analysis demonstrated that both SOD-1 forms were fully metalated with Cu and Zn. From 20 g of bacterial mass, 13.8 mg of pure wt Cu,Zn-SOD1 protein was obtained, and 80 mg of Cu,ZnSOD-1(G93A) was obtained from 60 g of bacterial mass.

2.2. Demetallation of Cu, ZnSOD1 at Elevated Temperatures in the Presence of EDTA

Demetallation of 10 µM wt Cu,Zn-SOD1 was monitored at 60° C, 70° C, and 80° C in the presence of 0, 1, 10, and 50 mM EDTA. The monitored isotopes were Cu-63 and Zn-66. The high and low-molecular-weight metal pools containing protein-metal and EDTA-metal complexes, respectively, were separated by a Sephadex G25 Superfine 1 mL column

and the metal content was continuously monitored by ICP MS. Examples of the demetallation of Cu,Zn-SOD1 and its G93A mutant in the presence of 1 mM EDTA at 70° C are presented in Figure 2

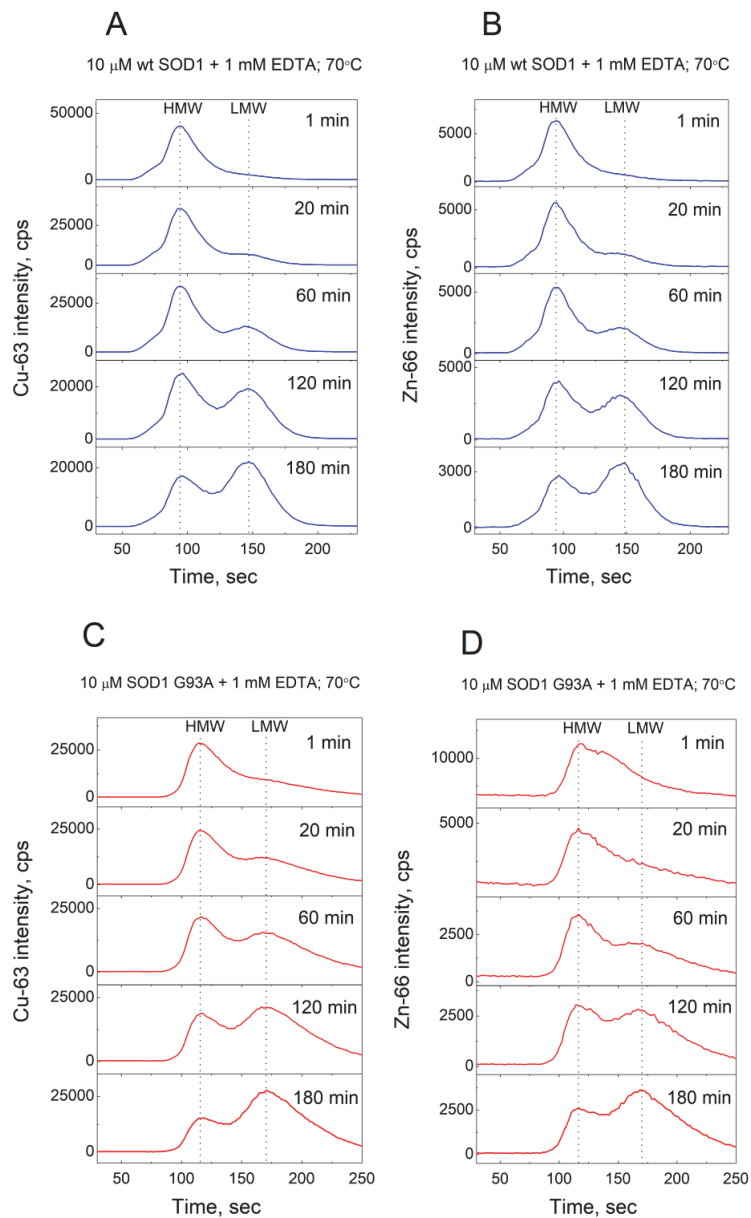


Figure 2. Demetallation of wt and G93A mutant Cu,Zn-SOD1 monitored by LC-ICP-MS. Conditions: 10 μ M wt Cu,Zn-SOD1 (A, B) and 10 μ M of its G93A mutant (C, D) in the presence of 1 mM EDTA at 70° C in 50 mM HEPES/50 mM NaCl, pH 7.3.

The separation of the HMW and LMW peaks allows integration using Origin software. Kinetic curves reflecting a decrease of the fractional content of metalated protein in time are presented in Figure 3.

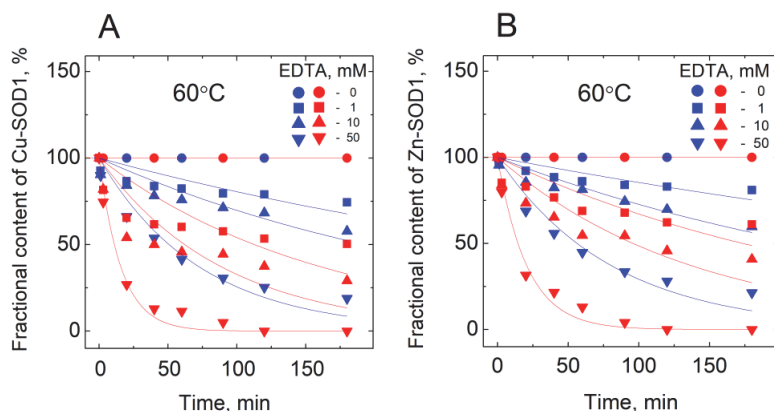


Figure 3. Demetallation of wt Cu,Zn-SOD1 and its G93A mutant in the presence of EDTA monitored by LC-ICP-MS. (A) fraction of Cu bound to-SOD1; (B) fraction of Zn bound to SOD1. Conditions: 10 μ M wt Cu,Zn-SOD1 (blue symbols) and 10 μ M of its G93A mutant (red symbols) in 50 mM HEPES/50 mM NaCl, pH 7.3 at 60° C.

The release of both the copper and zinc occurred concomitantly in all of the conditions shown in the Figure. From the kinetic curves, first-order rate constants were calculated, and their dependencies from the concentration of EDTA are presented in Figure 4.

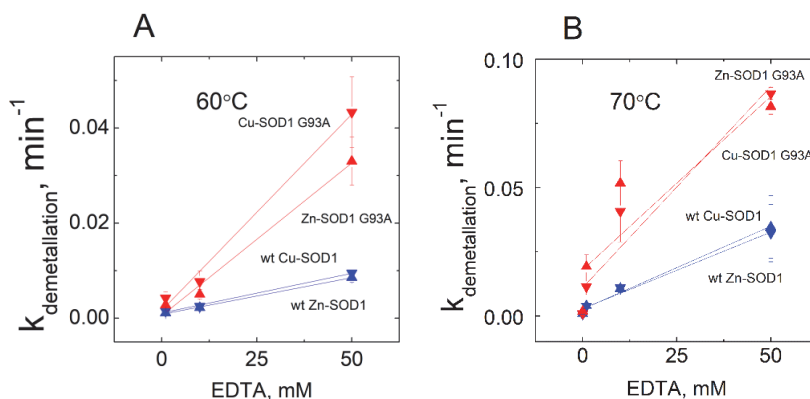


Figure 4. Dependence of the rate constant of demetallation of wt Cu,Zn-SOD1 and its G93A mutant on the EDTA concentration. Demetallation of wt Cu,Zn-SOD1 (blue symbols) and Cu,Zn-SOD1 G93A mutant (red symbols) at 60° C (A) and 70° C (B). Conditions: 10 μ M wt Cu,Zn-SOD1 and 10 μ M of its G93A mutant in 50 mM HEPES/50 mM NaCl, pH 7.3.

In the presence of DTPA, which has in comparison with EDTA more than 100 times higher binding affinity for Cu(II) and Zn(II) ions, only two times faster metal release was observed (data not shown).

In the absence of EDTA, a release of the metal ions was monitored in temperatures ranging from 60° to 85° C (Figure 5). Experiments at 70° and 80° C were performed in duplicates and the average difference between the parallel measurements was three fractional contents %.

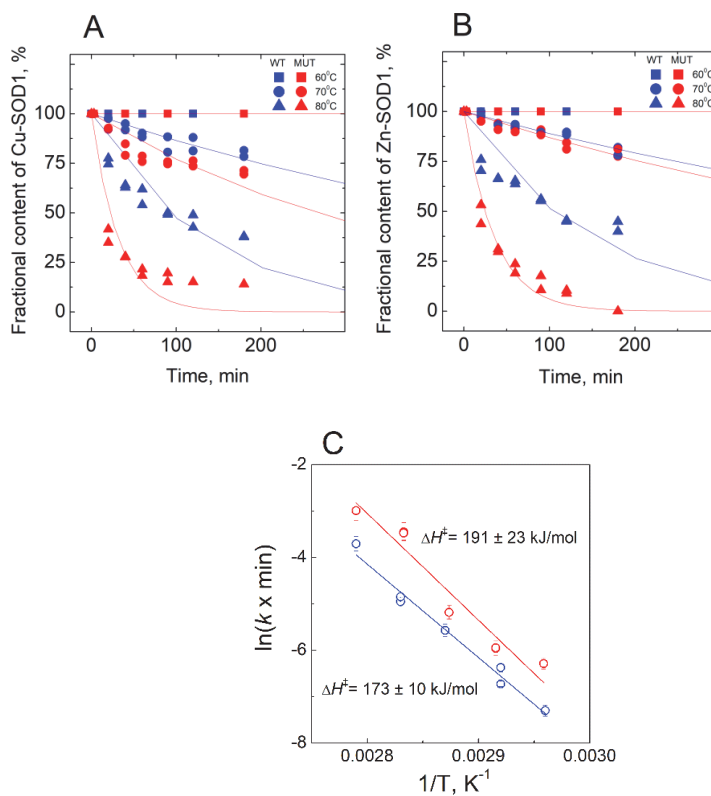


Figure 5. Demetallation of wt Cu,Zn-SOD1 and of its G93A mutant in the absence of EDTA monitored by LC-ICP-MS. **(A)** fraction of Cu bound to SOD1; **(B)** fraction of Zn bound to SOD1; **(C)** Arrhenius plots for the de-coppering of wt and G93A mutant Cu,Zn-SOD1. Conditions: 10 μM wt Cu,Zn-SOD1 (blue symbols) and 10 μM of its G93A mutant (red symbols) in 50 mM HEPES/50 mM NaCl, pH 7.3 at 60° C, 70° C and 80° C. EDTA at 1mM concentration was added to the samples before LC to obtain the LMW peak.

2.3. Fibrillization of Cu,ZnSOD-1 and its G93A Mutant

Fibrillization of Cu,Zn-SOD1 and its G93A mutant at 40° C are presented in Figure 6, which demonstrates that both proteins exposed similar fibrillization kinetics.

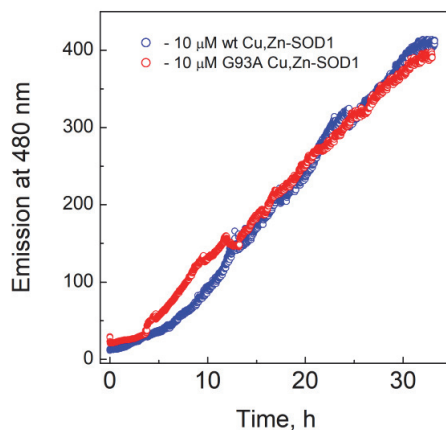


Figure 6. Fibrillization kinetics of Cu,Zn-SOD1. Conditions: 10 μM wt Cu,Zn-SOD1 (blue) and 10 μM of its G93A mutant (red) in 50 mM HEPES/50 mM NaCl, pH 7.3 at 40° C in the presence of 3.3 μM ThT.

3. Discussion

The major focus of the study was directed towards the determination of the Cu^{2+} and Zn^{2+} -binding affinities of wt SOD1, and its G93A mutant through competition with high-affinity metal-binding ligands, such as EDTA and DTPA. Demetallation of proteins was monitored by using the LC-ICP MS technique, allowing simultaneous and specific detection of the release for both copper and zinc ions. None of the ligands was able to demetallate these proteins at physiological temperatures, even at high millimolar concentrations, indicating either very high metal-binding affinity or the kinetic inertness of Cu,Zn-SOD1. Demetallation was also studied at elevated temperatures, where Cu^{2+} and Zn^{2+} ions were released from protein simultaneously and the process followed first-order kinetics until full demetallation. The rate of demetallation depended on the ligand concentration, but not on its affinity. Such behavior indicates that the rate-limiting step in the metal release is the opening of the active site to the ligand and the ligand-assisted demetallation. The release of metal ions is cooperative—e.g., the release of Cu^{2+} leads to a release of Zn^{2+} or vice versa—thus, it is not possible to determine the affinity of protein towards one of these ions, or to establish which ion is released first. From the Arrhenius plots of the de-coppering in the absence of chelators $\Delta H^\ddagger = 173 \pm 10$ kJ/mol for wt and 191 ± 23 kJ/mol for G93A Cu,Zn-SOD1 was determined. The obtained high ΔH^\ddagger value is indicative of the occurrence of protein conformational changes before demetallation and confirms that the rate-limiting step in the metal release is indeed thermal denaturation. Those activation energies fall into the range of the reported values for the proteins, as discussed in [24,25]. By extrapolating Arrhenius dependence to 40 °C, we found that in physiological conditions the metal release from wt Cu,Zn-SOD-1 could occur with a half-life of 3.5 month ($k_d = 4.37 \times 10^{-6}$ min $^{-1}$), and from Cu,ZnSOD-1 (G93A) with a half-life of 2.8 month ($k_d = 5.45 \times 10^{-6}$ min $^{-1}$). By using these values and considering that metal binding occurs with a speed below the diffusion limit $k_a = 10^9$ M $^{-1}$ s $^{-1}$, we can estimate the minimal values of the dissociation constants K_D for wt Cu,Zn-SOD1 and G93A mutant Cu,Zn-SOD1 of 7.3×10^{-17} and 9.1×10^{-17} M, respectively. The difference between the estimated dissociation rate constants between wt and mutant Cu,Zn-SOD1 is very small, which apparently does not influence the functioning of the enzyme. In a separate experiment, we established that fibrillization of the native and mutant Cu,Zn-SOD-1 occurs according to a very similar time curve, thus, there are no differences in the fibrillization propensity of these fully metalated protein forms.

All metal-binding ligands EDTA, DTPA, accelerated at elevated temperatures the metal release from wt and G93A Cu,Zn-SOD1 in a dose-dependent manner, which indicates that ligands should form a ternary complex with Cu,Zn-SOD1 in the activated intermediary state of thermal denaturation. This conclusion is confirmed by the fact that all demetallation curves led to full demetallation. The effect of chelators was slightly stronger in the case of the G93A Cu,Zn-SOD1, which might originate from the lower thermal stability of the mutated protein. Therefore, we can conclude that there exists no equilibrium between SOD-1 and free metal ions and metal removal is a part of an irreversible thermal denaturation process. The obtained results indicate that from metal chelator studies it is impossible to determine directly Cu²⁺ and Zn²⁺ -binding affinities for SOD-1, however, we can confirm that metal chelators facilitate metal release through the formation of the ternary complex, which is faster in the case of the Cu,Zn-SOD1 G93A mutant.

4. Materials and Methods

4.1. Expression and Purification of Cu,Zn-SOD1

Human wild-type Cu,Zn-SOD1 was produced according to the protocol presented in [31], by overexpression of protein in *Escherichia coli* strain BL21 Star (DE3). The plasmid containing human wt SOD1, and the yeast CCS coding sequences were kindly provided by Dr. Jinghui Luo (Paul Scherrer Institute). G93A mutant SOD1 was constructed using QuikChange Site-Directed Mutagenesis Kit (Agilent) and primers Gly93Ala_fw (GAC ACA TCG GCC ACA GCA TCT TTG TCA GCA GTC) and Gly93Ala_rev (GAC TGC TGA CAA AGA TGC TGT GGC CGA TGT GTC). The entire coding region was sequenced to verify the presence of the desired mutation. All the reagents were obtained from Sigma-Aldrich, with some exceptions: tryptone, yeast extract powder, and bacteriological agar were from Lab M. The plasmid miniprep kit GeneJET, the pre-stained protein ladder PageRuler™ and the protein staining solution PageBlue™ were from Thermo Scientific™. Protease inhibitor cocktail tablets cOmplete™ were from Roche.

Both wt-Cu,Zn-SOD1 and its G93A mutant were induced at OD₆₀₀ = 0.5-0.6 with 0.5 mM IPTG in the presence of 3 mM CuCl₂ (Sigma-Aldrich) and 30 μM zinc acetate (Scharlau). After induction, the culture was incubated for 18 h in a shaking incubator at 23 °C and 180 rpm (New Brunswick Scientific C25KC) for protein expression.

Purification of the expressed wt Cu,Zn-SOD1 proceeded, according to the protocol developed by [31], with minor modifications. The cell lysate was heated at 65 °C for 30 min, centrifuged at 24 500g and 4 °C for 35 min (Beckman Coulter Avanti centrifuge, rotor JA-20) and the precipitate was discarded. This was followed by fractional precipitation with ammonium sulfate with salt concentrations of 50%, 60%, and 90% of the saturation. After each step the solution was gently rotated for 2h at 4 °C following incubation and centrifugation at 24 500g and 4 °C for 15 min to separate the supernatant. After the final step, the solution was centrifuged for 30 min under the same conditions. Purification was carried out by size-exclusion chromatography (SEC) followed with ion exchange chromatography (IEX) on the ÄKTA explorer (Amersham Biosciences) chromatography system. For SEC, the HiLoad™ Superdex™ 75 26/60 column (GE Healthcare) was used with buffer 50 mM TRIS-HCl, pH 7.5. The sample containing dissolved pellets was filtered through a 5 μM microfilter before injection into SEC. The SEC was carried out using the following parameters: flow rate 2 mL/min; detection wavelengths 280 and 680 nm; collection at 1 mL fractions. The MALDI MS analysis was used to find the right fractions to collect. Prior IEX injection fractions containing wt-Cu/Zn-SOD1 were diluted 2.5 times and then concentrated. The IEX column used was 5 mL HiPrep™ DEAE FF (GE Healthcare) equilibrated with buffer 20 mM TRIS-HCl, pH 7.5. The elution was carried out at a flow rate 4 mL/min using two step gradients: 20 CV up to 25% and then 5 CV until 100% of buffer B (250 mM NaCl in 20 mM TRIS-HCl, pH 7.5). MALDI-MS was used for the analysis of the fractions. The wtSOD-1 containing fractions were then pooled and dialyzed against 20

mM ammonium acetate pH 7.4 or desalted by the SEC column before lyophilization on Christ Alpha 1-2 LD plus freeze dryer.

Purification of the G93A mutant of Cu,Zn-SOD1 followed a similar protocol, with several exceptions. The protein containing fraction was not heated as the G93A mutant Cu,Zn-SOD1 is more sensitive to high temperatures than wt Cu,Zn-SOD1. The fractional precipitation with ammonium sulphate was not applied either. Purification was conducted with SEC and the obtained fractions were investigated with MALDI MS. The buffer was exchanged to 20 mM ammonium acetate pH 7.4 and samples were lyophilized.

4.2. ICP-MS Analysis of Purified Proteins

Ultrapure Type 2 water with a resistivity of 18.2 MΩ/cm, produced by a Merck Direct-Q UV water purification system (Merck KGaA, Darmstadt, Germany), was used for all applications. The trace metal grade HNO₃ was from Fisher Scientific, and the multi-element calibration standard and the ICP-MS internal standard mix were from Agilent Technologies.

Inductively coupled plasma mass spectrometry (ICP-MS) on Agilent 7800 series instrument was used to measure the metal content in wt Cu,Zn-SOD1 and G93A mutant samples. Metal concentrations were determined by the external calibration method by using multi-element calibration standard solutions in the range of 0.50–50 ppb in 2% trace metal grade HNO₃. The protein samples were diluted in 2% HNO₃ to a final concentration of 0.1 μM and 0.3 μM. The measurements were performed in He mode. For the ICP-MS instrument control Agilent MassHunter 4.4 software version C.01.04 was used under the following conditions: RF power 1550 W, nebulizer gas flow 1.03 l/min, auxiliary gas flow 0.90 l/min, plasma gas flow 15 l/min, nebulizer type: MicroMist, isotopes monitored: Cu-63 and Zn-66. The obtained results were analyzed by the program Origin 9 Pro.

4.3. Metals Release Followed with LC-ICP-MS

Stock solutions of wt and G93A Cu,Zn-SOD1 were prepared in ultrapure Type 2 water, whereas stock solutions of ethylenediaminetetraacetic acid (EDTA, 99.995% trace metal basis) and diethylenetriaminepentaacetic acid (DTPA), both from Sigma/Merck (Merck KGaA, Darmstadt, Germany), were neutralized with 0.1 M NaOH to pH 7–8 and further diluted into reaction buffer composed from 50 mM HEPES, 50 mM NaCl, pH 7.3. Mobile phase and reagent solutions were prepared daily before the experiment.

Metal release from both 10 μM wt and G93A Cu,Zn-SOD1 was followed using LC-ICP-MS apparatus from an Agilent Technologies (Santa Clara, CA, USA). An Agilent Infinity HPLC system consisting of 1260 series μ-degasser, 1200 series capillary pump, Micro WPS autosampler and 1200 series MWD VL detector, was coupled with Agilent 7800 series ICP-MS instrument. The samples were prepared in the reaction buffer (50 mM HEPES, 50 mM NaCl, pH 7.3) and incubated under different temperatures from 60 to 85° C. Before measurement, the vials containing the reaction mixture were placed into the LC system autosampler for about a minute and then returned to the heater. To initiate metal release, the chelating ligand EDTA was used at different concentrations. The reaction was followed for 3 h, and, in some cases, up to 48 h. The demetallation of the SEC column before each experiment was conducted by injecting 5 mM EDTA (injection volume was 10 μL for all experiments). Desalting resin Sephadex G25 Superfine (Amersham/GE Healthcare, Buckinghamshire, UK), was used for the SEC separation of the HMW and LMW pools in 1 mL column at the flow rate 0.4 mL/min. The mobile phase in SEC was 200 mM NH₄NO₃ at pH 7.5, prepared daily from TraceMetal Grade nitric acid (Fisher Scientific UK Limited, Leicestershire, UK) and ammonium hydroxide 25% solution (Honeywell Fluka, Seelze, Germany), which is compatible with ICP-MS. For instruments' control and data acquisition, ICP-MS MassHunter 4.4 software Version C.01.04 from Agilent was used under the following conditions: RF power 1550 W; nebulizer gas flow 1.03 l/min;

auxiliary gas flow 0.90 l/min; plasma gas flow 15 l/min; nebulizer type: MicroMist; isotopes monitored: Cu-63 and Zn-66. The data were analyzed and visualized using the program Origin 9 Pro.

4.4. Metals Release in the Absence of the EDTA Followed with ICP

Metal release in the absence of the EDTA for both wt and G93A Cu,Zn-SOD1 was followed by incubating 10 μ M proteins in 50 mM HEPES, 50 mM NaCl, pH 7.3, at a subset of high temperatures (60°, 70°, 80° C). Prior to injection into the LC-ICP-MS system, the fraction of 20 μ L was collected and cooled on ice. Before the LC-ICP-MS run, 1 mM EDTA was added to get the LMW peak signal corresponding to the released Cu(II) and Zn(II) ions bound to the EDTA. The demetallation of the SEC column before each experiment was conducted by injecting 10 mM EDTA (injection volume was 10 μ L for all experiments). The LC-ICP-MS conditions were as described above, and the results were analyzed by the program Origin 9 Pro.

4.5. Fluorescence Spectroscopy

In the fibrillization kinetics' experiments, a freshly prepared stock solution of Cu,Zn-SOD1 and its G93A mutant were diluted to a final concentration of 10 μ M in 50 mM Hepes, pH 7.3, and 50 mM NaCl containing 5 μ M ThT. A 500 μ L sample was incubated in a 0.5-cm-path-length quartz cell, equilibrated at 40° C and equipped with a magnetic stirrer. The increase in ThT fluorescence was measured at 480 nm using excitation at 440 nm on a Perkin Elmer (Waltham, MA, USA) LS55 fluorescence spectrophotometer and the "fast" stirring regime was used.

5. Conclusions

In conclusion, we confirmed that fully metalated Cu,Zn-SOD1 G93A mutant has slightly faster metal release at elevated temperatures in the absence and presence of metal chelators, which indicates that mutation of distant G93 residue has an effect on the metal-binding properties of the enzyme, as suggested in [18]. At the same time, the fully metalated G93A mutant Cu,Zn-SOD1 exposed fibrillization behavior similar to that of the native Cu,Zn-SOD1. Thus, the fibrillization of G93A SOD-1 protein in transgenic mice expressing human G93A SOD-1 could be caused by some conditions existing in in vivo transgenic mice model. SOD-1 is a constitutively highly expressed protein in vivo constituting about 0.5–1% of the soluble protein expressed in brain and spinal cord. However, in the transgenic mouse model that expresses the G93A SOD-1 mutation, SOD protein is about 13% of total cellular protein [26,27]. It is speculated that at such high protein concentration protein is only partially metalated with zinc. Zinc-depleted SOD-1 is known to be pro-apoptotic [28,29] and exhibits increased fibrillization propensity, which both of which can cause neurodegeneration in the transgenic mouse model. It is important to mention that zinc supplementation protects ALS mutant G93A SOD-1 transgenic mice against the toxicity of ALS-associated SOD [30], which suggests that toxicity is connected with zinc deficiency in G93A SOD-1. Considering that the release of Zn from G94A is slow, being only slightly faster than that of the wt enzyme, the appearance of zinc-depleted SOD-1 arises most likely due to its incomplete metalation, rather than from the zinc depletion from the fully metalated G94A SOD-1.

Author Contributions: Conceptualization, P.P. and V.T.; methodology, J.S., J.G., K.V.; investigation, J. S., J.G., A.N., K.V., H.P., V.T.; resources, J.L., P.P.; data curation, J.S.; writing—original draft preparation, P.P.; writing—review and editing, J. S., J.G., J.L., V.T.; visualization, J.S., J.G., P.P.; supervision, P.P.; project administration, P.P.; funding acquisition, P.P. All authors have read and agreed to the published version of the manuscript

Funding: This work was supported by the Estonian Research Council grant (PRG 1289).

Institutional Review Board Statement**Informed Consent Statement:****Data Availability Statement:****Conflicts of Interest:** The authors declare no conflict of interest.**References**

1. Sheng, Y.; Abreu, I.A.; Cabelli, D.E.; Maroney, M.J.; Miller, A.F.; Teixeira, M.; Valentine, J.S., Superoxide dismutases and superoxide reductases. *Chem Rev* **2014**, *114*, 3854–3918.
2. Turrens, J.F., Mitochondrial formation of reactive oxygen species. *The Journal of physiology* **2003**, *552*, 335–344.
3. Culotta, V.C.; Yang, M.; O'Halloran, T.V., Activation of superoxide dismutases: Putting the metal to the pedal. *Biochim Biophys Acta* **2006**, *1763*, 747–758.
4. Furukawa, Y.; O'Halloran, T.V., Posttranslational modifications in Cu,Zn-superoxide dismutase and mutations associated with amyotrophic lateral sclerosis. *Antioxidants & redox signaling* **2006**, *8*, 847–867.
5. Valentine, J.S.; Doucette, P.A.; Zittin Potter, S., Copper-zinc superoxide dismutase and amyotrophic lateral sclerosis. *Annu Rev Biochem* **2005**, *74*, 563–593.
6. Fetherolf, M.M.; Boyd, S.D.; Taylor, A.B.; Kim, H.J.; Wohlschlegel, J.A.; Blackburn, N.J.; Hart, P.J.; Winge, D.R.; Winkler, D.D., Copper-zinc superoxide dismutase is activated through a sulfenic acid intermediate at a copper ion entry site. *J. Biol. Chem.* **2017**, *292*, 12025–12040.
7. Nedd, S.; Redler, R.L.; Proctor, E.A.; Dokholyan, N.V.; Alexandrova, A.N., Cu,Zn-superoxide dismutase without Zn is folded but catalytically inactive. *J. Mol. Biol* **2014**, *426*, 4112–4124.
8. Perry, J.J.; Shin, D.S.; Getzoff, E.D.; Tainer, J.A., The structural biochemistry of the superoxide dismutases. *Biochim Biophys Acta* **2010**, *1804*, 245–262.
9. Biliaderis, C.G.; Weselake, R.J.; Petkau, A.; Friesen, A.D., A calorimetric study of human CuZn superoxide dismutase. *Biochem J.* **1987**, *248*, 981–984.
10. Stathopoulos, P.B.; Rumpfheldt, J.A.; Karbassi, F.; Siddall, C.A.; Lepock, J.R.; Meiering, E.M., Calorimetric analysis of thermodynamic stability and aggregation for apo and holo amyotrophic lateral sclerosis-associated Gly-93 mutants of superoxide dismutase. *The Journal of biological chemistry* **2006**, *281*, 6184–6193.
11. Lepock, J.R.; Arnold, L.D.; Torrie, B.H.; Andrews, B.; Kruuv, J., Structural analyses of various Cu²⁺, Zn²⁺-superoxide dismutases by differential scanning calorimetry and Raman spectroscopy. *Archives of biochemistry and biophysics* **1985**, *241*, 243–251.
12. Potter, S.Z.; Zhu, H.; Shaw, B.F.; Rodriguez, J.A.; Doucette, P.A.; Sohn, S.H.; Durazo, A.; Faull, K.F.; Gralla, E.B.; Nersissian, A.M.; Valentine, J.S., Binding of a single zinc ion to one subunit of copper-zinc superoxide dismutase apoprotein substantially influences the structure and stability of the entire homodimeric protein. *Journal of the American Chemical Society* **2007**, *129*, 4575–4583.
13. Roe, J.A.; Butler, A.; Scholler, D.M.; Valentine, J.S.; Marky, L.; Breslauer, K.J., Differential scanning calorimetry of Cu,Zn-superoxide dismutase, the apoprotein, and its zinc-substituted derivatives. *Biochemistry* **1988**, *27*, 950–958.
14. Zhuang, X.; Liu, S.; Zhang, R.; Song, F.; Liu, Z., Identification of unfolding and dissociation pathways of superoxide dismutase in the gas phase by ion-mobility separation and tandem mass spectrometry. *Anal. Chem* **2014**, *86*, 11599–11605.
15. Sheng, Y.; Chattopadhyay, M.; Whitelegge, J.; Valentine, J.S., SOD1 aggregation and ALS: Role of metallation states and disulfide status. *Current topics in medicinal chemistry* **2012**, *12*, 2560–2572.
16. Shaw, B.F.; Valentine, J.S., How do ALS-associated mutations in superoxide dismutase 1 promote aggregation of the protein? *Trends in biochemical sciences* **2007**, *32*, 78–85.
17. Galalaldeen, A.; Strange, R.W.; Whitson, L.J.; Antonyuk, S.V.; Narayana, N.; Taylor, A.B.; Schuermann, J.P.; Holloway, S.P.; Hasnain, S.S.; Hart, P.J., Structural and biophysical properties of metal-free pathogenic SOD1 mutants A4V and G93A. *Archives of Biochem. Biophys.* **2009**, *492*, 40–47.
18. Museth, A.K.; Brorsson, A.C.; Lundqvist, M.; Tibell, L.A.; Jonsson, B.H., The ALS-associated mutation G93A in human copper-zinc superoxide dismutase selectively destabilizes the remote metal binding region. *Biochemistry* **2009**, *48*, 8817–8829.
19. Stieber, A.; Gonatas, J.O.; Gonatas, N.K., Aggregates of mutant protein appear progressively in dendrites, in periaxonal processes of oligodendrocytes, and in neuronal and astrocytic perikarya of mice expressing the SOD1(G93A) mutation of familial amyotrophic lateral sclerosis. *J. Neurol. Sci.* **2000**, *177*, 114–123.
20. Stieber, A.; Gonatas, J.O.; Gonatas, N.K., Aggregation of ubiquitin and a mutant ALS-linked SOD1 protein correlate with disease progression and fragmentation of the Golgi apparatus. *J. Neurol. Sci.* **2000**, *173*, 53–62.
21. Forman, H.J.; Fridovich, I., On the stability of bovine superoxide dismutase. The effects of metals. *J. Biol. Chem.* **1973**, *248*, 2645–2649.
22. Crow, J.P.; Sampson, J.B.; Zhuang, Y.; Thompson, J.A.; Beckman, J.S., Decreased zinc affinity of amyotrophic lateral sclerosis-associated superoxide dismutase mutants leads to enhanced catalysis of tyrosine nitration by peroxynitrite. *J. Neurochem* **1997**, *69*, 1936–1944.

23. Kirsipuu, T.; Zadoroznaja, A.; Smirnova, J.; Friedemann, M.; Plitz, T.; Tougu, V.; Palumaa, P., Copper(II)-binding equilibria in human blood. *Sci. Rep.* **2020**, *10*, 5686.
24. Qin, Z.; Balasubramanian, S.K.; Wolkers, W.F.; Pearce, J.A.; Bischof, J.C., Correlated parameter fit of arrhenius model for thermal denaturation of proteins and cells. *Annals of Biomed. Eng.* **2014**, *42*, 2392–2404.
25. Peterson, M.E.; Eienthal, R.; Danson, M.J.; Spence, A.; Daniel, R.M., A new intrinsic thermal parameter for enzymes reveals true temperature optima. *J. Biol. Chem.* **2004**, *279*, 20717–20722.
26. Gurney, M.E.; Pu, H.F.; Chiu, A.Y.; Dalcanto, M.C.; Polchow, C.Y.; Alexander, D.D.; Caliendo, J.; Hentati, A.; Kwon, Y.W.; Deng, H.X.; Chen, W.J.; Zhai, P.; Sufit, R.L.; Siddique, T., Motor-Neuron Degeneration in Mice That Express a Human Cu,Zn Superoxide-Dismutase Mutation. *Science* **1994**, *264*, 1772–1775.
27. Beckman, J.S.; Esetvez, A.G.; Barbeito, L.; Crow, J.P., CCS knockout mice establish an alternative source of copper for SOD in ALS. *Free Rad. Biol. & Med.* **2002**, *33*, 1433–1435.
28. Estevez, A.G.; Sampson, J.B.; Zhuang, Y.X.; Spear, N.; Richardson, G.J.; Crow, J.P.; Tarpey, M.M.; Barbeito, L.; Beckman, J.S., Liposome-delivered superoxide dismutase prevents nitric oxide-dependent motor neuron death induced by trophic factor withdrawal. *Free Rad. Biol. & Med.* **2000**, *28*, 437–446.
29. Estevez, A.G.; Spear, N.; Manuel, S.M.; Radi, R.; Henderson, C.E.; Barbeito, L.; Beckman, J.S., Nitric oxide and superoxide contribute to motor neuron apoptosis induced by trophic factor deprivation. *J. Neurosci.: Of. J. Soc. Neurosci.* **1998**, *18*, 923–931.
30. Ermilova, I.P.; Ermilov, V.B.; Levy, M.; Ho, E.; Pereira, C.; Beckman, J.S., Protection by dietary zinc in ALS mutant G93A SOD transgenic mice. *Neurosci. Lett.* **2005**, *379*, 42–46.
31. Ahl, I.M.; Lindberg, M.J.; Tibell, L.A., Coexpression of yeast copper chaperone (yCCS) and CuZn-superoxide dismutases in *Escherichia coli* yields protein with high copper contents. *Prot. Expres. Purif.* **2004**, *37*, 311–319.

Curriculum vitae

Personal data

Name: Julia Gavrilova
Date of birth: 09.10.1988
Citizenship: Estonian
Language skills: Russian, Estonian, English

Contact information

Address: Department of Gene Technology, Tallinn University of Technology,
Akadeemia tee 15, 12618, Tallinn, Estonia
Phone: +372 5694 8505
E-mail: julia.gavrilova1@gmail.com

Education

2015–2022 Tallinn University of Technology, PhD student
2011–2014 Tallinn University of Technology, Master's degree
"Affinity of zinc and copper ions to insulin monomers"
2007–2010 Tallinn University of Technology, Bachelor's degree
"The effect of environmental conditions and Zn⁺² ions on the fibrillization of insulin"
1995–2007 Tallinn Central Russian Gymnasium

Awards

2015 Award of the Estonian Society of Biochemistry for the article *"Affinity of zinc and copper ions for insulin monomers"*
2014 Estonian National Competition of Student Research Works – 3rd Prize
(in the field of health research)
2010 Estonian National Competition of Student Research Works – 3rd Prize

Publications

Smirnova, J., **Gavrilova, J.**, Noormägi, A., Valmsen, K., Pupart H., Luo, J., Tõugu, V., Palumaa, P. "Evaluation of Zn(II)- and Cu(II)-binding affinities of native Cu,Zn-SOD1 and its G93A mutant by LC ICP MS" (2022) International Journal of Molecular Sciences

Zarovni, N.; Corrado, A.; Guazzi, P.; Zocco, D.; Lari, E.; Radano, G.; Muhhina, J.; Fondelli, C.; **Gavrilova, J.**; Chiesi, A. (2015). Integrated isolation and quantitative analysis of exosome shuttled proteins and nucleic acids using immunocapture approaches. *Methods*, 87 (1), 46–58. DOI: 10.1016/j.ymeth.2015.05.028

Gavrilova, Julia; Tõugu, Vello; Palumaa, Peep (2014). Affinity of zinc and copper ions to insulin monomers. *Metallomics*, 6, 1296–1300. DOI: 10.1039/C4MT00059E

Noormägi, A.; **Gavrilova, J.**; Smirnova, J.; Tõugu, V.; Palumaa, P. (2010). Zn(II) ions co-secreted with insulin suppress inherent amyloidogenic properties of monomeric insulin. *Biochemical Journal*, 430 (3), 511–518. DOI: 10.1042/BJ20100627

Employment

20.09.2021–...	Tallinn University of Technology, Department of Gene Technology, engineer (0,50)
01.05.2021–...	Semetron AS (clinical diagnostics area sales manager)
2019–2021	Inbio OÜ (immunology, molecular diagnostics, and flow cytometry area product manager)
2017–2019	HansaBioMed Life Sciences Ltd (researcher)
2014–2016	BioBalt Holding OÜ (junior researcher)

Elulookirjeldus

Isikuandmed

Nimi: Julia Gavrilova
Sünniaeg: 09.10.1988
Kodakondsus: Eesti
Keeleoskus: Vene keel, Eesti keel, Inglise keel

Kontaktandmed

Address: Keemia ja biotehnoloogia instituut, Tallinna Tehnikaülikool,
Akadeemia tee 15, 12618, Tallinn, Estonia
Tel.: +372 5694 8505
E-mail: julia.gavrilova1@gmail.com

Hariduskäik

2015–2022 Tallinna Tehnikaülikool, doktoriõpe
2011–2014 Tallinna Tehnikaülikool, MSc
“Affinity of zinc and copper ions to insulin monomers”
2007–2010 Tallinna Tehnikaülikool, BSc, “The effect of environmental conditions and Zn⁺² ions on the fibrillization of insulin”
1995–2007 Tallinna Kesklinna Vene Gümnaasium, hõbemedal

Tunnustus

2015 Eesti Biokeemia Seltsi Auhind artikli “Tsink- ja vaskioonide afiinsus insuliini monomeeride suhtes” eest
2014 Üliõpilaste teadustööde riiklik konkurss – III preemia (terviseuuringute valdkonnas)
2010 Üliõpilaste teadustööde riiklik konkurss – III preemia

Publikatsioonid

Smirnova, J., **Gavrilova, J.**, Noormägi, A., Valmsen, K., Pupart H., Luo, J., Tõugu, V., Palumaa, P. “Evaluation of Zn(II)- and Cu(II)-binding affinities of native Cu,Zn-SOD1 and its G93A mutant by LC ICP MS” (2022) International Journal of Molecular Sciences

Zarovni, N.; Corrado, A.; Guazzi, P.; Zocco, D.; Lari, E.; Radano, G.; Muhhina, J.; Fondelli, C.; **Gavrilova, J.**; Chiesi, A. (2015). Integrated isolation and quantitative analysis of exosome shuttled proteins and nucleic acids using immunocapture approaches. *Methods*, 87 (1), 46–58. DOI: 10.1016/j.ymeth.2015.05.028

Gavrilova, Julia; Tõugu, Vello; Palumaa, Peep (2014). Affinity of zinc and copper ions to insulin monomers. *Metallomics*, 6, 1296–1300. DOI: 10.1039/C4MT00059E

Noormägi, A.; **Gavrilova, J.**; Smirnova, J.; Tõugu, V.; Palumaa, P. (2010). Zn(II) ions co-secreted with insulin suppress inherent amyloidogenic properties of monomeric insulin. *Biochemical Journal*, 430 (3), 511–518. DOI: 10.1042/BJ20100627

Töökogemus

20.09.2021–...	Tallinna Tehnikaülikool, Keemia ja biotehnoloogia instituut, insener (0,50)
01.05.2021–... 2019–2021	Semetron AS (müügijuht kliinilise diagnostika alal) Inbio OÜ (immunoloogia, molekulaardiagnostika ja läbivoolutsütomeetria alal tootejuht)
2017–2019	HansaBioMed Life Sciences Ltd (teadur)
2014–2016	BioBalt Holding OÜ (nooremteadur)

ISSN 2585-6901 (PDF)
ISBN 978-9949-83-884-4 (PDF)